NASA CR-111946

LTV ASTRONAUTICS DIVISION
Ling-Temco-Vought, Inc.
P. O. Box 6267
Dallas, Texas 75222

TITLE

SCOUT FIRST STAGE MOMENT DISTURBANCE STUDY

SUBMITTED UNDER

REPORT NO.	DATED
23.287	15 July 1966
PROJECT	**CONTRACT NO.**
Scout	NAS1-4664 -EDJ

J. A. Brassard

PREPARED
R. N. Knauber

REVIEWED
J. A. Brassard

APPROVED
M. D. Brinson

J. E. Mellugin

C. D. Buehrle

FACILITY FORM 602

N71-10824 (ACCESSION NUMBER) (THRU)
(PAGES) (CODE)
CR-111946 (NASA CR OR TMX OR AD NUMBER) (CATEGORY)

SEP 1971
RECEIVED
NASA STI FACILITY
INPUT BRANCH

ABSTRACT

AST-52621 R2

TITLE OF REPORT

Scout First Stage Moment Disturbance Study

ORIGINATING AGENCY AND LOCATION	CLASSIFICATION		
	REPORT	ABSTRACT	TITLE
LTV Astronautics Division LTV Aerospace Corporation Dallas, Texas	U	U	U

AUTHORS	ISSUE DATE	LIMITATIONS ON DISTRIBUTION (IF ANY)
J. A. Brassard R. N. Knauber J. E. Melugin	7-15-66	None

ORIGINATING AGENCY'S REPORT NO.	DOD REFERENCES			OTHER IDENTIFYING REPORT NOS.
	CONTRACT NO.	PROJECT NO.	TASK NO.	
23.287	NAS-1-4664			

INDEXING

A. SUMMARY SENTENCE(S):

B. KEY WORDS: First stage.

Disturbing moments.

WEAPON SYSTEMS NUMBERS, MODEL NUMBERS, ETC.

ABSTRACT

A study was conducted to determine why the pitching and yawing motions of the Scout vehicle in flight do not agree with the predicted motions. Data from several flights were analyzed and an unexplained residual moment determined for each vehicle. Various potential causes of this residual moment were considered including thrust misalignment, wind measurement accuracy, and possible errors in the predicted jet vane effectiveness and aerodynamic characteristics. It was determined that the jet vane effectiveness as calculated from Algol motor firing test data is apparently in error due to improper reduction of the data, and that the transonic aerodynamic stability margin may be less than predicted. Recommended follow-on action includes review and revision of the jet vane test data and wind tunnel tests with simulated rocket exhaust pluming.

TABLE OF CONTENTS

	Page No.
List of Figures	4
List of Symbols	6
1.0 Summary	9
2.0 Introduction	10
3.0 Discussion	12
3.1 Vehicle Configuration	12
3.2 Equations of Angular Motion	13
3.2.1 Aerodynamic Moments	16
3.2.2 Control Moments	17
3.2.3 Thrust Misalignment Moments	17
3.3. Residual Moments	17
3.3.1 Pitch Up at Lift-Off	18
3.3.2 Initial Pitch Program	25
3.3.3 Transonic Region (Mach 0.5 to 1.5)	27
3.3.4 Supersonic Region (Mach 1.5 to 4.0)	27
3.3.5 Coast	28
3.4 Potential Sources of Residual Moments	29
3.4.1 Thrust Misalignment	30
3.4.2 Jet Vane Effectiveness	36
3.4.3 Aerodynamic Characteristics	45
3.4.4 Vehicle Assembly Tolerance Investigation	52
3.4.5 Center of Pressure and Thrust Misalignment as a Function of Jet Vane Effectiveness	54
4.0 Conclusions and Recommendations	61
References	65
Appendix A, Method of Least Squares	67
Appendix B, Scout First Stage Parameter Time Histories	74
Appendix C, Effects of Reduced Jet Vane Effectiveness- Supplementary Data	96

LIST OF FIGURES

Figure No.	Title	Page No.
3.1-1	Vehicle Configuration	14
3.2-1	Sign Convention and Reference System	15
3.3-1	Residual Pitching Moment Summary	19
3.3-2	Scout Vehicle S-131 First Stage Flight Parameters	20
3.3-3	Scout Vehicle S-131 First Stage Pitch Data	21
3.3-4	Scout Vehicle S-131 First Stage Yaw Data	22
3.3-5	Scout Vehicle S-131 Summary of Pitching Moments	23
3.3-6	Scout Vehicle S-131 Summary of Yawing Moments	24
3.3-7	Scout S-131 Pitch-Up at Lift-Off Summary	26
3.4.1-1	Effective Thrust Misalignment Time Histories	32
3.4.1-2	Miscellaneous Known Pitching Moments Induced by Thrust Vector - Vehicle S-131	34
3.4.1-3	Yawing Moment Due to Thrust Misalignment Induced by Aerodynamic and Control Forces - Vehicle S-131	35
3.4.2-1	Jet Vane Effectiveness versus Time - First Fourteen Seconds of Flight - Pitch and Yaw	38
3.4.2-2	Jet Vane Effectiveness Vs. Time - Least Squares Polynomial Curve Fit of Flight Data	39
3.4.2-3	Static Test Instrumentation Summary-Algol II A-3 & II B-31	41
3.4.2-4	Algol IIB-31 Test Results	42
3.4.2-5	Jet Vane Effectiveness Summary	44
3.4.2-6	Effect of Reduced Jet Vane Effectiveness On Residual Moments - Scout Vehicle S-131	46
3.4.3-1	Pitching and Yawing Moment Coefficient versus Angle of Attack and Angle of Sideslip	48
3.4.3-2	Effective Center of Pressure versus Mach Number	51
3.4.4-1	Definition of Tolerance Buildup	53
3.4.5-1	Pitch Center of Pressure History as a Function of Control Effectiveness - Vehicle S-131	56
3.4.5-2	Yaw Center of Pressure History as a Function of Control Effectiveness - Vehicle S-131	57
3.4.5-3	Pitch Thrust Misalignment as a Function of Control Effectiveness - Vehicle S-131	59
3.4.5-4	Yaw Thrust Misalignment as a Function of Control Effectiveness - Vehicle S-131	60
B-1	Vehicle S-123 Data Summary	75
B-2	Vehicle S-130 Data Summary	76
B-3a	Vehicle S-133 Data Summary	77
B-3b	Vehicle S-133 Data Summary	78
B-4	Vehicle S-134 Data Summary	79
B-5	Vehicle S-135 Data Summary	80
B-6a	Vehicle S-136 Data Summary	81
B-6b	Vehicle S-136 Data Summary	82
B-7	Vehicle S-137 Data Summary	83

LIST OF FIGURES (Cont'd)

				Page No.
B-8a	Vehicle	S-138	Data Summary	84
B-8b	Vehicle	S-138	Data Summary	85
B-9a	Vehicle	S-139	Data Summary	86
B-9b	Vehicle	S-139	Data Summary	87
B-10a	Vehicle	S-140	Data Summary	88
B-10b	Vehicle	S-140	Data Summary	89
B-11a	Vehicle	S-141	Data Summary	90
B-11b	Vehicle	S-141	Data Summary	91
B-12a	Vehicle	S-142	Data Summary	92
B-12b	Vehicle	S-142	Data Summary	93
B-13a	Vehicle	S-143	Data Summary	94
B-13b	Vehicle	S-143	Data Summary	95

C-1	Effect of Reduced Jet Vane Effectiveness on Residual Pitch Moment - Vehicle S-133	97
C-2	Pitch Center of Pressure History as a Function of Control Effectiveness - Vehicle S-133	98
C-3	Pitch Thrust Misalignment History as a Function of Control Effectiveness - Vehicle S-133	99
C-4	Effect of Reduced Jet Vane Effectiveness on Residual Moment - Vehicle S-137	100
C-5	Pitch Center of Pressure History as a Function of Control Effectiveness Vehicle S-137	101
C-6	Pitch Thrust Misalignment History as a Function of Control Effectiveness - Vehicle S-137	102
C-7	Effect of Reduced Jet Vane Effectiveness on Residual Moment - Vehicle S-142	103
C-8	Pitch Center of Pressure History as a Function of Control Effectiveness - Vehicle S-142	104
C-9	Yaw Center of Pressure History as a Function of Control Effectiveness - Vehicle S-142	105
C-10	Pitch Thrust Misalignment History as a Function of Control Effectiveness - Vehicle S-142	106
C-11	Yaw Thrust Misalignment History as a Function of Control Effectiveness - Vehicle S-142	107

LIST OF SYMBOLS

C_{L_ϵ}	slope of fin lift coefficient with fin misalignment angle, per degree
$C_{N_\alpha}, C_{Y_\beta}$	slope of normal or side force coefficient with angle of attack or sideslip respectively, per degree
$C_{N_\delta}, C_{Y_\delta}$	slope of fin tip force coefficient with deflection angle, in pitch or yaw respectively, per degree
$C_{m_\alpha}, C_{n_\beta}$	slope of pitching or yawing moment coefficient with angle of attack or sideslip respectively, per degree
C_{m_o}, C_{n_o}	pitching or yawing moment coefficient at zero angle of attack or sideslip respectively
$C_{m_{\dot\theta}}, C_{n_{\dot\psi}}$	pitching or yawing damping moment coefficient, per radian
d	reference length, 2.58 ft.
F	force, lbs.
h	altitude, ft.
I_{YY}, I_{ZZ}	pitching or yawing moment of inertia, SLUG-ft^2
L	jet vane lift, lbs.
L_δ	jet vane effectiveness, lbs/degree
ℓ	moment arm, ft.
M_i	pitch moment (subscript denotes source) , ft.- lbs.
M	Mach number
ΔM	residual pitch moment, ft. lbs.
N_i	yawing moment (subscript denotes source), ft.- lbs.
ΔN	residual yaw moment, ft. - lbs.
q	dynamic pressure, lbs/ft.^{2}
S	reference area, 5.25 ft.^{2}
T	booster thrust (actual), lbs.
$T_{vac.}$	vacuum booster thrust, lbs.
V	relative air velocity, ft./second

X	body station, inches or feet
$X_{C.G.}$	center of gravity location, body station, inches or feet
X_{C_p} or C.P.	aerodynamic center of pressure, body station, inches or feet
X_T	booster nozzle throat location, body station, inches or feet
X_δ	control surface center of pressure location, body station, inches or feet
$\bar{Y}$	lateral shift in body segment centerline due to manufacturing tolerances, inches or feet
α	angle of attack, degrees or radians.
β	angle of sideslip, degrees or radians
δ_p, δ_Y	pitch or yaw control surface deflection angle, degrees
ϵ_T	thrust misalignment angle, degrees or radians
ϵ_{FIN}	fin misalignment angle, degrees
θ_c	commanded pitch program angle, degrees or radians
θ_e	pitch attitude error, degrees or radians
$\dot{\theta}$	angular rate about the body pitch axis, rad/sec. or deg/sec.
$\ddot{\theta}$	angular acceleration about the body pitch axis, rad/sec^2
ψ_e	yaw attitude error, degrees or radians
$\dot{\psi}$	angular rate about the body yaw axis, rad/sec or deg/sec.
$\ddot{\psi}$	angular acceleration about the body yaw axis, rad/sec^2

Subscripts

J.V.	jet vane
S	side force
δ	partial with respect to deflection angle
ϕ	angularity
$\odot$	concentricity
$\perp$	perpendicularity
$\parallel$	parallelism
p	pitch

ψ	yaw
e	error
EFF.	effective
APP.	apparent
PRED.	predicted

1.0 SUMMARY

A study was conducted under Contract NAS 1-4664 to determine why the pitching and yawing motions of the Scout vehicle in flight do not agree with the predicted motions under the influence of winds measured about the time of launch. The meterological, radar tracking and telemetered flight data have been used in conjunction with the predicted stability and control characteristics to calculate the moments acting on the vehicle. Data from about fifteen flights were analyzed and an unexplained "residual" moment was determined for each vehicle. The various potential causes of this residual moment considered were thrust misalignment, wind measurement accuracy, and possible errors in the predicted jet vane effectiveness and aerodynamic characteristics. It is apparent that no single factor is solely responsible and that thrust misalignment, jet vane effectiveness, and transonic aerodynamic stability are likely candidates.

Thrust misalignment due to bending and center of gravity offset can cause consistent pitch-up moments, but they are of significantly lesser magnitude than the residual moment. The test data upon which the predicted jet vane effectiveness is based was reviewed for accuracy and is apparently in error. Side force data measured during a later jet vane test indicates a significantly lower jet vane effectiveness than that determined from the vane loads. This side forced data correlates well with that determined from flight data. The aerodynamic stability margin as derived from flight data is apparently less than predicted in the transonic region. A number of recommendations are made for resolving these and other uncertainties.

2.0 INTRODUCTION

Correlation of the Scout post flight trajectory simulation with the flight measured vehicle trajectory and control deflections indicates that moments are acting on the vehicle that are not accounted for by the predicted aerodynamic and control characteristics. These moments would, of course, include those caused by thrust misalignment. The magnitude of the thrust misalignment angle required to generate the calculated moments exceeded the predicted maximum of 0.25 degrees on several flights. For this reason the residual moment has been treated as a separate entity that includes thrust misalignment as well as any other moment sources such as uncertainties in the predicted vehicle aerodynamics, control effectiveness, flight wind profile, etc. These moments which are not included in the pre-flight analysis will affect the controllability limits, wind restrictions, and trajectory dispersion.

A significant pitch-up moment at launch has been experienced on most vehicles and the resulting commanded control deflections during the first pitch program have exceeded the available control throw for initial pitch rates of about 4 degrees per second, although only one-half of the available deflection is predicted for this rate. Later in the flight the predicted control deflections approach zero in the region of minimum predicted static stability margin but flight results indicate a consistent control deflection requirement of about 3 to 5 degrees trailing edge down. The existence of these moments has been noted in other studies on the Scout vehicle including the first stage control system performance analysis performed by Honeywell as reported in Reference 1, and the flight loads analysis performed on vehicle S-133 as reported in Reference 2.

The residual moment has been calculated and presented separately in the post flight analyses of vehicles S-130 and subsequent. Incorporation of this moment in the post flight trajectory simulation results in better correlation with the observed radar trajectory and good correlation between the measured and simulated control deflections. As the results of several flights accumulated it became apparent that the residual moment in the pitch plane exhibits a characteristic time history profile. This profile coincides with the control deflections during the first pitch program, becomes a pitch-down moment when the vehicle is in the transonic region and becomes a pitch-up moment in the supersonic region near maximum dynamic pressure/mimimum static margin. It was anticipated that this characteristic profile would provide a means of determining the most likely causes of the residual moment and provide a basis for recommended action to define the magnitude of the individual contributing factors. The data could then be incorporated into the preflight trajectories for accurate definition of the flight restrictions and trajectory profile and in the dispersion analysis. This report presents the results of the study and the recommended follow-on action.

3.0 DISCUSSION

The pitching and yawing motion of the Scout vehicle in flight does not agree with the predicted motion under the influence of winds measured just prior to or after the time of launch. Therefore, the approach to the first stage post flight analysis is to define the moments acting on the vehicle by the use of all available meteorological, radar tracking, and telemetered flight data. This procedure has revealed the existence of discrepancies or unexplained residual moments of significant magnitude (±30,000 ft.-lbs). These residual moments have been used in the post flight trajectory calculation to achieve a more accurate simulation. The residual moment is most noticeable in the pitch plane where a characteristic time history is evident. The objective of the following sections is to define the equations, assumptions and methods used to determine the moments. The characteristics of the Scout first stage are then discussed and various analyses presented which define the probable sources of the unexplained moments. The purpose of this study was not to predict the unexplained moments, but to investigate the problem to the extent that positive recommendations can be made which will lead to this capability.

3.1 Vehicle Configuration

The Scout launch vehicle utilizes a "strapped down" gyro guidance system to provide the body displacement reference in pitch, yaw and roll. A programmer provides torquing voltages to the pitch displacement gyro to command the vehicle to fly a preselected trajectory. A proportional control system featuring a combination of moveable jet vanes immersed in the rocket exhaust and aerodynamic fin tip control surfaces, operated by electro-hydraulic servo actuators, is used to control the vehicle throughout the entire first stage burning period. The jet vanes provide the majority of the control force

during the thrusting phase. The aerodynamic fin tips provide all the control force during the coast phase following burnout of the Algol motor.

During subsonic and transonic flight the vehicle is aerodynamically stable. Later in the first stage burning phase the forward movement of the center of pressure caused by increased Mach number and flexibility effects results in a near zero static margin.

The specific Scout motor configuration analyzed consists of an Algol II first stage, Castor second stage, X-259 third stage and an X-258 or an FW-4S fourth stage. The external configuration shown in Figure 3.1-1 has a 34 inch diameter heat shield with the nose at Scout station -25 and aerodynamic fins on the base section. The only exception to this configuration used in the analysis is vehicle S-133 which had a 34 inch diameter heatshield and the nose at station -10 with a 22 inch nose boom. The external symmetry of the Scout vehicle is altered by the various protuberances such as wiring tunnels, launch fittings, antennas, and reaction control jets.

3.2 Equations of Angular Motion

The equations describing the pitch and yaw motion of the Scout vehicle during first stage flight are assumed to consist of moments due to aerodynamics, control surface deflections and thrust misalignment.

$$I_{yy}\ddot{\theta} = \Sigma M = M_{AERO} + M_{CONTROL} + M_{ET} \qquad (1)$$

$$I_{zz}\ddot{\psi} = \Sigma N = N_{AERO} + N_{CONTROL} + N_{ET} \qquad (2)$$

The angular relations and sign conventions used in this analysis are shown in Figure 3.2-1. Thrust misalignment is not known and cannot readily be separated from other uncertainties. Therefore, a residual moment is inserted into the equations and thrust misalignment is eliminated as a separate entity. The equations of pitch and yaw motion then become.

$$I_{yy}\ddot{\theta} = M_{AERO} + M_{CONTROL} + \Delta M \qquad (3)$$

$$I_{zz}\ddot{\psi} = N_{AERO} + N_{CONTROL} + \Delta N \qquad (4)$$

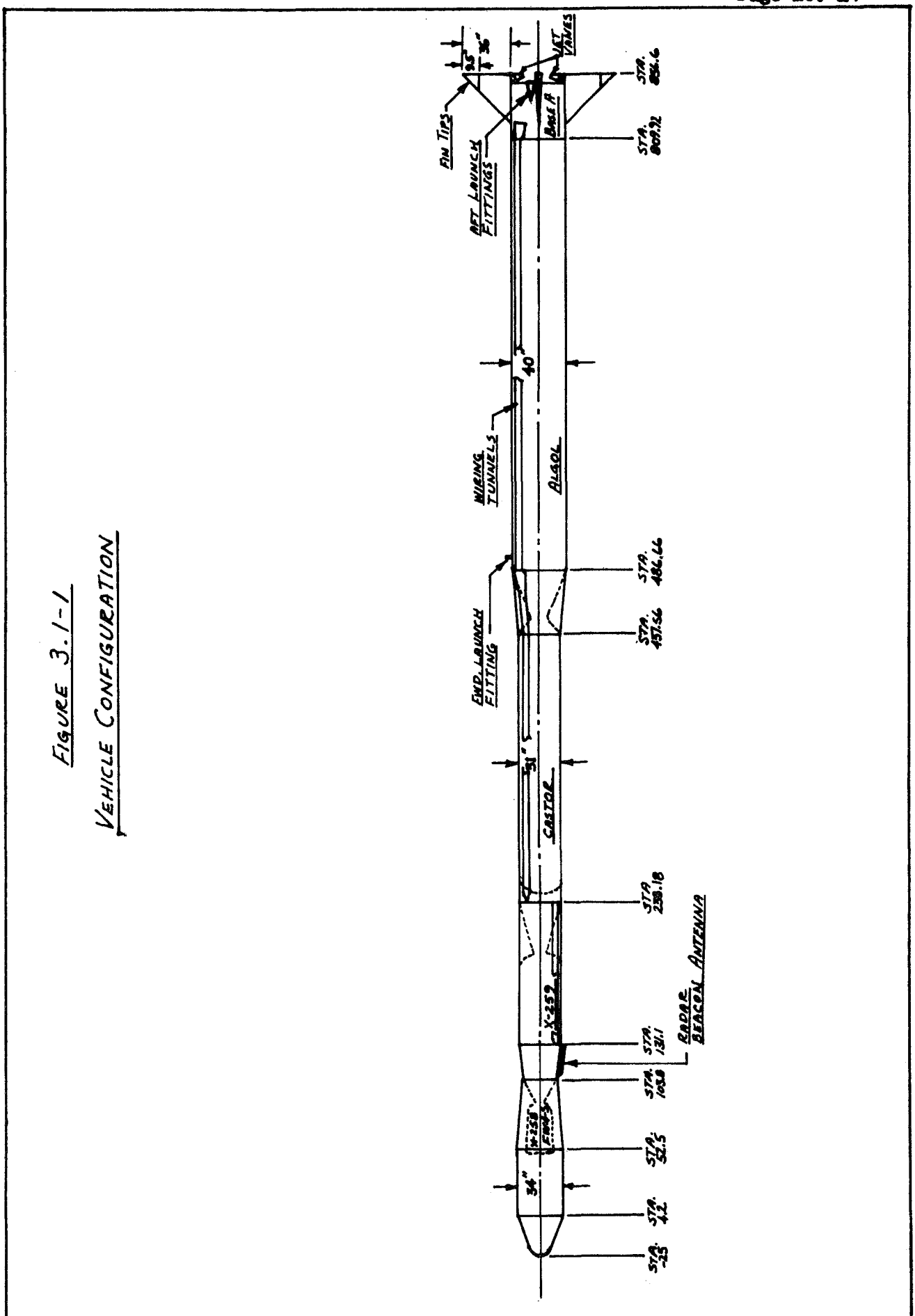

Figure 3.1-1

Vehicle Configuration

FIGURE 3.2-1
SIGN CONVENTION AND REFERENCE SYSTEM

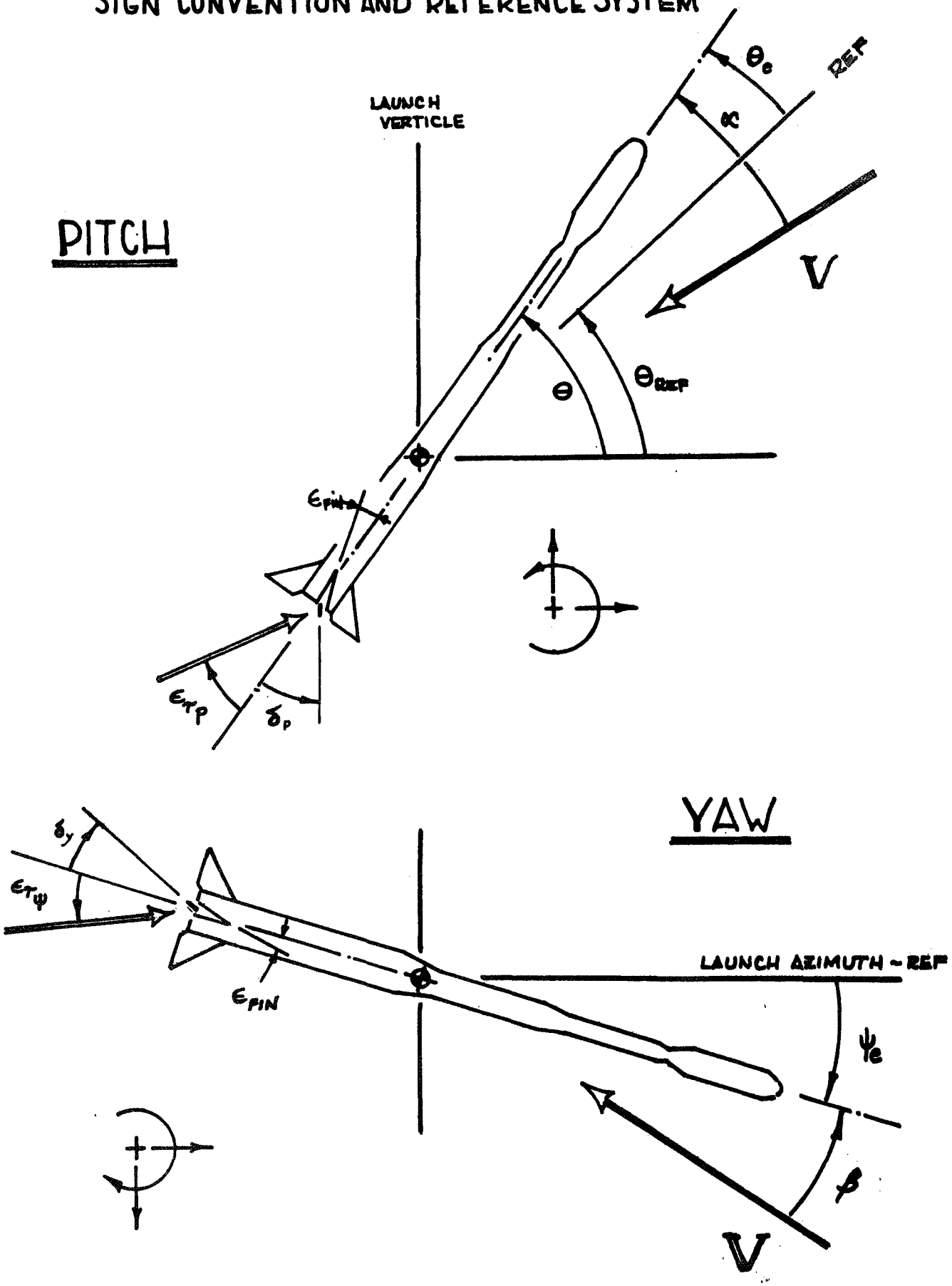

The residual moments are:

$$\Delta M = I_{yy}\ddot{\theta} - M_{AERO} - M_{CONTROL} \quad (5)$$

$$\Delta N = I_{zz}\ddot{\psi} - N_{AERO} - N_{CONTROL} \quad (6)$$

The vehicle angular accelerations are obtained by differentiation of the telemetered rate gyro date. The other moments are described below.

3.2.1 Aerodynamic Moments

The aerodynamic contributions to the moments acting on the vehicle include the basic aerodynamic characteristics derived from wind tunnel tests and analytical methods as presented in Reference 3. In calculating moments the following aerodynamic terms are included.

$$M_{AERO} = C_{M_\alpha} qS(X_{CG}-X_{CP})\alpha + C_{M_{TD}} qSd + C_{L_E} qS(X_{CG}-X_{CP_{FIN}})\epsilon_{FIN} + C_{m_{\dot\theta}} \frac{qSd^2}{2V}\dot\theta \quad (7)$$

$$N_{AERO} = C_{Y_\beta} qS(X_{CG}-X_{CP})\beta + C_{L_E} qS(X_{CG}-X_{CP_{FIN}})\epsilon_{FIN} + C_{n_{\dot\psi}} \frac{qSd^2}{2V}\dot\psi \quad (8)$$

The static aerodynamic characteristics include the effects of external protuberances, aeroelasticity, and fin misalignment. The effects of combined angle of sideslip and angle of attack are not included. The center of pressure is assumed to be invariant with angle of attack to 5 degrees and is adjusted for angle of attack at larger angles.

The pitch and yaw damping derivatives are assumed to be due to the pitching and yawing velocities. The damping due to rate of change of angle of attack and sideslip are assumed negligible.

The calculated aerodynamic moments are based on the predicted coefficients and the post flight calculated relative velocity, Mach number, dynamic pressure, angles of attack and sideslip and telemetered pitch and yaw rates.

These parameters are determined by analysis of the radar tracking data, meteorological data and telemetered information for each flight.

3.2.2 Control Moments

The control moments include jet vane lift and aerodynamic fin tip force.

$$M_{CONTROL} = 2\,(L_\delta + C_{N\delta}\,qS)(X_{CG} - X_\delta)\,\delta_P \qquad (9)$$

$$N_{CONTROL} = 2\,(L_\delta + C_{N\delta}\,qS)(X_{CG} - X_\delta)\,\delta_Y \qquad (10)$$

The jet vane effectiveness is assumed to be proportional to the booster vacuum thrust and is linear with deflection angle as determined from static motor test firing data presented in Reference 3 . The fin tip normal force coefficient is also assumed linear with deflection angle and invariant with angle of attack. The post flight calculated thrust, Mach number, dynamic pressure and the telemetered control surface deflections are used with the predicted coefficients to determine the total control moment in pitch and yaw. The use of telemetered control surface deflections circumvents any problem of variation in control system response characteristics.

3.2.3 Thrust Misalignment Moments

The thrust misalignment is not known and cannot be readily separated from other uncertainties during first stage flight. Therefore, the residual moment term included in the analysis includes any thrust misalignment.

3.3 Residual Moments

The equations used to define the residual moments in pitch and yaw are:

$$\Delta M = I_{yy}\ddot{\theta} - C_{N\alpha}\,qS(X_{CG} - X_{CP})\,\alpha - C_{m_0}\,qSd - C_{L_\epsilon}\,qS(X_{CG} - X_{CP_{FIN}})\,\epsilon_{FIN} - C_{m_\theta}\,q\,\frac{Sd^2}{2V}\,\dot{\theta} - 2(L_\delta + C_{N\delta}\,qS)(X_{CG} - X_\delta)\,\delta_P \qquad (11)$$

$$\Delta N = I_{zz}\ddot{\psi} - C_{Y\beta} qS (X_{cs} - X_{cg})\beta - C_{L_\epsilon} qS (X_{cs} - X_{cp_{FIN}})\epsilon_{FIN}$$
$$- C_{n_{\dot{\psi}}} q \frac{Sd^2}{2V}\dot{\psi} - 2(L_\delta + C_{Y\beta} qS)(X_{cs} - X_\delta)\delta_M \qquad (12)$$

The residual moments calculated for the post flight analysis may be due to thrust misalignment, errors in post flight data, and/or errors in predicted aerodynamic data or jet vane effectiveness. The jet damping effect is not included in the moment equations since the magnitude of this moment is insignificant in comparison to the other individual moments and the residual moment.

The first stage moment disturbances have been calculated as part of the post flight analysis for fifteen Scout flights. The calculated residual pitching moment on each of these flights has a similar time history. A summary of all residual pitching moments is shown in Figure 3.3-1. A representative flight, that of the S-131 Systems Evaluation Vehicle, is discussed below. The time histories of the related flight parameters for this vehicle are shown in Figures 3.3-2 through 3.3-4. These are typical of the parameters which occur on other missions. The calculated pitch and yaw moments including the residual moments are shown in Figures 3.3-5 and 3.3-6 respectively. Summary data for other vehicles are presented in Appendix B.

3.3.1 Pitch-Up at Liftoff

From liftoff to initiation of the first pitch program at approximately three seconds flight time the vehicle is programmed to fly vertically to clear the launch tower.

On most flights prior to the first pitch program input the vehicle experiences a pitch-up disturbance of several thousand foot-pounds. This phenomenon has concerned the Range Safety Personnel since the pitch-up causes

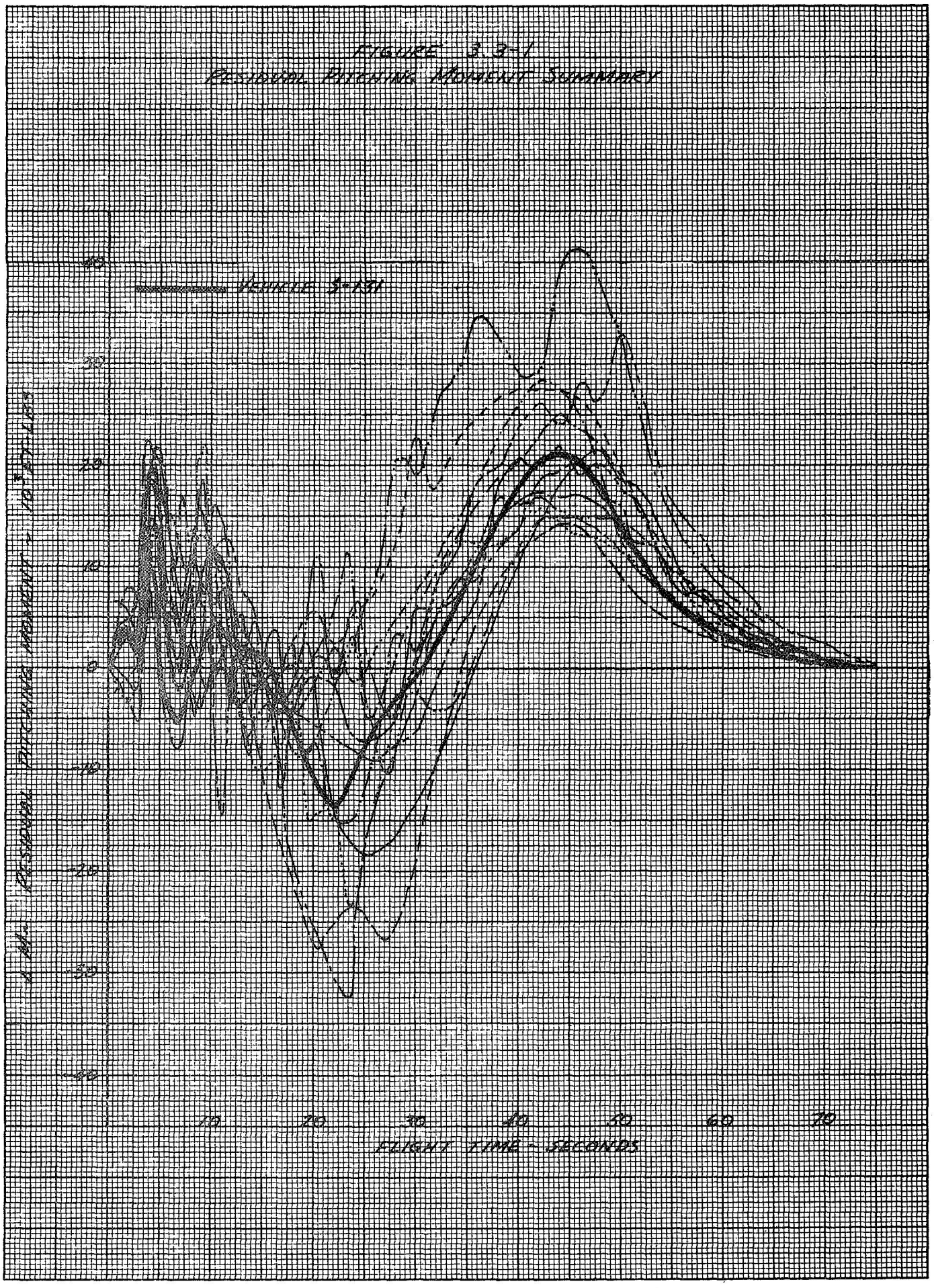
FIGURE 3.3-1
RESIDUAL PITCHING MOMENT SUMMARY
VEHICLE S-13A
60
40
20
0
-20
-40
-60
RESIDUAL PITCHING MOMENT - DEGREES/SEC²
10
20
30
40
50
60
70
FLIGHT TIME - SECONDS

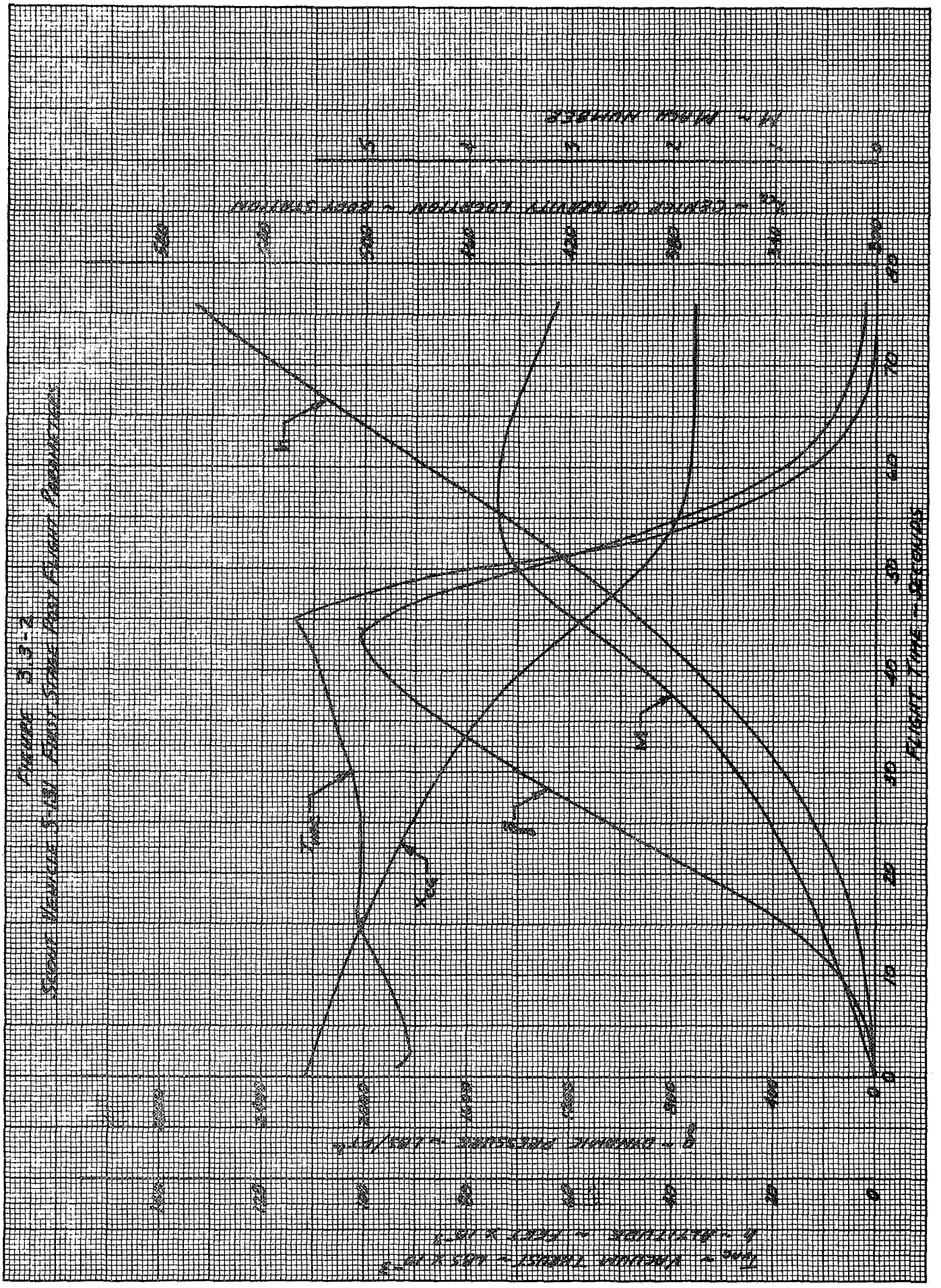
Flight time - seconds
Engine speed - r.p.m.
Engine boost pressure - lbs/sq.in.
Throttle position
Mixture control position
Airscrew pitch control position
Radiator shutter position
Oil temperature - °C
Oil pressure - lbs/sq.in.
Cylinder head temperature - °C

FIGURE 3.3-3
SCOUT VEHICLE S-131 FIRST STAGE ROLL DATA

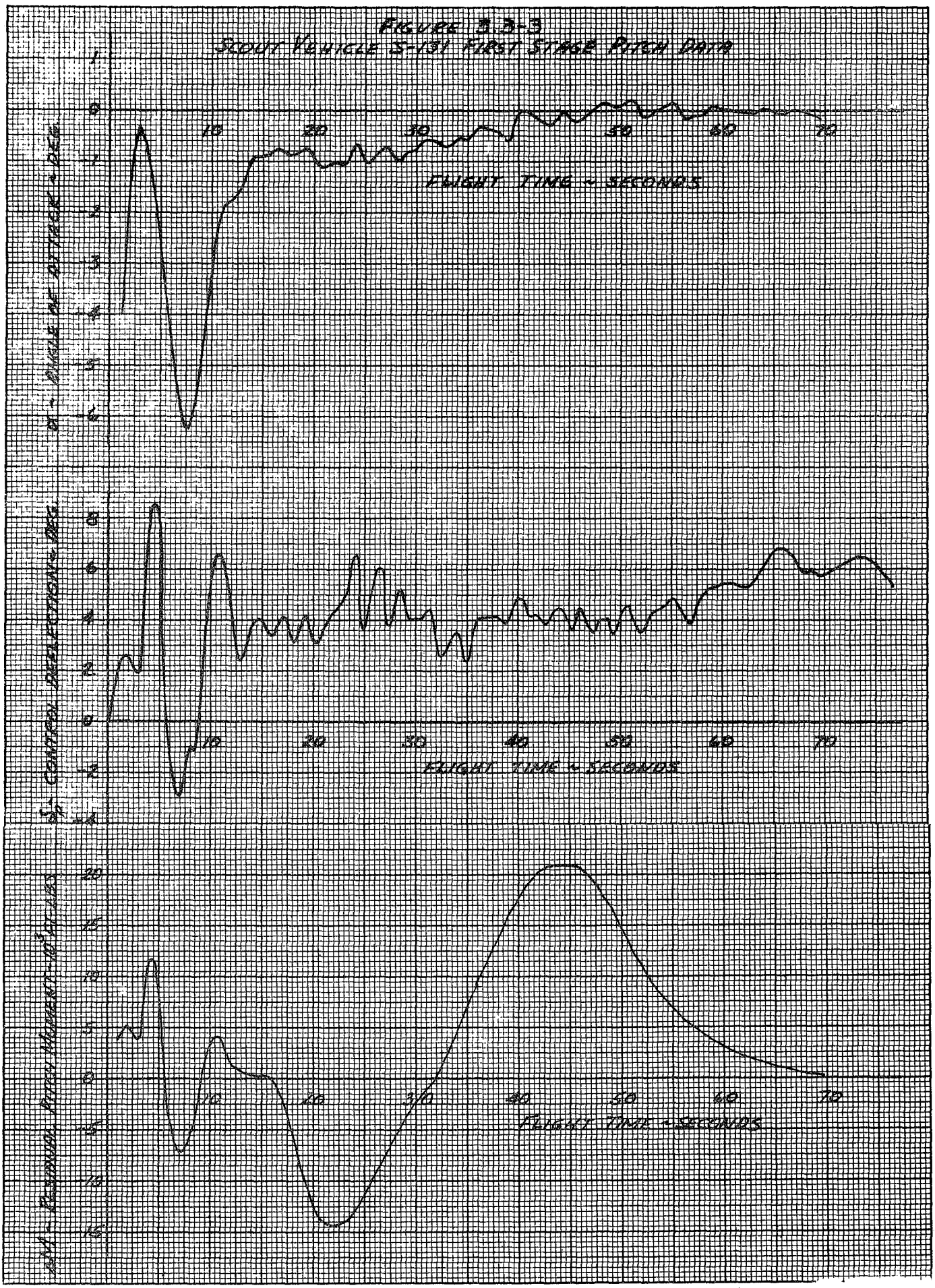

FIGURE 3.3-4
SCOUT VEHICLE S-13L FIRST STAGE YAW RATE

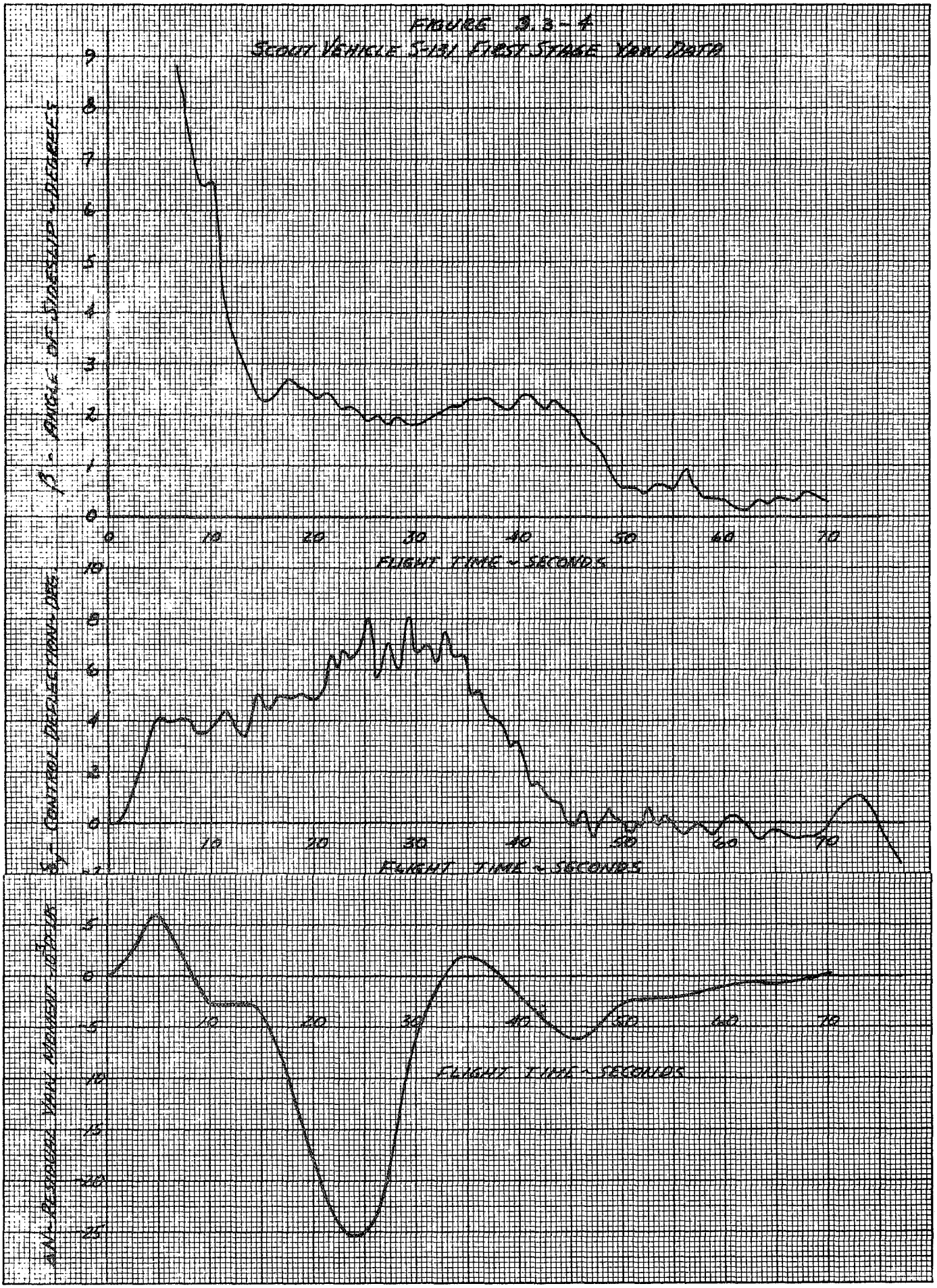

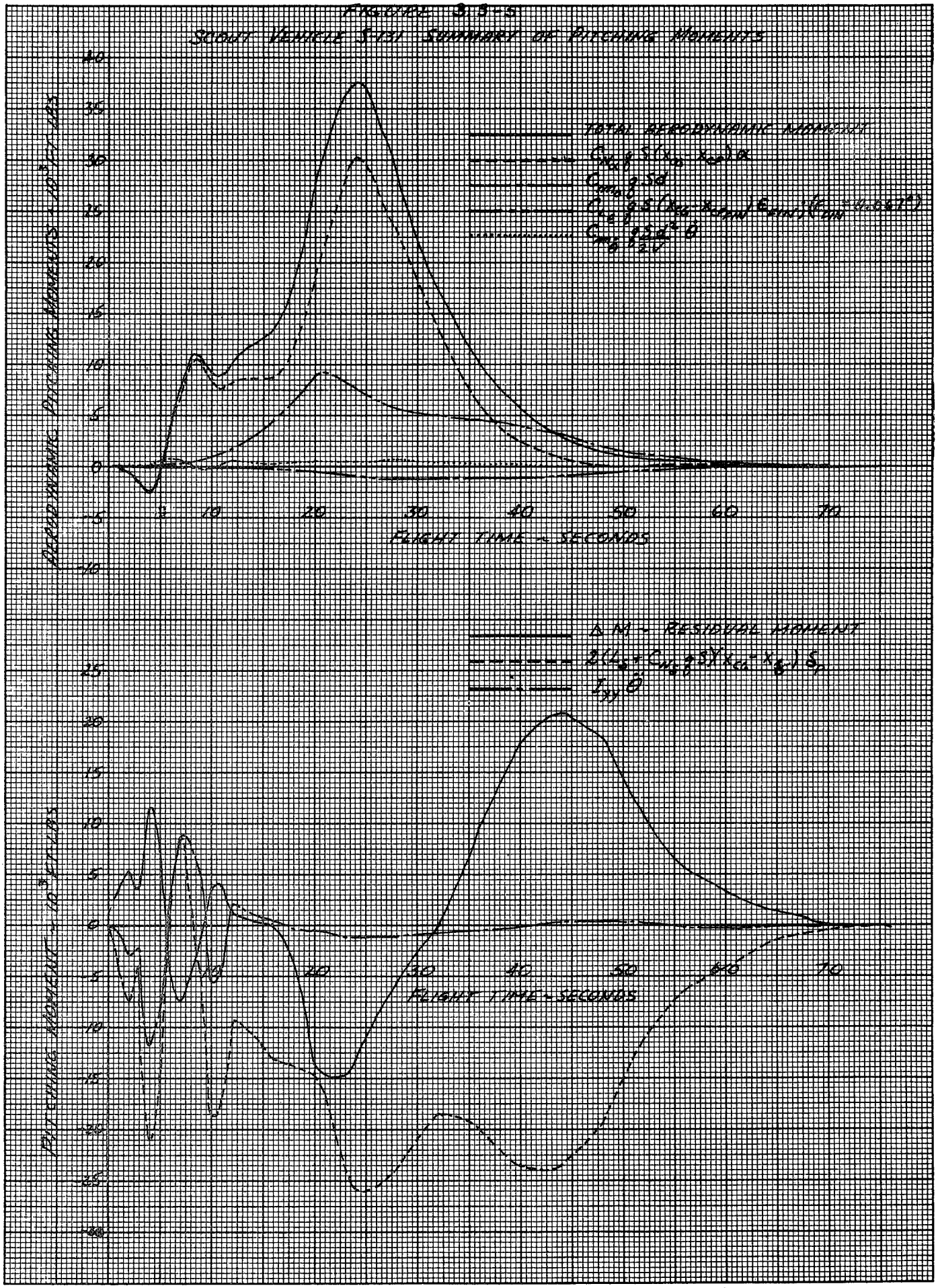
FIGURE 3.3-5
SCOUT VEHICLE S-IVI SUMMARY OF PITCHING MOMENTS
TOTAL AERODYNAMIC MOMENT
$C_{N_\alpha} \bar{q} S(x_{cp} - x_{cg})\alpha$
$C_{m_{q_\alpha}} \bar{q} S d$
$C_{N_\delta} \bar{q} S(x_{cg} - x_{cpw}) \delta_{max} (\delta_{max} = 0.0872)$
$C_{m_\delta} \bar{q} S d \delta$
PITCHING MOMENT - RADIANS/SEC²
FLIGHT TIME - SECONDS
ΔM - RESIDUAL MOMENT
$2(A_{s^2} C_{N_\delta} \bar{q} S)(x_{cp} - x_{cg}) \delta_p$
$I_{yy} \ddot{\theta}$
PITCHING MOMENT - RADIANS/SEC²
FLIGHT TIME - SECONDS

Figure 3.3-6

Scout Vehicle S-13 Summary of Yawing Moments

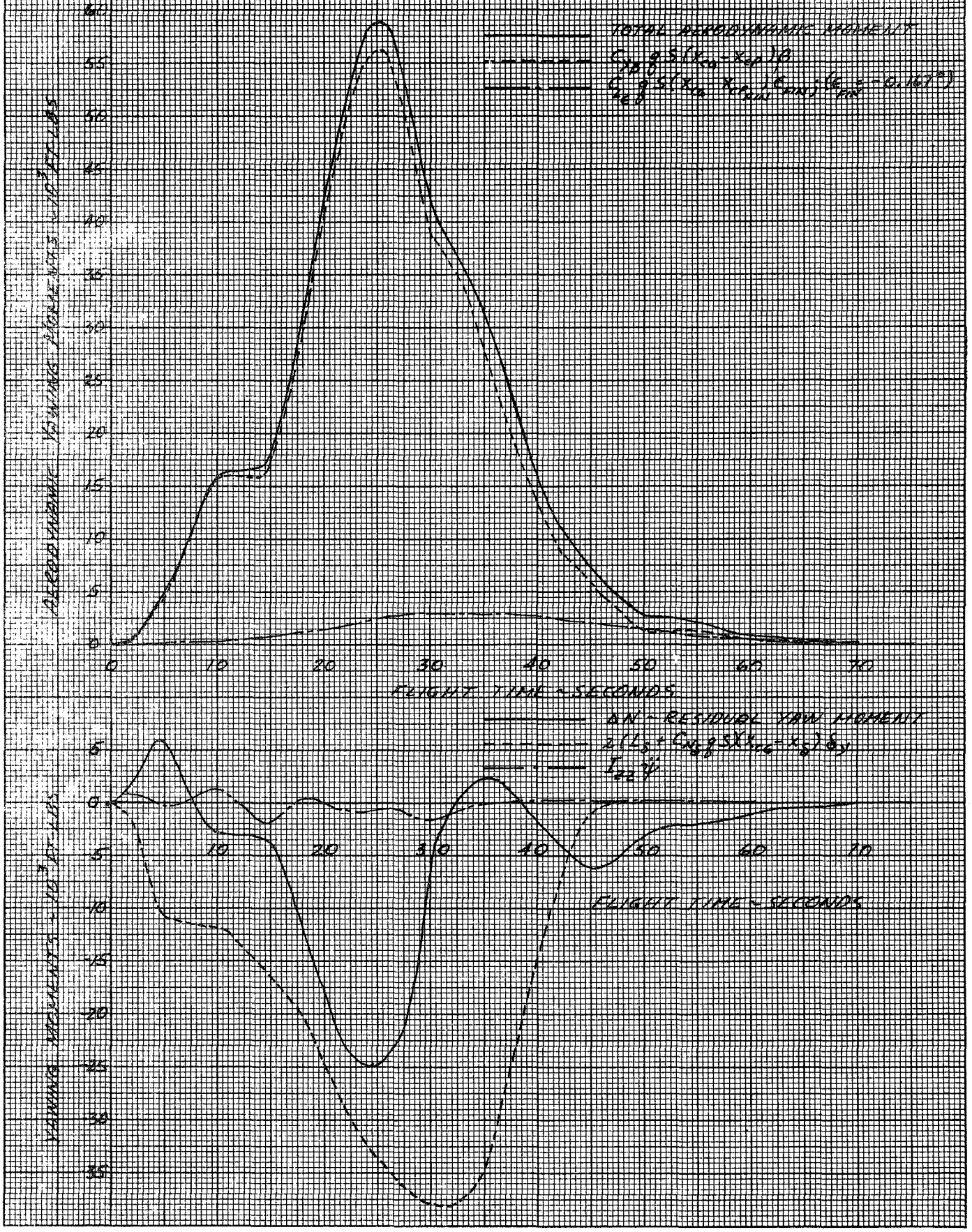

an uprange trajectory dispersion early in the flight.

The attitude time history and moments acting on Vehicle S-131 are shown in Figure 3.3-7. The dynamics of the launcher and vehicle during the first few tenths of a second when the vehicle is unloading and leaving the launcher induces a pitch-up "tip-off" rate of approximately 0.25 degrees per second. The calculated pitch-up moments acting on the vehicle after lift-off but prior to the first pitch program may be due to an asymmetric pressure distribution on the vehicle caused by interaction of the rocket exhaust with the ground and the launch tower, or biased Algol moter thrust misalignment similar to the observed Castor pitch-up thrust misalignment.

Vehicle S-127 had the largest pitch-up of any successful Scout flight with a pitch-up moment of approximately 9000 ft-lbs during the first three seconds. An uprange dispersion of approximately 20 feet occurred which caused the vehicle to fly back over the launcher.

3.3.2 Initial Pitch Program

After the first three seconds of flight a pitch program is initiated which commands the vehicle to pitch down range at a rate of from 2 to 4 degrees per second. Commanded initial pitch rates in excess of about 3.9 deg/sec can cause surface deflections to briefly reach their physical stops at about 18.5 degrees. Recent flights with initial pitch rates of about 3 deg/sec have had peak deflections of 10 to 15 degrees trailing edge down during this period. A second transient of almost equal magnitude occurs at about 8 to 10 seconds flight time when the pitch program is stepped down to a much lower rate. During this time period control is supplied almost entirely by the jet vanes due to the ineffectiveness of the aerodynamic fin tips at low dynamic pressure. Angles of attack and sideslip undergo large transients during this period due to the high pitching rate and low forward velocity but decrease rapidly as the initial pitch program is accomplished and forward velocity is increased.

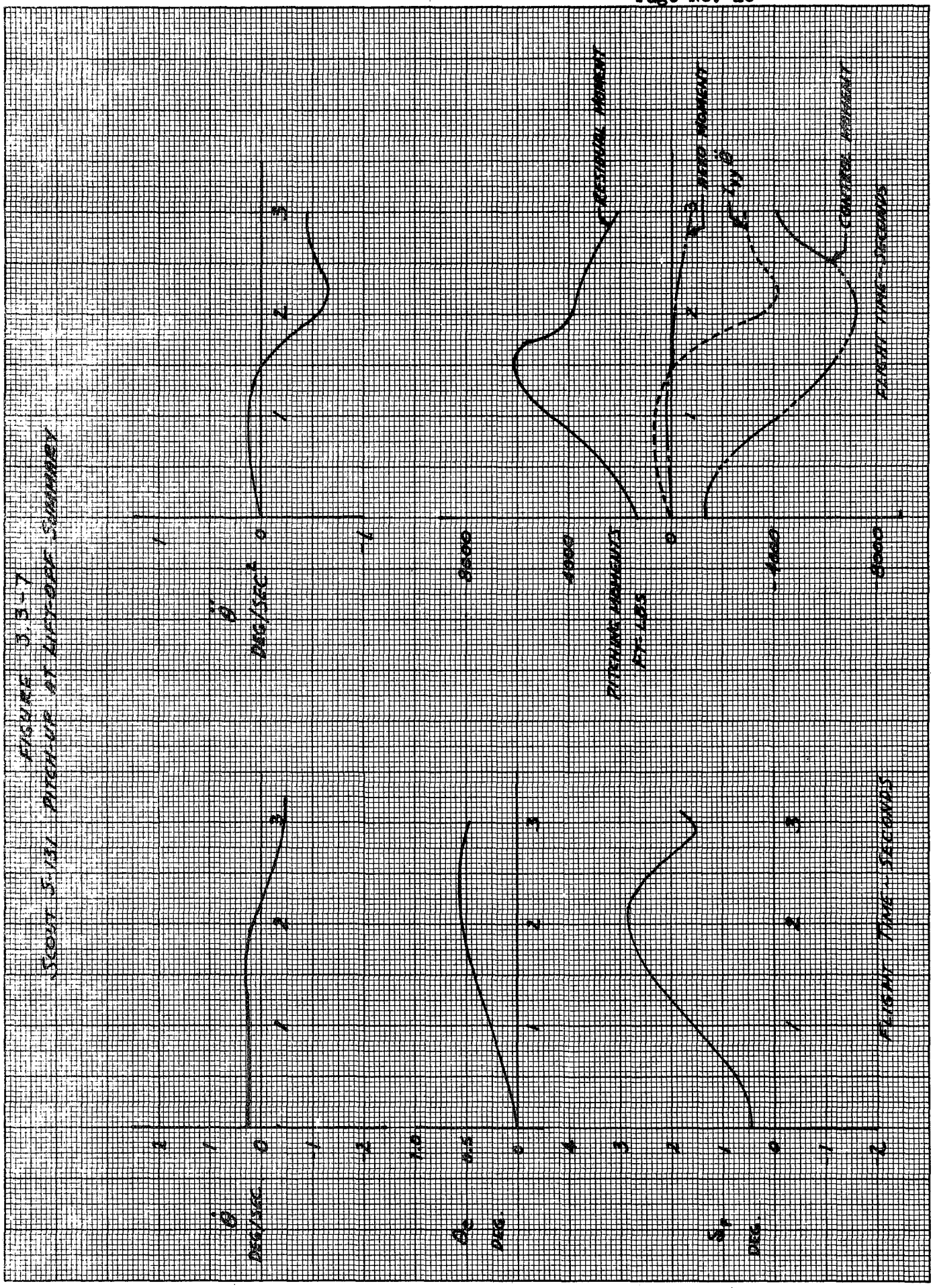
FIGURE 3.3-7
SCOUT S-181 PITCH-UP AT LIFT-OFF SUMMARY
PITCH RATE, DEG/SEC
PITCH ANGLE, DEG
PITCH MOMENT, FT-LBS
PITCH MOMENT
CENTER OF GRAVITY
FLIGHT TIME, SECONDS

During the first pitch program, residual pitch-up moments occur which are proportional to the control deflections. This can be seen in Figure 3.3-5 by comparing the residual moment with the computed control moment. This indicates a possible reduced effectiveness of the jet vanes.

3.3.3 Transonic Region (Mach 0.5 to 1.5)

When the transients associated with the first pitch program have decayed, the vehicle has entered the transonic region of flight (Mach 0.5 to 1.5). This phase includes the time from 15 to 30 seconds after liftoff. During this phase the vehicle undergoes rapid changes in static stability. The predicted static margin increases from 175 inches at Mach 0.5 to 215 inches at Mach 1 and then decreases to 105 inches at Mach 1.5. At Mach 0.8 the pitching moment coefficient at zero angle of attack, Cm_o, due to protuberances, reaches its maximum value and produces a pitch-up moment of 9000 ft-lbs.

In the transonic region the residual pitching moment changes from a nose-up moment to a negative (nose-down) moment near Mach 1.0 and then reduces to zero near Mach 1.5. The magnitude of this residual pitch down moment averages from 10,000 to 20,000 ft-lbs at Mach 1.0. The residual moment in yaw at Mach 1.0 is about -25000 ft-lbs (nose-left) on vehicle S-131 but varies in both magnitude and direction from vehicle to vehicle. Corelation of these moments with jet vane effectiveness and static stability is discussed in sections 3.4.2 and 3.4.3 of this report.

3.3.4 Supersonic Region (Mach 1.5 to 4.0)

In the supersonic region of first stage flight the vehicle experiences its maximum dynamic pressure. The maximum dynamic pressure occurs at 40 to

45 seconds flight time and in the Mach number range of 2.0 to 3.0. In this region the predicted static stability of the vehicle including flexibility effects is near zero. The effects of pluming of the rocket exhaust may become significant at high altitude, but it has not been considered in the aerodynamic predictions. At about 45 seconds flight time the thrust of the Algol II motor begins to decay with a resultant loss of jet vane control. Dynamic pressure also decreases rapidly at this point causing decreasing fin tip control effectiveness. The simultaneous decrease in motor thrust and dynamic pressure causes a decreasing system natural frequency which appears as a dynamic instability; i.e., increasing amplitude with decreasing frequency. Analog studies of the vehicle response during this period are presented in Reference 4.

The residual pitching moment begins increasing to positive values in the supersonic region and reaches a maximum near peak dynamic pressure. On vehicle S-131 the pitch-up moment reached 21,000 ft-lbs. Other vehicles also have this characteristic but the magnitude of the moment varies from about 14,000 to 41,000 ft-lbs.

The residual yawing moment during this period is of a lower magnitude and does not have a consistent direction as it does in pitch. Control deflections in yaw are usually near zero past 45 seconds flight time whereas the pitch deflections are usually 3 to 5 degrees trailing edge down.

3.3.5 Coast

The Algol II motor thrust has a long decay time and reduces to zero at about 75 to 80 seconds after ignition. In some cases a short coast period is necessary in order to reduce dynamic pressure prior

to second stage ignition. During the first stage coast period control is supplied only by the moveable fin tips which are decreasing in effectiveness. The altitude during the first stage coast is above 100,000 ft. In addition to low control effectiveness wind velocities usually increase significantly above 100,000 feet as shown in References 5 and 6 causing increasing trim angles of attack and sideslip. The wind profiles measured at the time of Scout launchings are made by radiosonde balloon and are limited to altitudes below about 100,000 feet. Due to this lack of data the moments can not be calculated during the coast period.

3.4 Potential Sources of Residual Moments

The nature of the unexplained pitch moment history indicates several possible causes. The almost consistent pitch-up at liftoff suggests either a consistent thrust misalignment or consistent interaction of the vehicle and the rocket exhaust gases in the vicinity of the launcher. The proportionality of the residual moment with the control surface deflections during the first pitch program suggests a reduced jet vane effectiveness. The large pitch and yaw moments in the transonic region indicate reduced aerodynamic stability. The large pitching moment near maximum dynamic pressure and the sudden drop-off with both dynamic pressure and thrust level suggests a possible aerodynamic uncertainty and/or thrust misalignment possibly coupled with a reduced jet vane effectiveness.

Evaluation of the above postulation was accomplished by several means. An attempt was made to reduce the calculated residual moment by altering jet vane effectiveness and aerodynamic center of pressure estimated from the moment analysis. A least squares curve fitting method was also

employed to determine the best estimate of jet vane effectiveness during the flight and the best estimate of the aerodynamic pitching moment at several Mach numbers. An investigation of the assembly tolerances was made. The amount of Algol motor case bending in storage was estimated to determine if storage procedures may induce a consistent pitch-up thrust misalignment. The jet vane test data was reviewed for accuracy and repeatability. The basic aerodynamic data was also reviewed for phenomenon which may alter the predicted stability characteristic.

Detailed discussion of these tasks are presented in the following paragraphs.

3.4.1 Thrust Misalignment:

3.4.1.1 The analysis of thrust misalignment for this study is limited to the calculation of an effective thrust misalignment form the residual moments and the estimation of possible thrust misalignment bias in the pitch plane resulting from horizontal storage of the motor, vehicle mass asymmetry and vehicle bending in flight.

Calculations made by Aerojet-General Corporation indicate that the Algol motor can have a thrust misalignment of 0.20 degrees, considering the effects of motor center of gravity offset, nozzle misalignment, case bending and gas flow misalignment. The thrust misalignment orientation is assumed to be random from motor to motor. Flight experience has shown that the Scout second stage (Castor motor) has a consistent pitch-up thrust misalignment of about 0.10 degree. This is readily obtained from flight data since it is the only significant disturbing energy source on the second stage. It is possible that the Algol motor may exhibit the same characteristic thrust misalignment and cause a portion of

the first stage residual moments, since a consistent pitch-up moment is calculated early in flight and toward burnout of the motor.

3.4.1.2 The equivalent thrust misalignment calculated from the residual moment is assumed to act at the longitudinal nozzle throat location (X_T), that is:

$$\epsilon_T = \frac{\Delta M}{T(X_T - X_{CG})} \qquad (13)$$

The effective pitch thrust misalignment was calculated for 15 vehicles from the residual moments. Ten vehicles were used for calculation of equivalent yaw thrust misalignment. A least squares polynomial curve fitting method was used to determine a best estimate average time history of both the pitch and yaw thrust misalignment. Several orders of polynomials were generated; the constant value and the 4th order which provide the best fit are shown in Figure 3.4.1-1. The calculated average value in pitch may have some meaning considering the Castor motor pitch-up thrust misalignment bias.

3.4.1.3 A number of conditions exist on the Scout vehicle that introduce disturbing moments that are similar for every flight. These moments were calculated for the S-131 vehicle and include thrust misalignment due to center of gravity offset and vehicle bending, and jet damping.

The Scout vehicle has built in mass asymmetry due to wiring tunnels, antennaes, launch fittings, etc. This asymmetry causes the first stage center of gravity to shift toward the tower side of the vehicle. The effective thrust misalignment caused by this asymmetry varies from 0.011 degrees at ignition to 0.0165 degrees at burnout. The moment produced by this center of gravity location is presented in Figure 3.4.1-2. A maximum pitch-up moment of 840 ft.-lbs. occurs at web burnout (45 second flight time). The magnitude of the yaw thrust

FIGURE 3.4.1-1
EFFECTIVE THRUST MISALIGNMENT TIME HISTORIES
LEAST SQUARES POLYNOMIAL CURVE FIT OF FLIGHT DATA

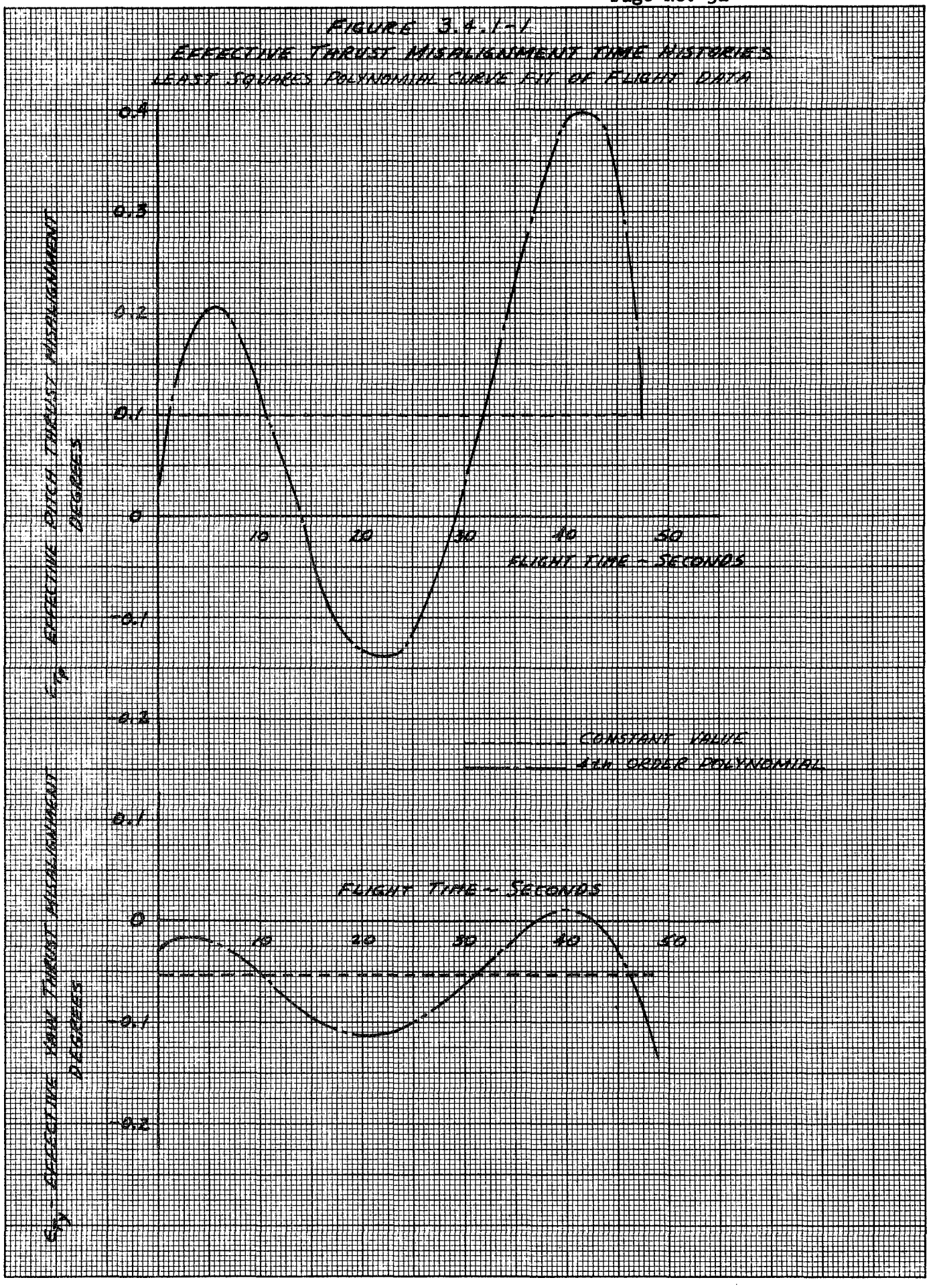

misalignment due to these asymmetries is about 5 per cent of the pitch contribution.

The thrust misalignment induced by aerodynamic loads and control forces acting on the structure were calculated for Vehicle S-131. The resulting pitch moment is presented in Figure 3.4.1-2. A maximum value of 1500 ft.-lbs nose-down occurs at 30 seconds flight time. The yaw thrust misalignment moment induced by the aerodynamic loads and control forces is presented in Figure 3.4.1-3 and reaches a maximum value of 7700 ft-lbs nose-left at 40 seconds flight time. The thrust misalignment due to vehicle flexibility can be significant.

The pitch jet damping moment was calculated for vehicle S-131 and the results are presented in Figure 3.4.1-2. The maximum occurred during the first pitch program where it reached 560 foot-pounds nose-up. The sum of the pitching moments mentioned above is also presented in Figure 3.4.1-2. This sum is relatively low when compared to the residual pitching moment.

3.4.1.4 A preliminary analysis was made of the Algol motor case bending due to horizontal storage. The motor was assumed to be a simply supported steel tube with a 0.1 inch wall thickness. The weight of the motor was assumed to be uniformly distributed over the length and the propellant was assumed to provide no restraining force to bending. The calculated case deflection is 0.14 inch midway between the two end supports and the angles at either end are approximately 0.073 degrees. Due to the storage position this deflection would always be in the pitch plane and the angle would be such that the thrust vector would cause a nose-up moment. However, unless the propellant influences the bending, the steel case should return to the unbent shape when the vehicle is raised to the vertical position on the launcher. Limited information on the Algol storage procedures indicates

FIGURE 3.2.1-2
MISCELLANEOUS KNOWN PERTURBATIONS
INDUCED BY THRUST VECTOR
VEHICLE 5-131

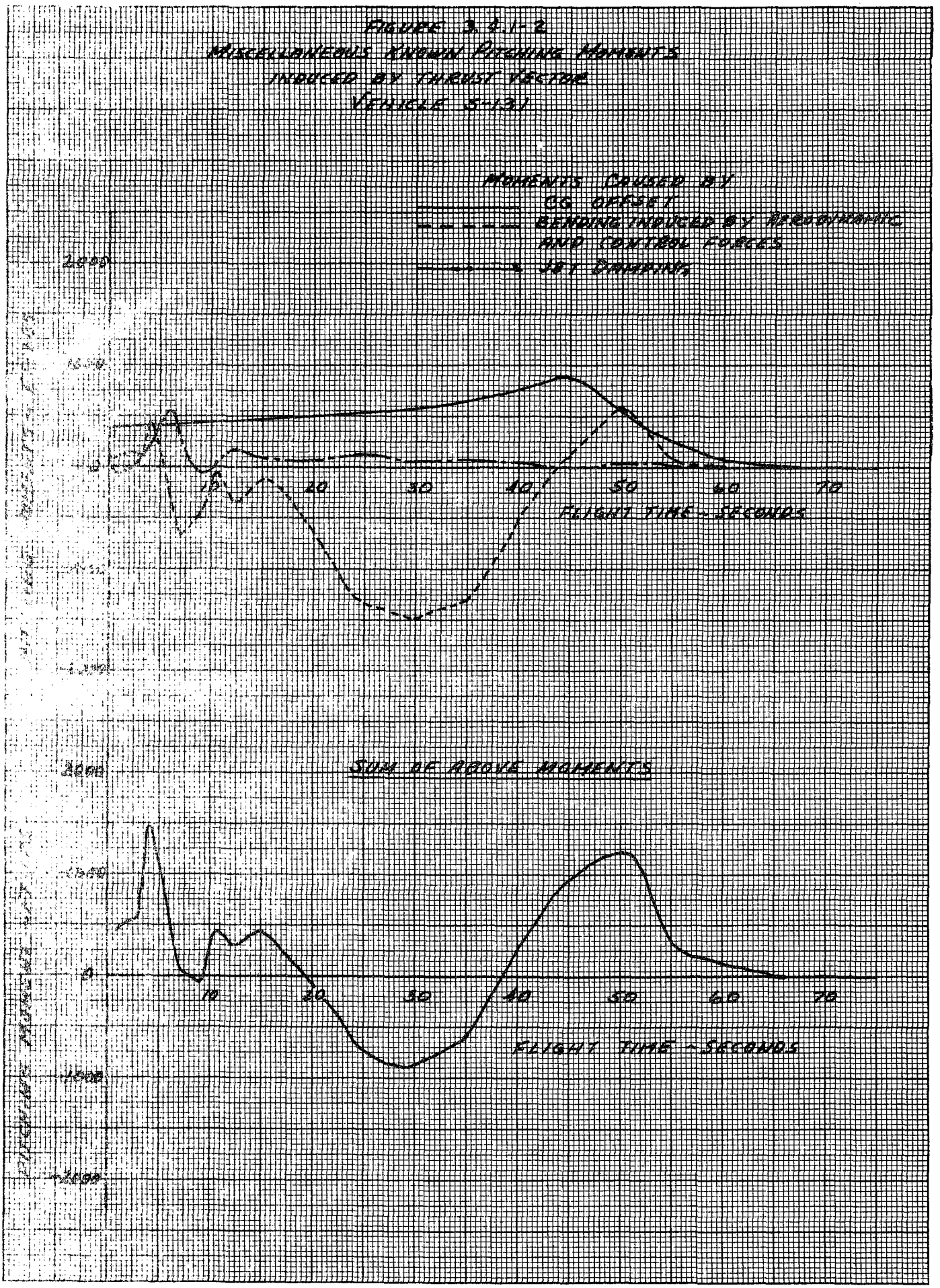

FIGURE 3.A.1-3
YAWING MOMENT DUE TO THRUST MISALIGNMENT
INDUCED BY AERODYNAMIC AND CONTROL RATES
VEHICLE S-13

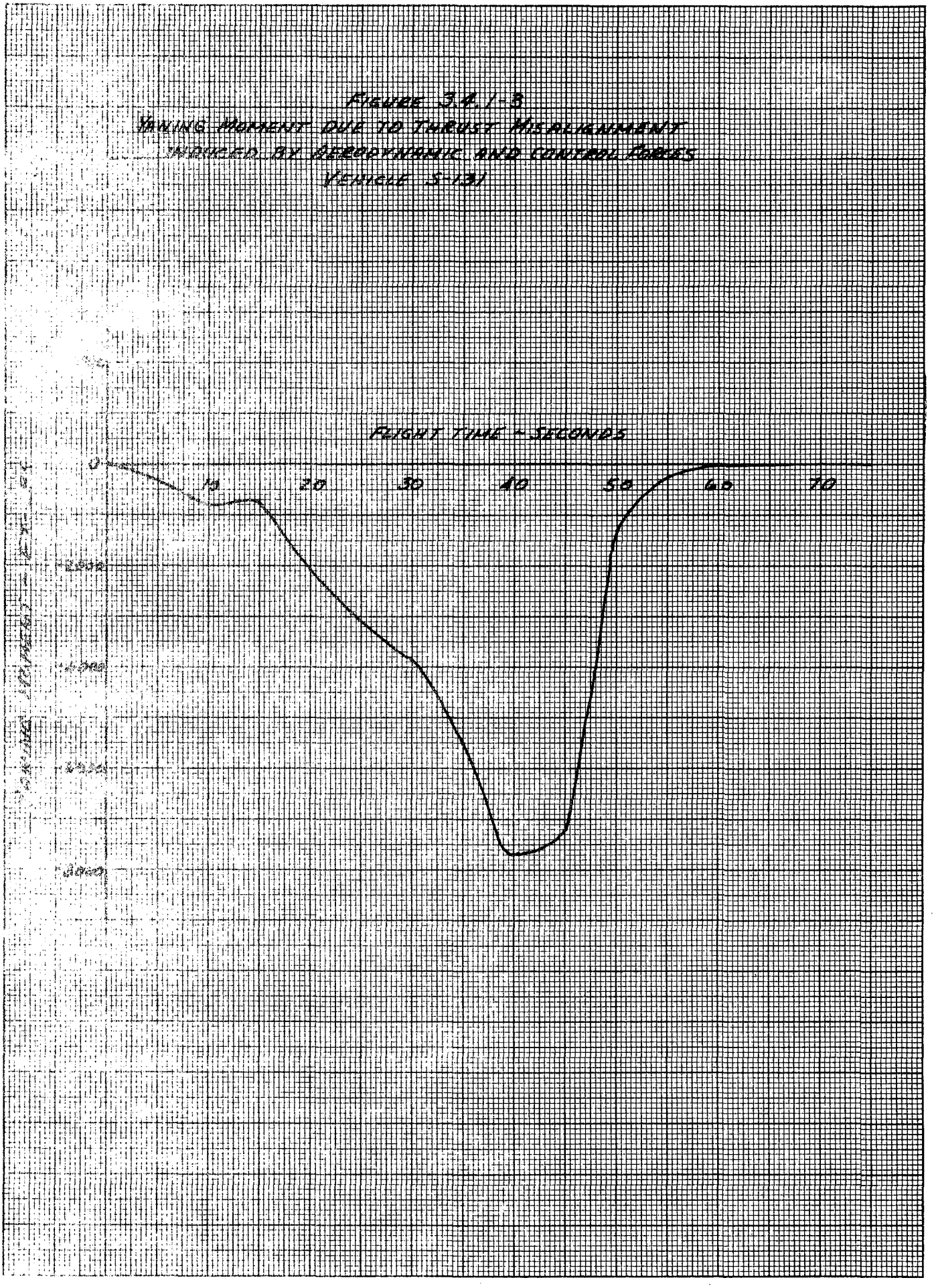

that both simple supports and full-length supports have been used. No significant amount of case bending should occur with a full-length support. In either case the thrust misalignment due to storage would be significantly lower than 0.073 degrees.

3.4.2 Jet Vane Effectiveness

3.4.2.1 As discussed in Section 3.3 the residual moment time history has exhibited a characteristic shape (Figure 3.3-1). During the first 10 to 15 seconds after lift off the residual moment varies directly with the response of the control deflections to the commanded pitch program. During this period it is assumed that the effect of deviations from the predicted aerodynamics are negligible because of the relatively low dynamic pressure and that the thrust misalignment does not vary coincidently with the control deflections. The residual moment can then be set equal to the difference between the predicted and the apparent jet vane control moment and the jet vane effectiveness determined;

$$\Delta M = (L_{\delta_{PRED}} - L_{\delta_{EFF}})(X_\delta - X_{CG})\delta \qquad (14)$$

$$L_{\delta_{EFF}} = L_{\delta_{PRED}} - \frac{\Delta M}{(X_\delta - X_{CG})\delta} \qquad (15)$$

The moment data was evaluated using the method of least squares, reference Paragraph 3.4.2.2, from which a jet vane effectiveness of about 23 lbs/degree was computed compared to the value of about 49 lbs/degree based on static test data (Reference 3) currently used for jet vane effectiveness.

Based on these preliminary analyses, the jet vane effectiveness determined from flight data (Paragraph 3.4.2.2) is about 40 to 60 per cent of the predicted. In order to determine the reasons for this difference, the jet vane effectiveness published in Reference 3 was reviewed. This review included the Algol IIA-3 test data which was used to derive the data presented in Addendum D of Reference 3 and the results of the more recent Algol IIB-31 test.

3.4.2.2 The jet vane effectiveness was evaluated utilizing the method of least squares for the period of flight from lift-off to 14 seconds flight time where deviations from predicted aerodynamic moments would have relatively little effect. In this evaluation the values of calculated jet vane effectiveness were weighted in favor of larger deflection angles to minimize scatter induced by small angle deflections. The results are shown in Figure 3.4.2-1 for both the pitch and yaw planes. The data, although scattered during the first few seconds where deflections are generally low, indicates a reduced jet vane effectiveness in both pitch and yaw and an increase in effectiveness with time. Jet vane lift of 20 to 30 pounds per degree deflection are indicated at those time points where deflections are unusually large. This represents a 40 to 60 percent reduction from the predicted values.

The jet vane effectiveness was also evaluated for the entire first 55 seconds of flight from the residual moment data. The resulting polynomial approximations shown in Figure 3.4.2-2 are compared with the predicted jet vane effectiveness from Addendum D to Reference 3. It is apparent that jet vane effectiveness is not the sole contributor to the unexplained pitching moment, in that negative effectiveness would be required during portions of the flight.

The current estimates of jet vane effectiveness are based on ground level motor firings and assume no variation in effectiveness with increasing altitude. The Algol nozzle flow is overexpanded at sea level, fully expanded at about 8000 feet, and underexpanded at higher altitudes. It is quite possible that these flow characteristics influence the jet vane effectiveness.

3.4.2.3 The static test firings for the Algol IIA-3 and IIB-31 motors were almost identical with regard to measurements and data reduction, but

FIGURE 3.4.2-1
JET VANE EFFECTIVENESS VERSUS TIME
FIRST FOURTEEN SECONDS OF FLIGHT
PITCH AND YAW

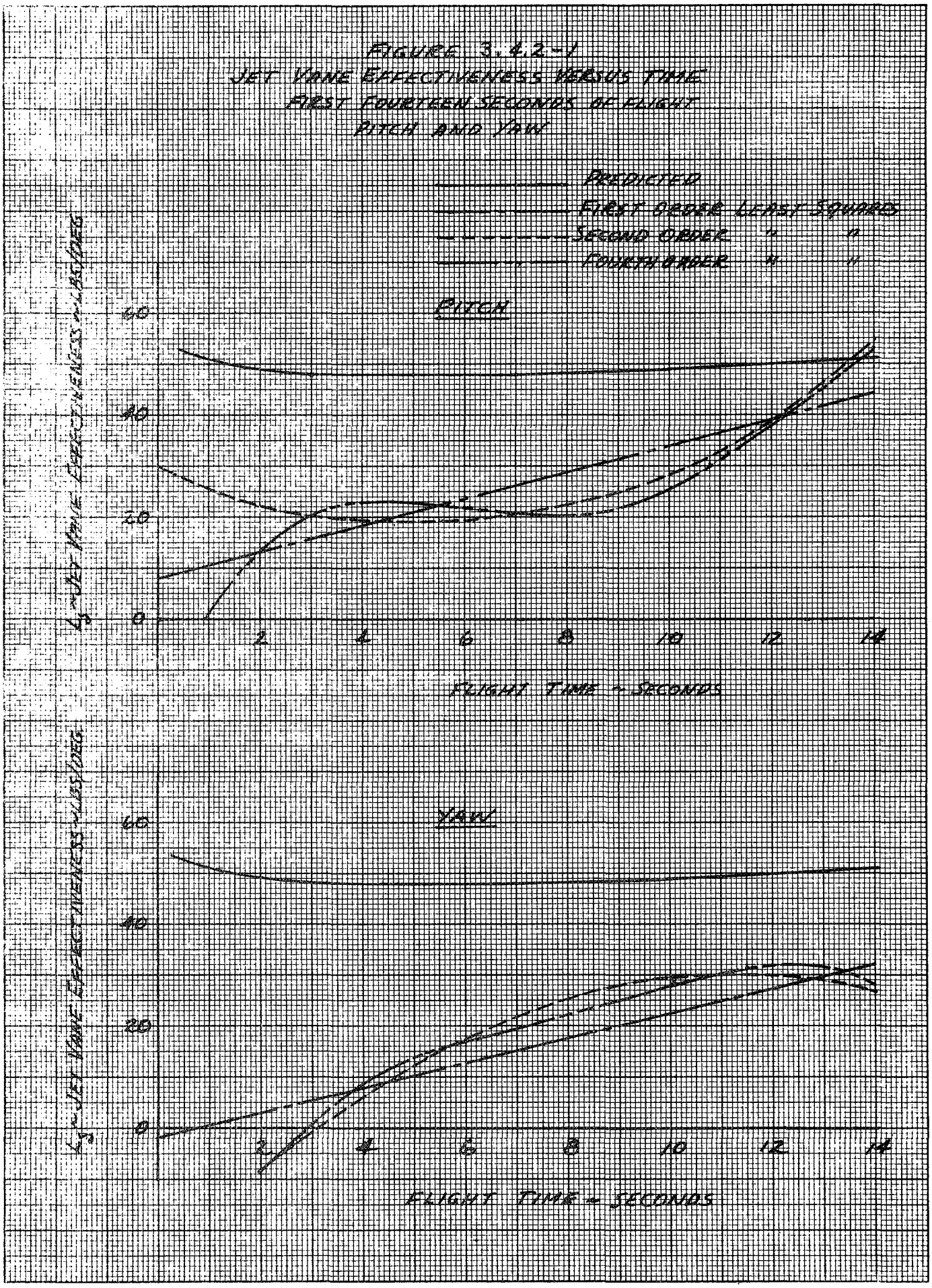

FIGURE 3.4.2-2
JET VANE EFFECTIVENESS VS. TIME
LEAST SQUARES POLYNOMIAL CURVE FIT
OF FLIGHT DATA

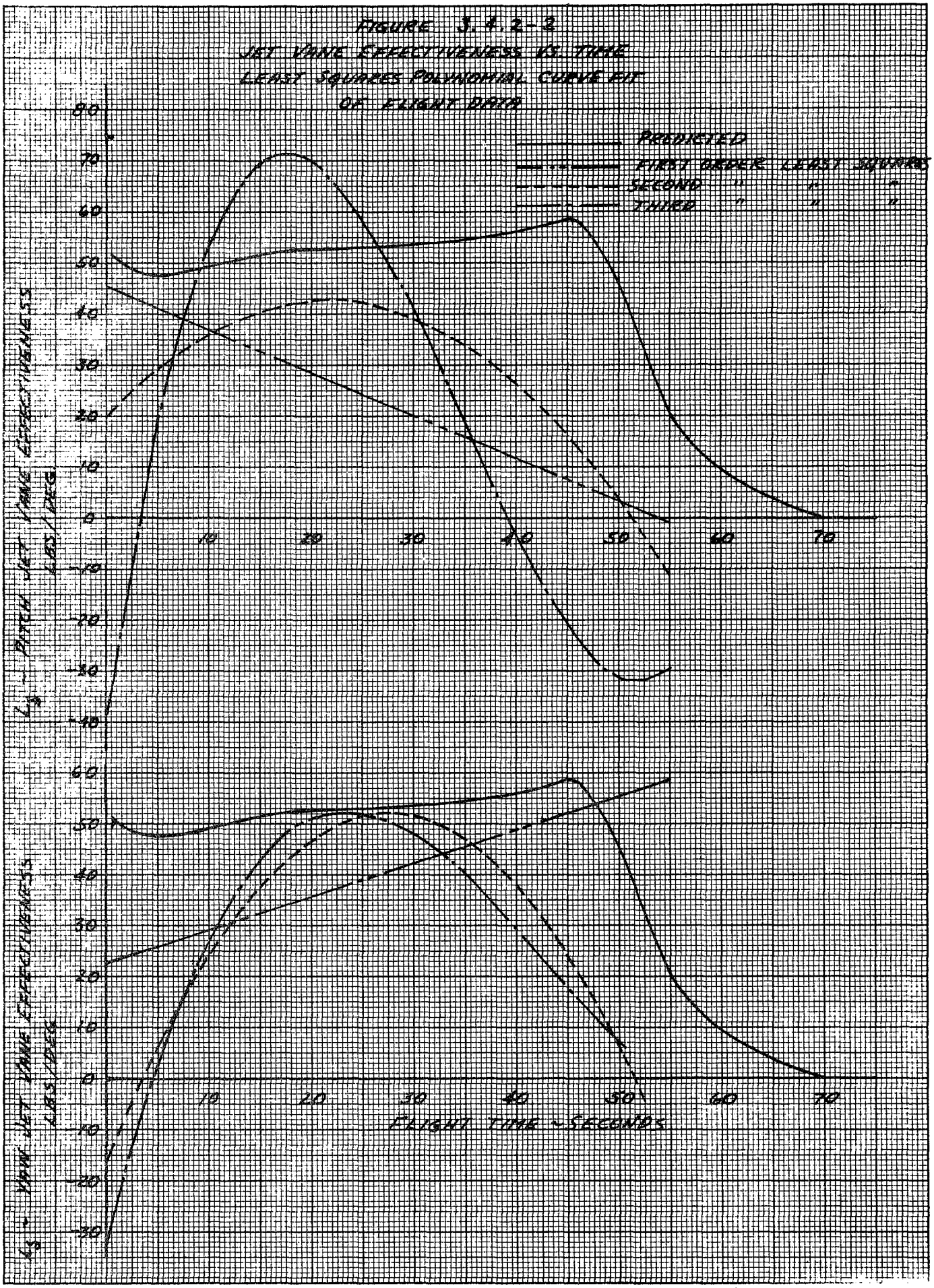

the IIB-31 motor was also instrumented for side force measurements.

A description of the tests is presented in References 7 and 9, a brief summation follows: two jet vanes were installed aft of the nozzle exit plane in the same relative position as on the Scout vehicle and located 180 degrees apart, top and bottom in the pitch plane. The vane shafts are mounted in six component balances which measure the forces normal to and along the vane axis and the hinge moment. The balances are mounted in a structure which attaches to the aft ring of the motor. For the IIB-31 test the motor was mounted in a multi-component test fixture and load cells were installed in the yaw plane between the motor and ground supports to measure the side forces on the motor. A sketch of the measured forces used to resolve the vane lift, drag, and side force loads is shown in Figure 3.4.2-3.

The data from the IIB-31 test has not been utilized to date in the vane effectiveness predictions so it was analyzed during this study to compare with the earlier test data. The test plan and test results are documented in References 8 and 9 respectively, however, pertinent figures and data are included in this report.

The jet vane deflection history shown on Figure 3.4.2-4 was designed for the test to simulate a flight condition control deflection time history. The test data which represents the computed jet vane lift during the static firing is also shown on Figure 3.4.2-4. The lift curve for jet vane #3 did not start out from zero but had about a -40 lb. bias. At 38 seconds where the measured deflections went to zero for approximately 3.0 seconds, the corresponding calculated lift on both vanes #1 and #3 decreased to a value of about -60 pounds. At 60 seconds after ignition the vane deflection program was accidentally shorted out and both the measured deflections and the calculated lift ended at zero. In this analysis a zero

FIGURE 3.4.2-3

STATIC TEST INSTRUMENTATION SUMMARY
ALGOL IIA-3 & IIB-31

STING BALANCE

-3 AND -31

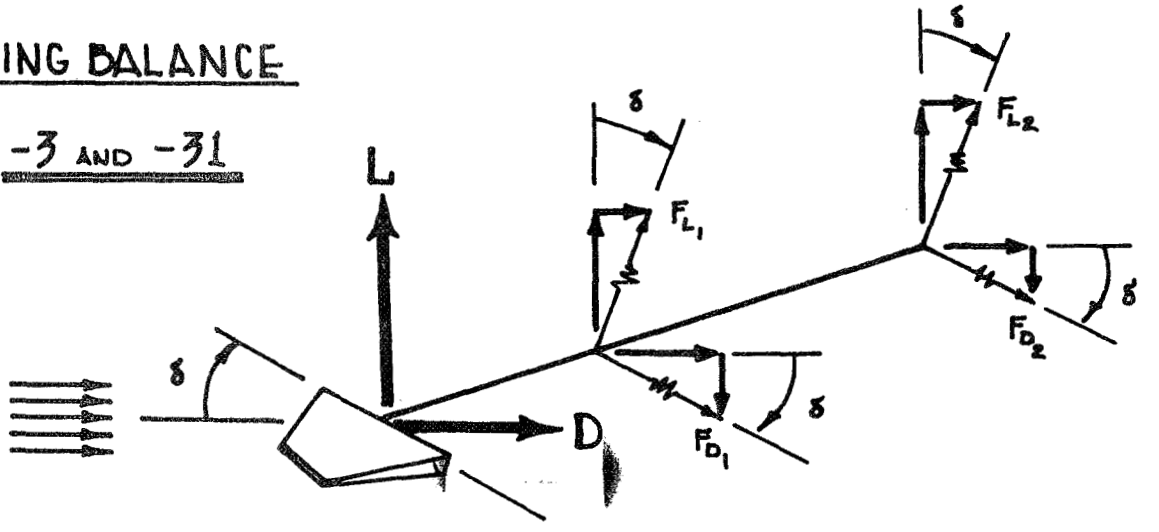

SIDE FORCE

-31 ONLY

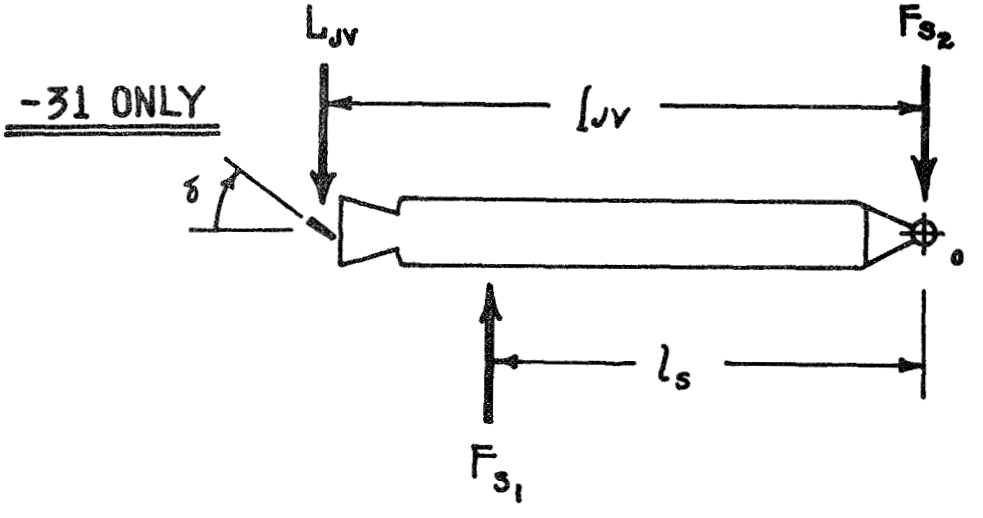

$$\sum M_o = 0 = L_{JV}\, l_{JV} - F_{S_1}\, l_S \quad ; \quad L_{JV} = \frac{F_{S_1}\, l_S}{l_{JV}}$$

FIGURE 3.4.2-4

ALGOL II B-31 TEST RESULTS

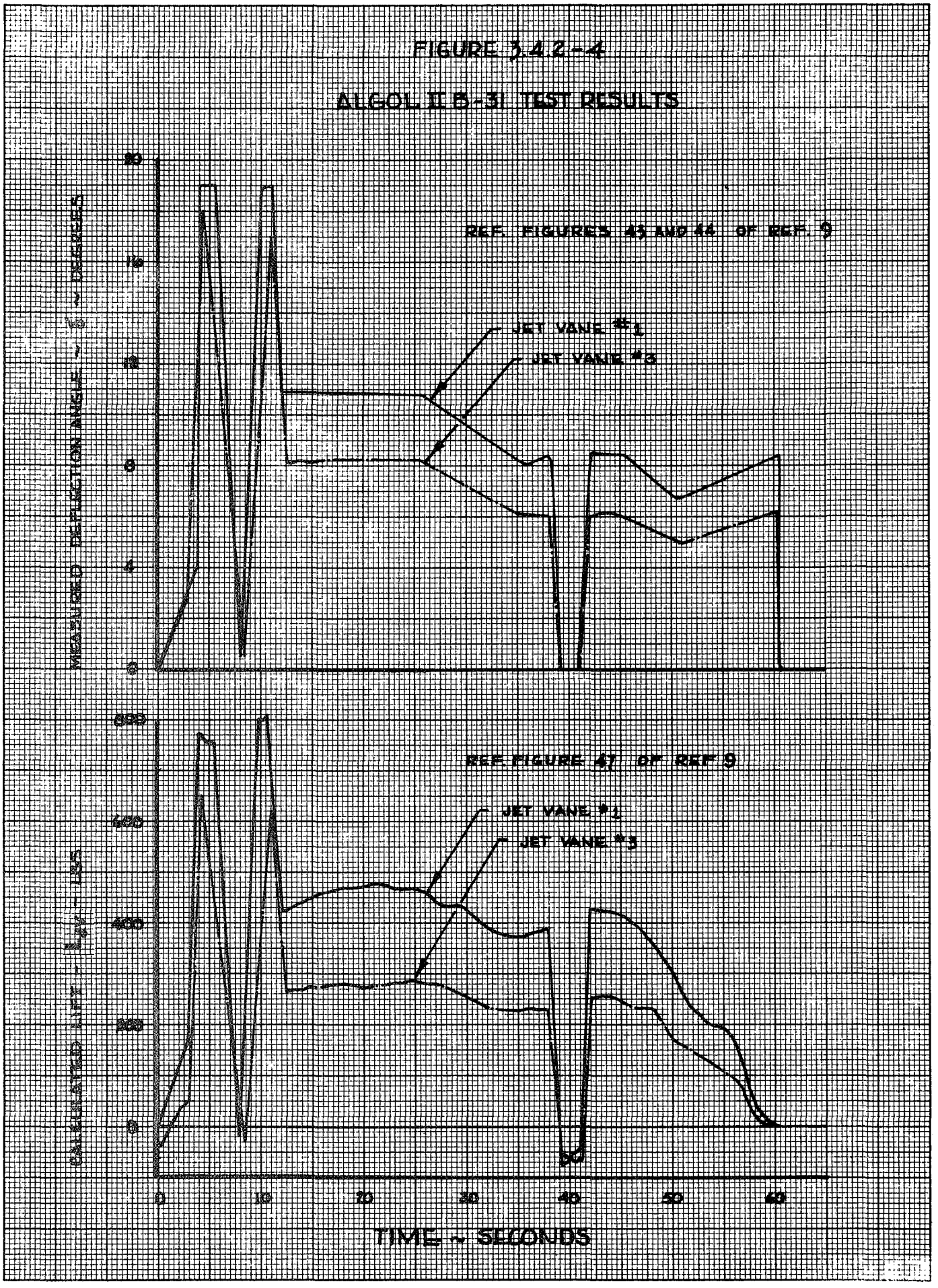

shift was assumed and the lift data includes a +50 pound correction to the calculated lift values presented in Figure 3.4.2-4.

The jet vane effectiveness computed from the IIB-31 test is shown on Figure 3.4.2-5 for comparison with the IIA-3 data in terms of lift per degree deflection, and also lift per degree deflection per pound of vacuum thrust (L_δ/Tvac). The L_δ/Tvac is assumed constant during boost.

The measured side loads from the IIB-31 motor test were used to check jet vane effectiveness independently of sting balance data. This was accomplished by summing moments about the forward thrust pivot (Figure 3.4.2-3) such that:

$$F_{J.V.} = \frac{F_S \ell_S}{\ell_{J.V.}} \qquad (16)$$

$$L_\delta = \frac{F_{J.V.}}{\delta} \qquad (17)$$

$$\frac{L_\delta}{T_{VAC}} = \frac{F_{J.V.}}{\delta T_{VAC}} \qquad (18)$$

The jet vane effectiveness calculated according to equations (16)through (18) are shown on Figure 3.4.2-5 for comparison with the computed lift data from the IIA-3 and IIB-31 vane sting balance measurements.

The vane effectiveness determined form the IIB-31 computed sting balance lift data is about 10 to 20 percent lower than that based on the IIA-3 test data. The vane effectiveness determined from the IIB-31 measured side force data, however, is about one-half of that based on the computed sting balance lift data and correlates closely with the vane effectiveness calculated from flight data(Figure 3.4.2-1).

3.4.2.4 Based on the indications of reduced jet vane effectiveness from side force measurement data of the IIB-31 tests and the least squares evaluation from flight calculated residual moments, a jet vane effectiveness value(L_δ/Tvac) of 0.00024 per degree was assumed for re-evaluation of

FIGURE 3.4.2-5

JET VANE EFFECTIVENESS SUMMARY

BASED ON TEST DATA

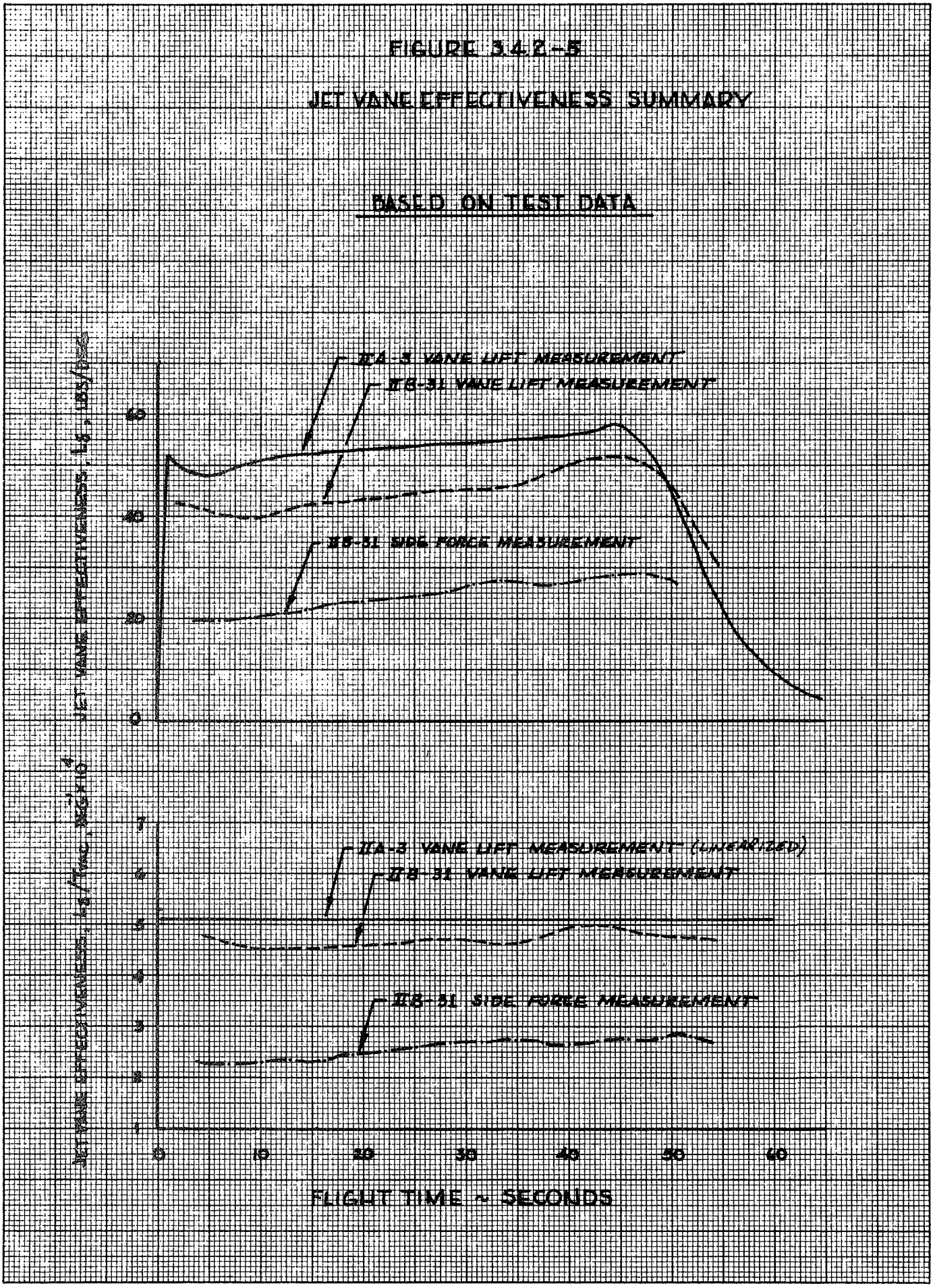

the residual moment. The residual moments for the S-131 vehicle based on jet vane effectiveness (L_j/T_{vac}) of 0.00051 per degree and 0.00024 per degree are shown on Figure 3.4.2-6.

The reduced jet vane effectiveness reduces the residual moment fluctuations during the first ten seconds. After about 10 seconds flight time the residual moment based on the lower jet vane effectiveness increases negatively by a near constant increment. This increases the magnitude of the residual moment in the transonic region and reduces it in the supersonic region. If jet vane effectiveness alone were considered in attempting to eliminate the residual moment the resultant effectiveness as shown in Figure 3.4.2-2 would have to fluctuate considerably with flight time. The other potential error sources must be considered in conjunction with jet vane effectiveness to eliminate the residual moments.

3.4.2.5 The reports on the Algol IIA-3 and IIB-31 test firings (References 7 and 9) were reviewed in an attempt to explain the apparent difference between the predicted jet vane effectiveness based on test results and that experienced in flight. A review of the sting balance measurement system and data reduction procedure revealed an apparent error in the method of determining the total lift on the jet vanes. A more detailed evaluation of these data is recommended subsequent to this study to re-evaluate the results.

3.4.3 Aerodynamic Characteristics

The aerodynamic moments acting on the Scout vehicle during first stage flight are calculated based on the predicted aerodynamic characteristics as presented in Reference 3, radar observation of the trajectory, meteorological data and telemetered attitude errors. The calculated angles of attack and sideslip are subject to error resulting from measurement and data reduction

FIGURE 3.4.2-6

EFFECT OF REDUCED JET VANE EFFECTIVENESS ON RESIDUAL MOMENTS - SCOUT VEHICLE S-131

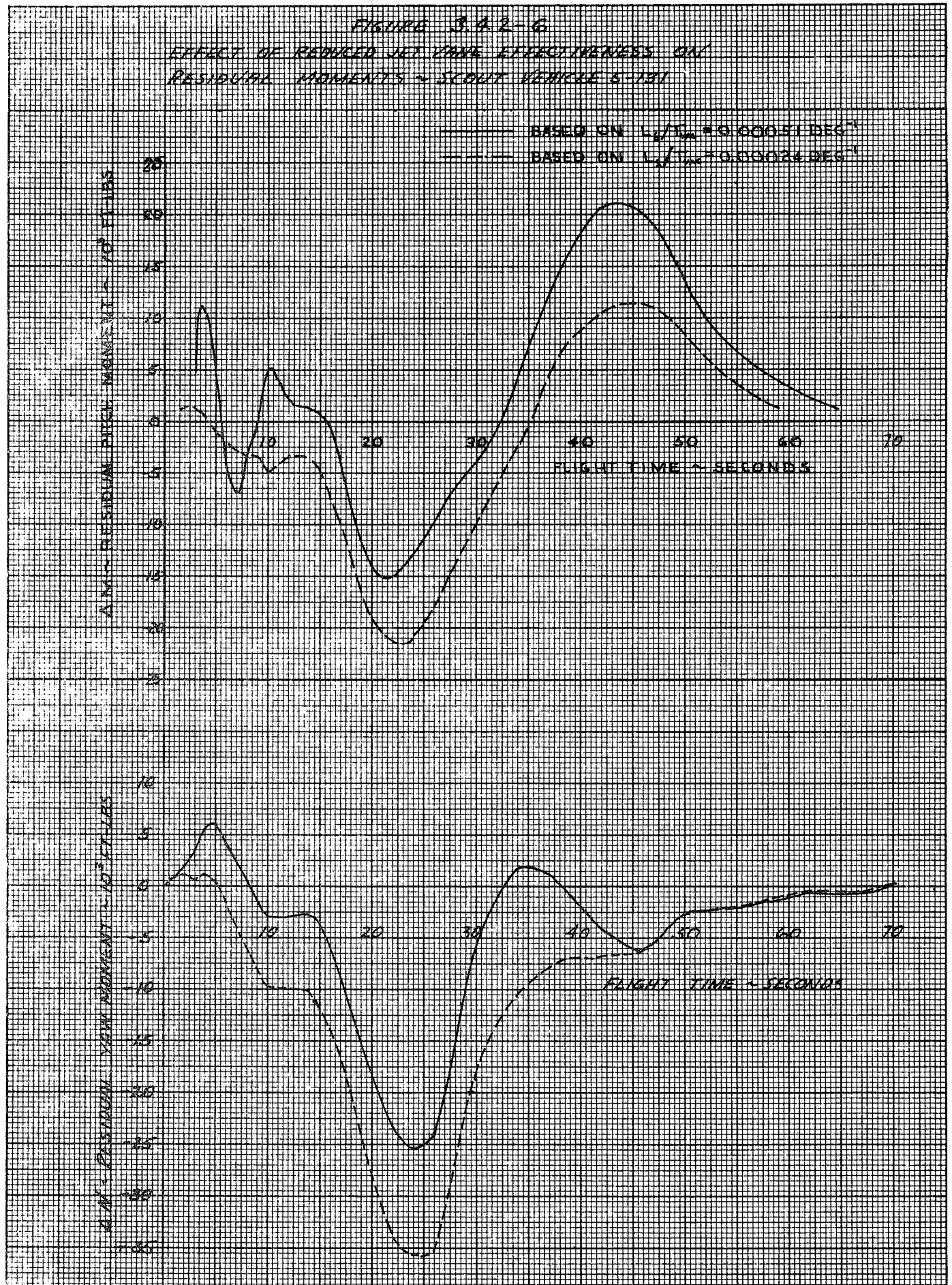

inaccuracies. A considerable error in the calculated angle of attack can occur since wind information may be obtained several hours before or after launch time. On any particular flight an error of this type would result in a residual moment, but errors of this type are assumed to be random when considering many flights. Deviations in the predicted aerodynamic coefficients would consistently cause residual moments. The method of least squares was used in an attempt to determine these deviations.

3.4.3.1 Moment Coefficients

The residual moments in pitch and yaw were transformed to an incremental change in aerodynamic pitching and yawing moment coefficients for Mach numbers of 1, 2 and 3, using the following equations:

$$\Delta C_{m_{\alpha}} = \frac{\Delta M}{qSd} \tag{19}$$

$$\Delta C_{n_{\alpha}} = \frac{\Delta N}{qSd} \tag{20}$$

The resulting incremental moment coefficients were correlated with the calculated angles of attack and angle of sideslip by the method of least squares. Data from 14 flights were used to calculate pitching moment coefficient and 9 flights were used to calculate yawing moment coefficient. The incremental coefficients were added to the predicted values and are shown in Figure 3.4.3-1 for pitch and yaw. The pitch and yaw stability margins appear to be significantly less than predicted at Mach 1.0. The correlation between pitch and yaw stability at this Mach number is quite close. The larger than predicted pitching moment coefficient at zero angle of attack supersonically (C_{m_0}) may be the result of not accounting for either a possible reduced jet vane effectiveness or a consistent pitch-up thrust misalignment. Some error in the predicted C_{m_0} might be expected since it was determined from limited wind tunnel data for a simulated 20 inch diameter

FIGURE 3.4.3-1
PITCHING AND YAWING MOMENT COEFFICIENT VERSUS ANGLE OF ATTACK AND ANGLE OF SIDESLIP

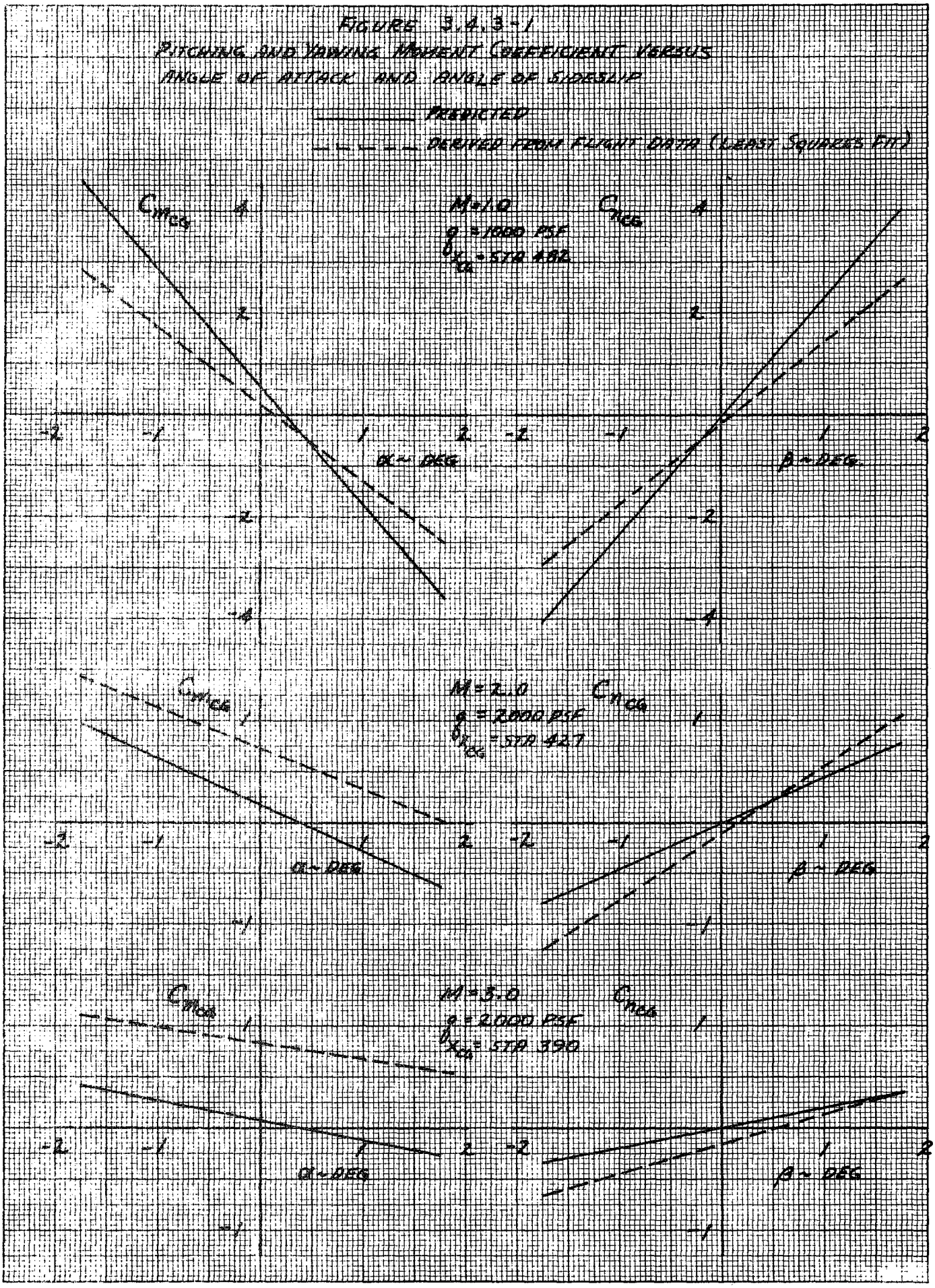

heatshield Scout configuration. (Ref. 12 and 13)

The most significant result is the effectively reduced stability at transonic speed. This may be partially caused by the rocket exhaust plume interaction with the boundary layer. Several studies have been performed by the NASA which indicate that an expanding exhaust plume from an underexpanded rocket nozzle can induce flow separation in the boundary layer flow ahead of the plume at supersonic speeds. References 10 and 11 indicate that a finned body may have a reduced stability as a result of the rocket exhaust plume. The effect of the rocket exhaust plume on the aerodynamic stability derivatives has not been considered on the Scout. A wind tunnel test simulating the rocket exhaust plume would be necessary to accurately predict such an effect on stability.

The pitching moment coefficient at zero angle of attack (C_{mo}) due to protuberances was derived from wind tunnel tests of a model simulating a 20-inch diameter heatshield configuration. Rigid body aerodynamic data for the present configuration without protuberances has been determined from wind tunnel tests for the Mach number range from 0.6 to 1.0. This is the region in which the aerodynamic stability is apparently significantly less than predicted. There is no wind tunnel data for the present 34 inch diameter heatshield configuration with protuberances. The predicted aerodynamic stability derivatives do not include the reduction in stability which occurs at simultaneous angles of attack and sideslip as indicated by the wind tunnel test reported in Reference 12. Data of this type is not available for the present configuration. It is possible that one or more of the above mentioned error sources may be creating the large residual moment experienced in the transonic region.

3.4.3.2 Center of Pressure Versus Mach Number

The effective center of pressure in pitch and yaw for Mach numbers above 0.5 were calculated for several vehicles from the residual moment by the following equations:

$$X_{CP_{EFF_P}} = X_{CP_{PRED}} - \frac{\Delta M}{C_{M_\alpha} q S \alpha} \tag{21}$$

$$X_{CP_{EFF_Y}} = X_{CP_{PRED}} - \frac{\Delta N}{C_{Y_\beta} q S \beta} \tag{22}$$

No reduction in jet vane effectiveness was considered in these calculations. Least squares polynomial approximations of these data were made in the same manner as the jet vane data was analyzed. A weighting function proportional to the calculated angle of attack and angle of sideslip was used to reduce the spread of the effective center of pressure resulting from errors in these angles. The resulting polynomial approximations of pitch and yaw center of pressure are compared with the predicted values in Figure 3.4.3-2. The effective center of pressure in pitch deviates significantly from the predicted value. The effective yaw center of pressure deviated form the predicted values but follows the general forward movement with increasing Mach number. Since the yaw values are in better agreement with predictions than the pitch values there is reason to suspect some other form of pitching moment which is not a strong function of angle of attack. This could be either thrust misalignment or an increaseed pitching moment at zero angle of attack as discussed in Paragraph 3.4.3.1.

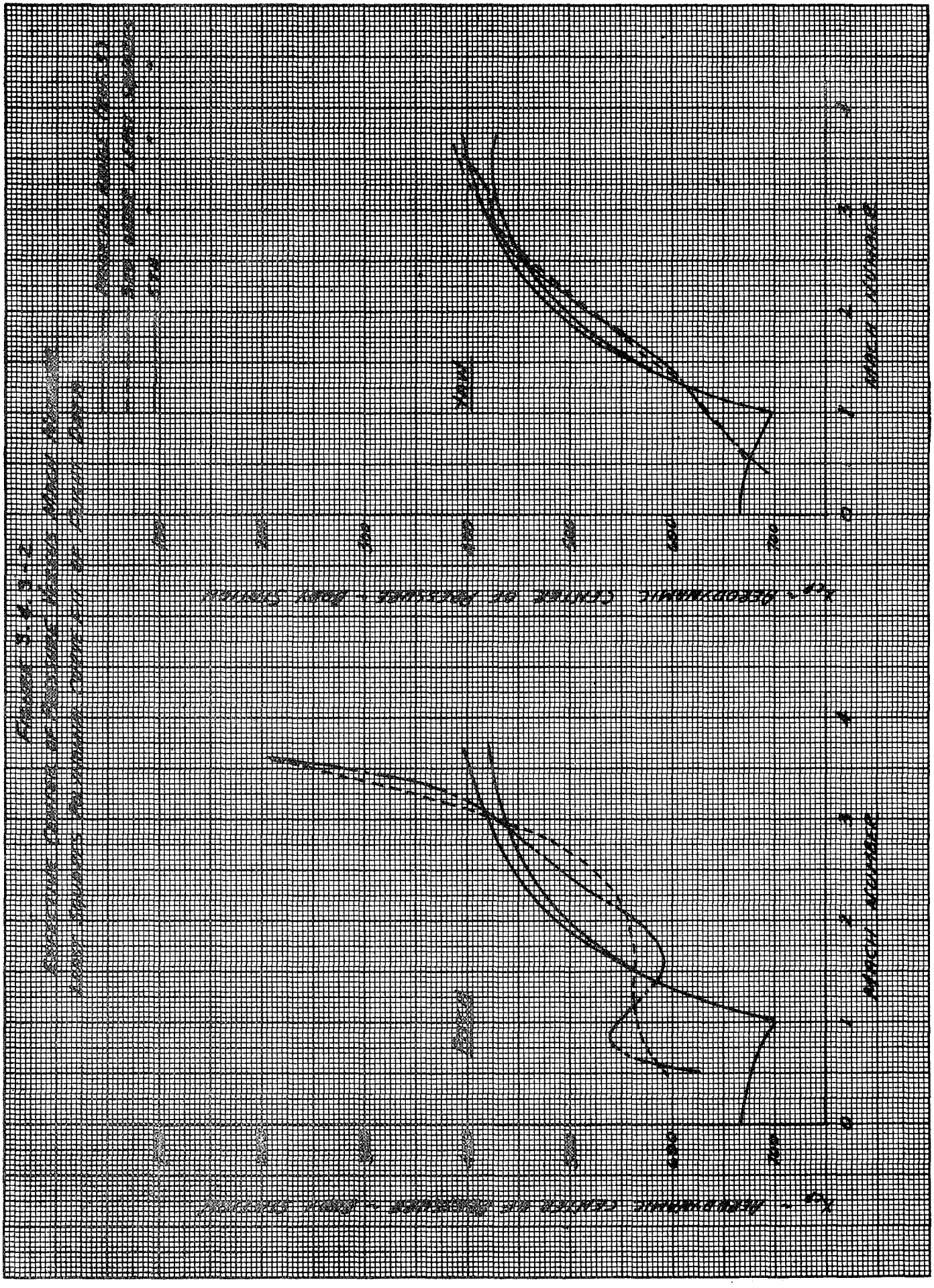

3.4.4 Vehicle Assembly Tolerance Investigation

Vehicle assembly tolerances are a potential contributing factor to the control deflections experienced during boost. If the vehicle has a permanent deflected shape it will influence the aerodynamic trim requirements as well as inducing a thrust misalignment moment.

The manufacturing tolerances considered in this analysis are established by Reference 14 and the rocket motor manufacturers' drawings and are defined in terms of parallelism, perpendicularity, and concentricity of adjacent vehicle sections. Figure 3.4.4-1 shows how the tolerance build-up affects the center of gravity and local angle of attack. These were combined in a random manner (root-sum-square, RSS) to define an induced thrust misalignment. This assumes that each section is built at its maximum tolerance, but that the tolerance build-up on adjacent sections is random and not accumulative.

The booster thrust contribution to the pitching moment due to accumulated tolerances from the Algol nozzle to the vehicle center of gravity is given by:

$$M_T = T \bar{\gamma}_i \tag{23}$$

where,

$$\bar{\gamma}_i = \left[\bar{\gamma}^2_{\odot_{BASE\,A'}} + \bar{\gamma}^2_{\odot_{ALGOL}} \cdots + \bar{\gamma}^2_{\parallel_{BASE\,A'}} + \bar{\gamma}^2_{\parallel_{ALGOL}} \cdots + \bar{\gamma}^2_{\perp_{BASE\,A'}} + \bar{\gamma}^2_{\perp_{ALGOL}} + \cdots \right]^{1/2} \tag{24}$$

The aerodynamic pitching moment due to the accumulated tolerances over the length of the vehicle is given by:

$$M_\alpha = \Sigma C_{N\alpha_i} \alpha_i S q \, (X_{cg} - X_{cp_i}) \tag{25}$$

FIGURE 3.4.4-1
DEFINITION OF TOLERANCE BUILD-UP

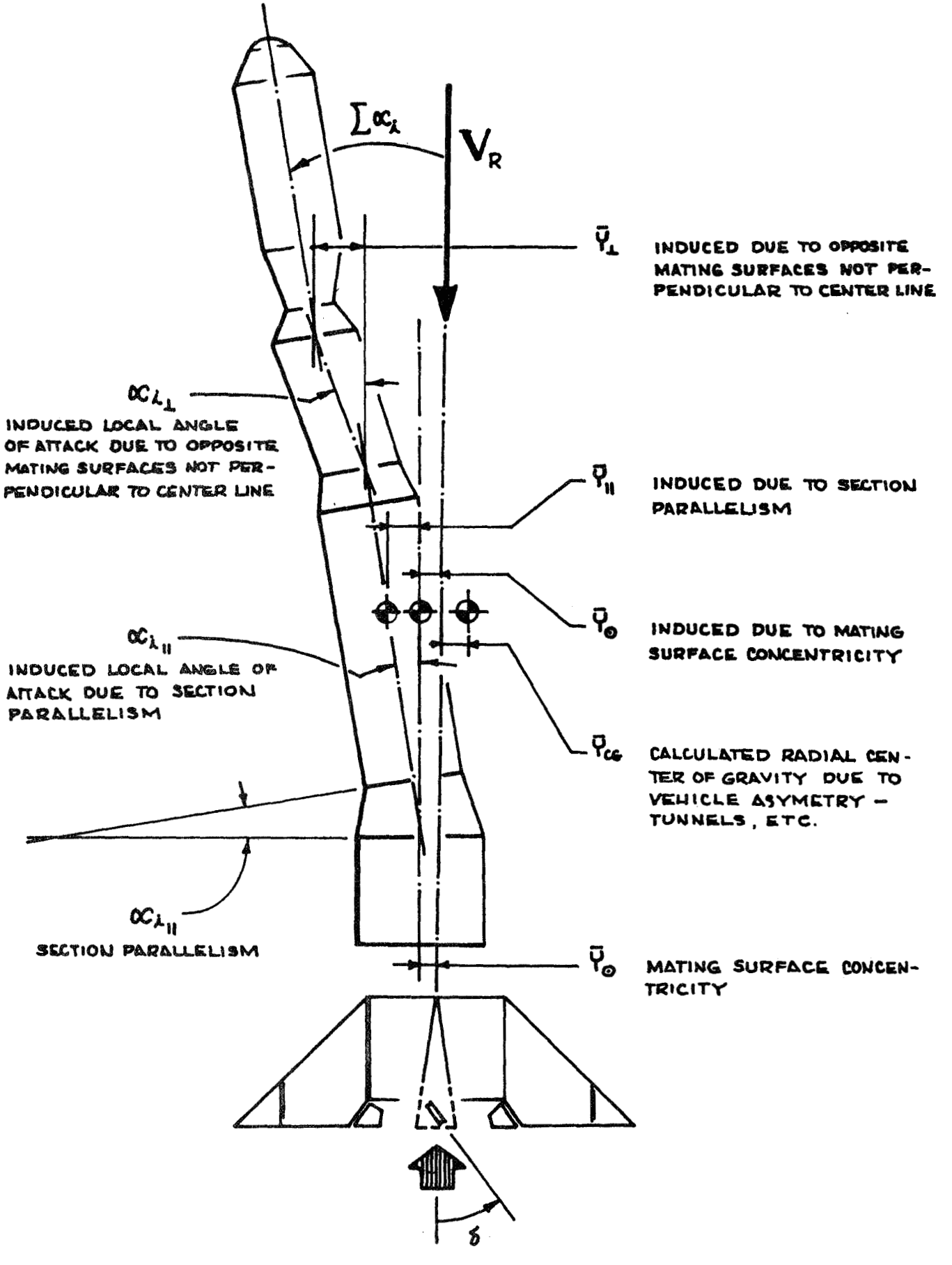

where $C_{N_{\alpha_i}}$ is the lift coefficient of the local section, i.e. heatshield, 2nd and 3rd stage cylinder, etc.; x_i is the RSS of the angular tolerances between the center of gravity and the local section; and X_{cpi} is the center of pressure of the local section.

The summation of moments for this analysis were calculated based on the conditions of flight for the S-131 vehicle at the time of maximum dynamic pressure (t = 43 seconds). The resulting moments, assuming that the vehicle shape is deflected nose up, are about 4000 ft.-lbs. of aerodynamic moment and 1670 ft.-lbs. of induced thrust misalignment moment. The total pitch-up moment including about 840 ft.-lbs. due to built in vehicle asymmetry is about 6510 ft.-lbs. The calculated residual moment for the S-131 vehicle at this time is 21,000 ft.-lbs. nose-up. Although the moments defined here constitute a sizable percentage of the residual moment, it has to be assumed that the vehicle is always assembled with some nose-up deflected shape in order to help explain the consistent nose-up residual moment experienced on all flights at supersonic velocities. In the transonic region this pitch-up moment would be contrary to the residual pitch-down moment usually experienced in flight. It is, however, recommended that the vehicle tooling and assembly fixtures and alignment measurements be checked to determine if a consistent body deflection is being built in.

3.4.5 Center of Pressure and Thrust Misalignment as a Function of Jet Vane Effectiveness

3.4.5.1 As discussed in paragraph 3.4.2, consideration has been given to the effects of a change in the jet vane effectiveness on the residual moment. In addition, calculations have been made to determine the differences in the apparent center of pressure and thrust misalignment that result from assuming a jet vane effectiveness reduced from the predicted value of

0.0051 per degree (L_j/T_{vac}) to the flight determined value of 0.00024 per degree. The center of pressure was computed based on equations (21) and (22) and the thrust misalignment on equation (13).

The results of these center of pressure computations are presented in Figures 3.4.5-1 and 3.4.5-2. Also presented are the predicted center of pressure and the center of gravity. This evaluation is based simply on revising the predicted C.P. to give aerodynamic moments which eliminate the residual moment for the S-131 vehicle (reference equation 1), whereas the effective center of pressure evaluation presented in paragraph 3.4.3.2 is based on a least squares procedure to determine the average C.P. time history from a number of flights.

The center of pressure history based on a jet vane effectiveness of 0.00051 per degree shows an apparent reduction in static margin transonically and an apparent increase in pitch static margin supersonically but with considerable fluctuation in this range. This randomness of the center of pressure as a function of time is due in part to the small angle of attack (see Figure 3.3-3) which then requires large changes in C.P. to significantly influence the moments. The effective C.P. location during the transonic phase of the flight is based on wind tunnel test data but neglects any possible destabilizing effect due to exhaust plume or reduced stability due to combined angles of attack and sideslip. It is not likely that the aerodynamic characteristics in flight vary this much from the predicted data so this could indicate an increase in jet vane effectiveness with increasing altitude at least through this region.

Similar presentations for vehicles S-133, 137, and 142 are presented in Appendix C.

FIGURE 3.4.5-1

PITCH CENTER OF PRESSURE HISTORY
AS A FUNCTION OF CONTROL EFFECTIVENESS
VEHICLE S-131

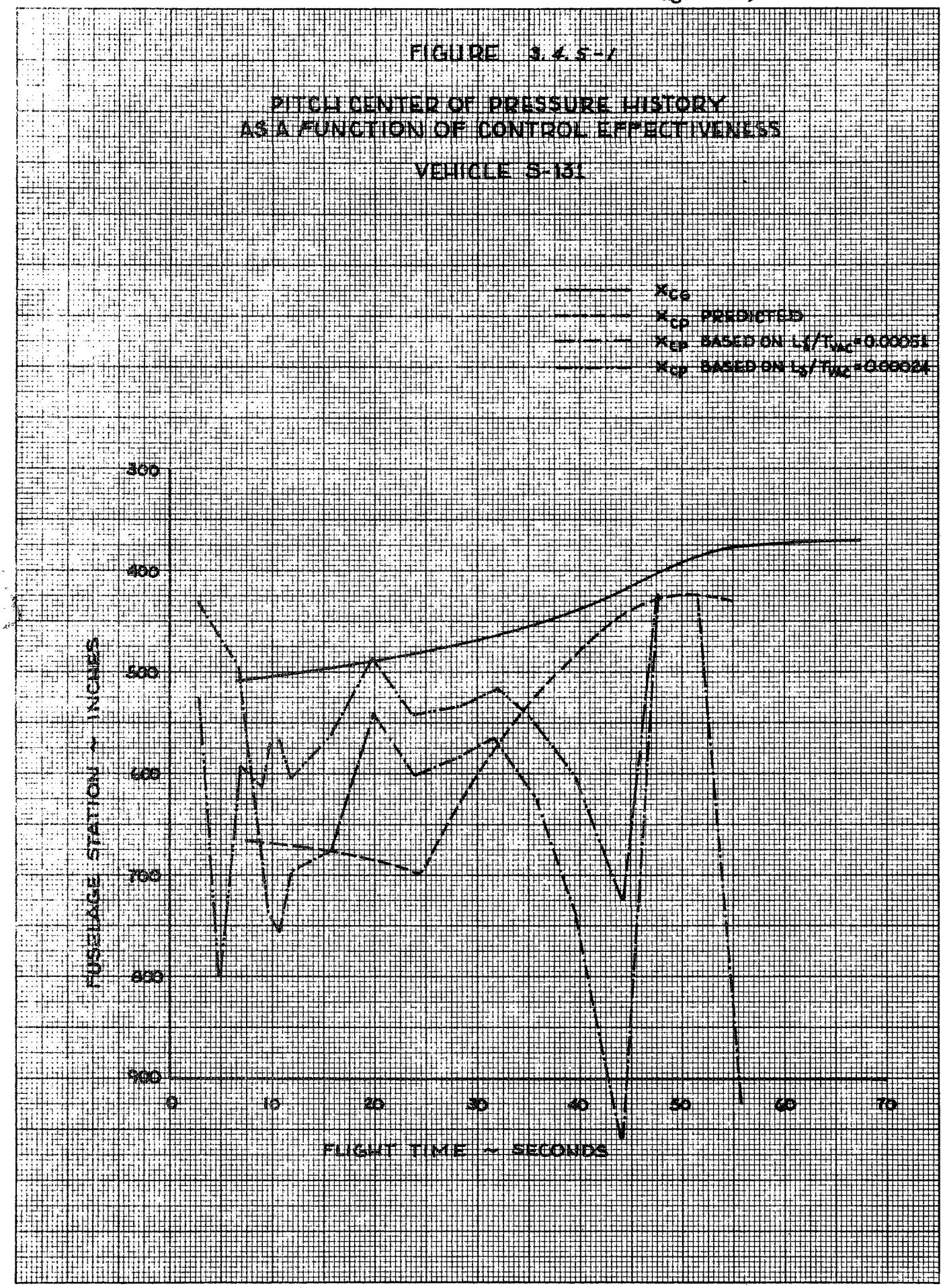

FIGURE 3.4.5-2

YAW CENTER OF PRESSURE HISTORY
AS A FUNCTION OF CONTROL EFFECTIVENESS

VEHICLE S-131

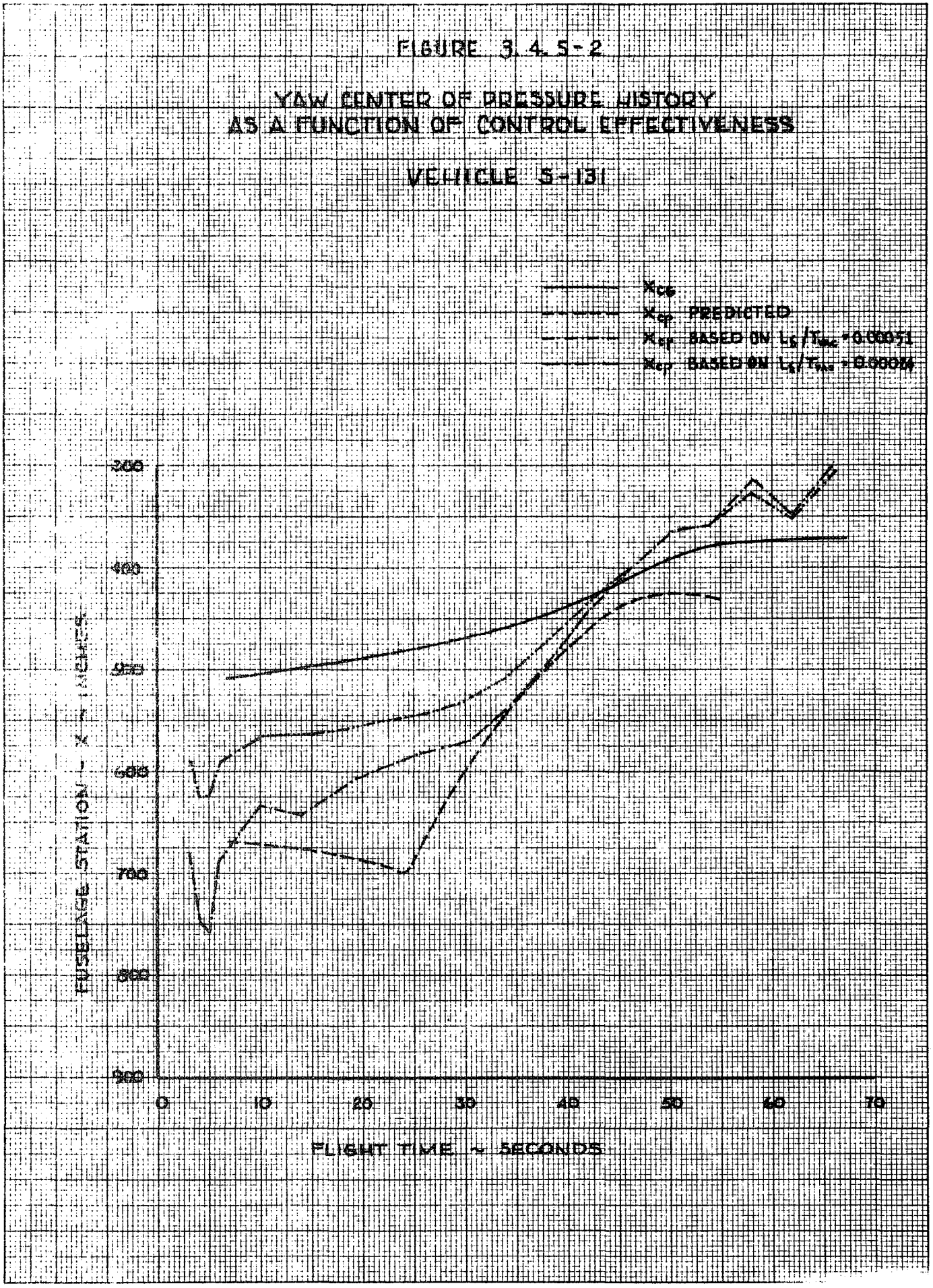

3.4.5.2 The evaluation of the apparent thrust misalignment was carried out in the same way as the center of pressure analysis. The thrust misalignment history for the S-131 vehicle is presented in Figures 3.4.5-3 and 3.4.5-4.

As would be expected, the thrust misalignment time history exhibits the same characteristic shape as the residual moment due to the relatively small variations in thrust level and center of gravity location. Substitution of the reduced jet vane effectiveness of 0.00024 per degree reduces the apparent pitch plane thrust misalignment subsonically, increases it transonically, and again reduces it supersonically as shown in Figure 3.4.5-3. The transonic increase in nose-down thrust misalignment is not consistent with the apparent nose-up bias indicated by the method of least squares analysis discussed in paragraph 3.4.1. This may indicate again an increase in jet vane effectiveness in this region coupled with a reduced aerodynamic static margin. Similar presentations for vehicle S-133, 137, and 142 are included in Appendix C.

It appears that the most promising procedure for determining individual contributions when a number of uncertainties exist lies in the least squares method defined in Appendix A.

FIGURE 3.4.5-3

PITCH THRUST MISALIGNMENT HISTORY
AS A FUNCTION OF CONTROL EFFECTIVENESS

VEHICLE S-13L

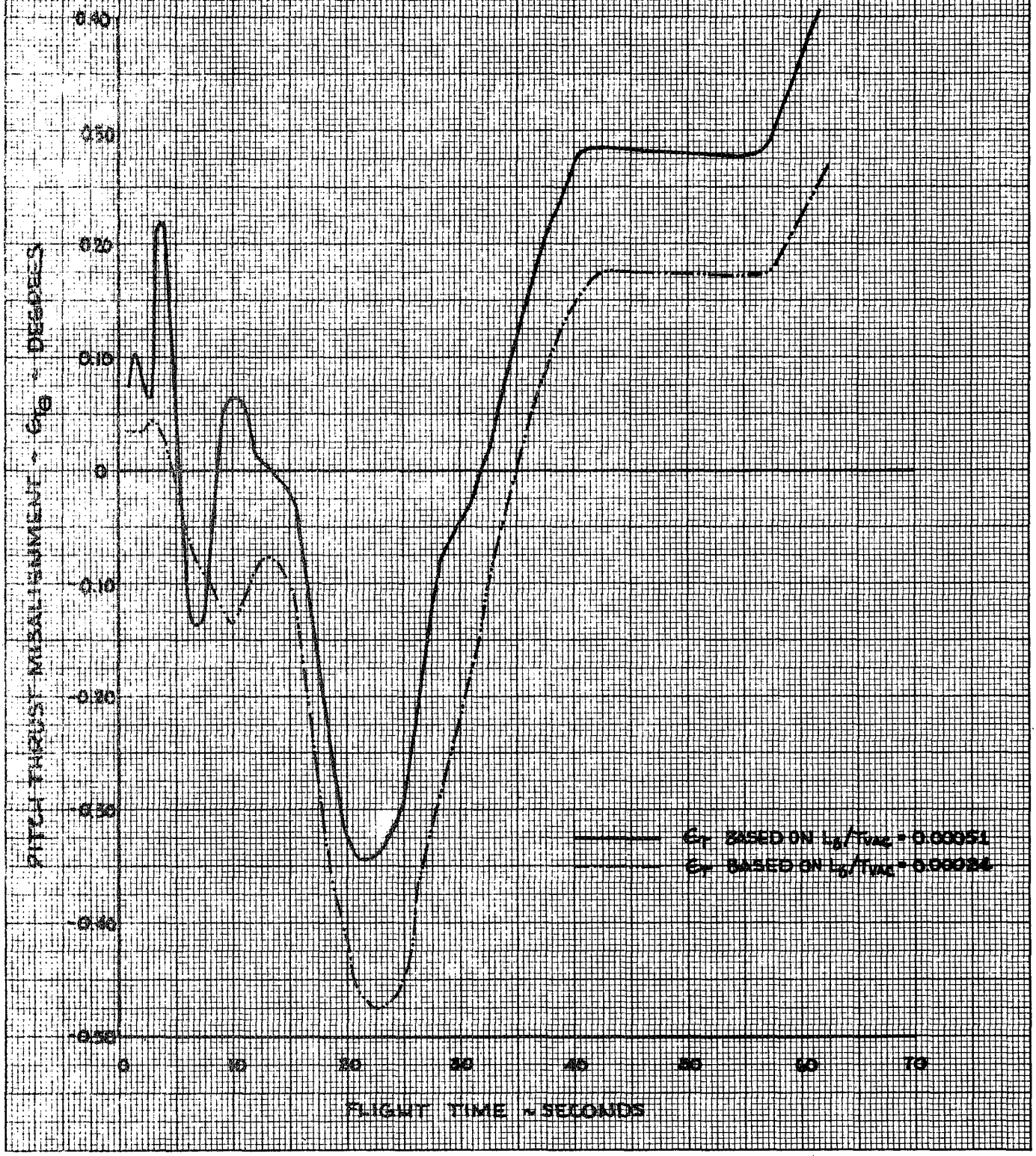

FIGURE 3.4.5-4

YAW THRUST MISALIGNMENT HISTORY
AS A FUNCTION OF CONTROL EFFECTIVENESS

VEHICLE S-13 I

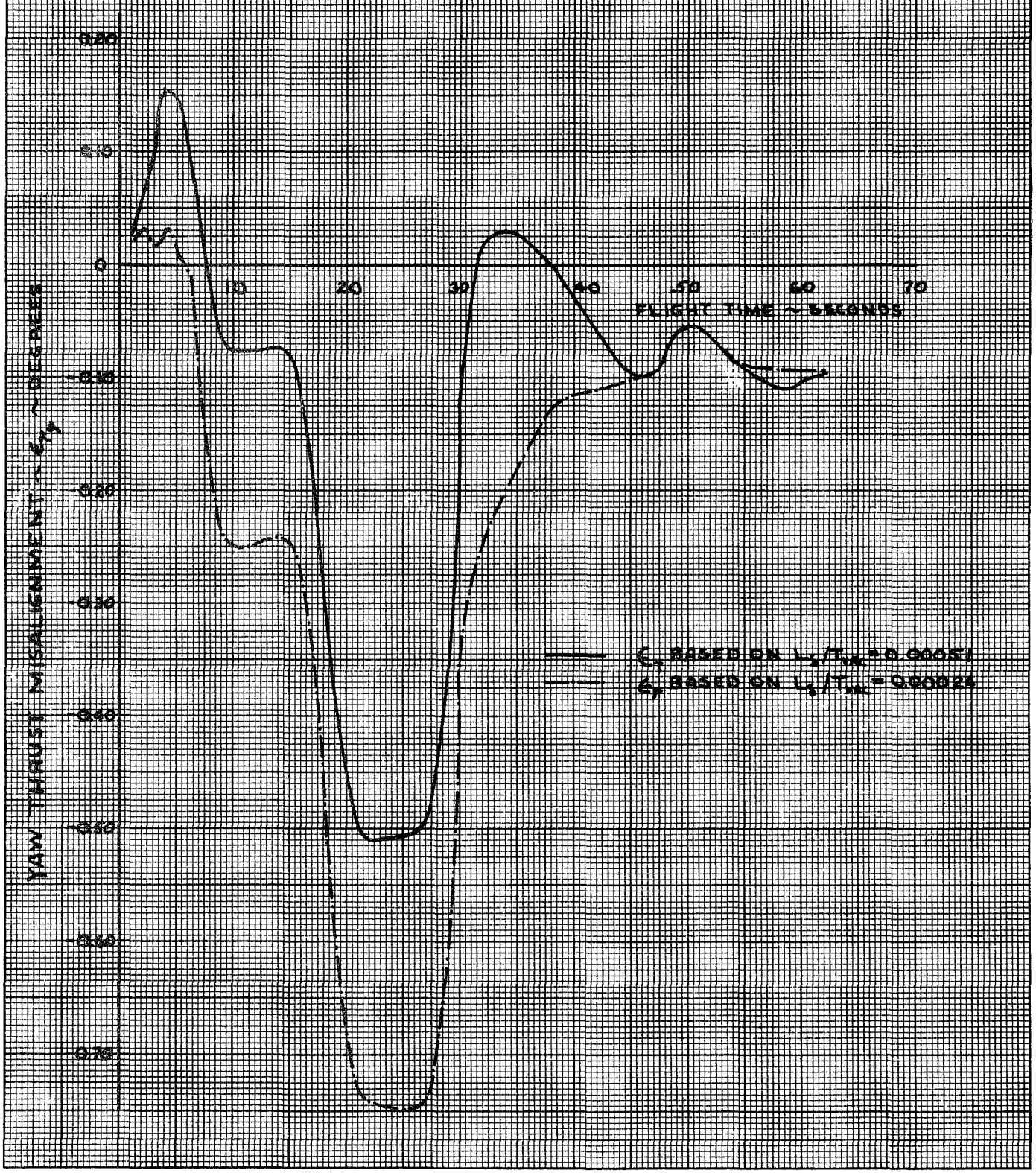

4.0 CONCLUSIONS AND RECOMMENDATIONS

The characteristics of the residual moment time history in the pitch plane and subsequent analyses of the various factors that can contribute to the residual moment make it apparent that more than one factor is involved. As noted in the previous discussions thrust misalignment, flow interference near the launcher, launcher tip-off, jet vane effectiveness, vehicle aerodynamic characteristics, and wind measurement accuracy can all contribute to the residual moments calculated during the flight. Errors in determining the wind at flight time will be a factor for each individual flight but might be expected to average out over a large number of flights. Thrust misalignment is theoretically random in orientation and not expected to exceed 0.25 degrees but experience with the upper stages, where thrust misalignment can be defined, has shown that a bias in orientation can exist and that the misalignment angle can be larger than would be predicted by theoretical means. The difficulty in determining thrust misalignment makes it all the more important that the other potential disturbance sources and their magnitudes be defined. It is recommended, therefore, that all future static firings of the Algol motor be accurately instrumented to measure thrust misalignment in both the pitch and yaw planes.

The pitch-up phenomenon at lift-off may be attributed to the presence of the launcher which induces a tip-off to the vehicle and could cause jet flow interference during the vertical boost which may cause a pressure asymmetry on the base and the fins. It is recommended that the base"A" and fins be instrumented on several vehicles for pressure differential between the tower side and the range side. With these data

and the measured attitude data from flight records it should be possible to predict the limits of the pitch-up and define any existing thrust misalignment bias.

The jet vane effectiveness during the flight shows every indication of being different than that currently defined. During the first pitch program the control effectiveness is about one-half of predicted. Later in the flight when aerodynamic effects become significant and other uncertainties enter into the picture, the jet vane effectiveness is more difficult to determine, but it is likely that the vane effectiveness varies as the nozzle flow aft of the exit plane expands with increasing altitude. The current jet vane predictions are based solely on firing data collected at the altitude of the test site. A preliminary review of the Algol ground firing test set-up and instrumentation indicates an apparent error in the data reduction of the measured jet vane loads data. It is notable that the side force measurements from the Algol IIB-31 test, when converted to jet vane effectiveness, correlate well with the effectiveness calculated from flight data during the first pitch program. It is recommended that the following tasks be performed expeditiously: (1) review in detail the Algol test instrumentation and calibration procedures and data reduction for both the IIA-3 and IIB-31 tests and re-define, if necessary, the jet vane effectiveness as determined from these firings; (2) calculate the Algol exhaust flow characteristics in the plane of the jet vanes as a function of altitude and velocity and revise the vane lift time history as required; and (3) instrument the control actuation mechanism on several vehicles to measure the control hinge moments and bending moments for determination of in-flight control effectiveness.

The vehicle aerodynamic characteristics were evaluated under the assumption that the entire residual moment was due to differences between the predicted and actual aerodynamics. Jet vane effectiveness (L_δ/T_{vac}) values of 0.00051 per degree (predicted) and 0.00024 per degree (flight results) were assumed in determining the residual moment. In both cases the most significant factor determined is that the stability margin is apparently less than predicted in the transonic region. The supersonic results were less conclusive due to wide fluctuations in the calculated center of pressure. In order to define the vehicle aerodynamics of the current configuration and to improve the post flight determination of the aerodynamic moments the following recommendations are made: (1) conduct wind tunnel tests at transonic and supersonic velocities which include the effects of protuberances, combined angles of attack and sideslip, and rocket exhaust pluming; (2) evaluate the vehicle tooling and assembly fixtures and alignment measurements to determine if a consistent body deflection is being built into the vehicle; (3) utilize a wind measurement procedure such as exhaust trail observation which will give the wind profile at the time of launch rather than depend upon measurements made several hours before or after the flight.

The least squares procedure was used in this study to determine the apparent thrust misalignment, jet vane effectiveness, and center of pressure independently. This procedure previously has been applied to the problem of reducing flight test data and can be used, as defined in Appendix A, to evaluate the total moment disturbance problem. The complexity of the problem prohibited its further development during this study but it is recommended that

this procedure be developed and utilized for the first stage moment analyses. As the number of uncertainties are reduced by completion of the previously recommended tests and studies, the remaining uncertainties can be better definded and the preflight prediction accuracy improved.

REFERENCES

1. "Analysis of Scout First Stage Control System Performance" Honeywell Aeronautical Division Report R-ED 1178, 2 February 1962.

2. K. G. Pratt, H. C. Lester, "Scout Vehicle Flight Loads," NASA Langley Research Center, 1 September 1965. Paper presented at the AIAA Structural Dynamics and Aeroelasticity Conference, Boston, Mass., August 30 - September 1, 1965.

3. "Aerodynamics Design Data Report" LTV Report #AST/EIR-12431, Revised 30 June 1965.

4. "Stability and Control Report" LTV Report #AST/EIR-13381, Revised 30 June 1965.

5. "Meteorological Observations Above 30 Kilometers" NASA SP-49, 1964. Part of Proceedings of the Conference on Meteorological Support for Aerospace Testing and Operation held at Colorado State University, July 11-12, 1963.

6. Smith, W., Katchen, L., Sacher, P., Swartz, P., Theon, J., "Temperature, Pressure, Density, and Wind Measurements with Rocket Grenade Experiment, 1960-1963," NASA TR-R-211, Goddard Spaceflight Center, Greenbelt, Maryland, October 1964.

7. "Final Static-Test Firing Report Algol Solid Motor Program," Contract NAS1-1330, Aerojet General Corporation, Report 0498-01FFR-1; 16 August 1963, Confidential.

REFERENCES (Cont'd)

8. "Test Plan for the Quality Assurance Static Test Firing of Algol Motor IIB-31," Contract JAS103833, Test Plan IIB-31 Rev. A, Aerojet-General Corporation, 1 September 1964.

9. "Algol Motor IIB-31 Static Test Firing Report," Contract NAS 1-3833, Aerojet-General Corporation, 23 November 1964.

10. Salmi, Reino J., NASA TND-284, "Effects of Jet Billowing on Stability of Missile-Type Bodies at Mach 3.85," Lewis Research Center, June 1960.

11. Fetterman, David E. Jr.; "Effects of Simulated Rocket-Jet Exhaust on Stability and Control of a Research-Type Airplane Configuration at a Mach Number of 6.86," NASA TMX-127, Langley Research Center, October 1959.

12. Robinson, Ross B.; "Aerodynamic Characteristics in Pitch and Sideslip of a 1/15-Scale Model of the Scout Vehicle at a Mach Number of 2.01," NASA TN D-793, Langley Research Center, Langley Field, Virginia, May 1961.

13. Kelly, Thomas C, ; "Transonic Wind-Tunnel Investigation of the Static Longitudinal Aerodynamic Characteristics of Several Configurations of the Scout Vehicle and of a Number of Related Models," NASA TND-794, Langley Research Center, Langley Field, Virginia, May 1961.

14. "Tolerance Specification for Section Assemblies of Scout," LTV Specification 309-2B dated 28 June 1965.

15. Solilnikoff, I. S.; Sokolnikoff, E. S.; "Higher Mathematics for Engineers and Physicists," Second Edition, McGraw-Hill Book Company Inc., New York and London, 1941.

APPENDIX A

METHOD OF LEAST SQUARES

A.1 Description

The least squares approach is in theory one of the best methods for extracting meaningful information from scattered data. It is based on minimization of data scatter which is assumed to have a normal distribution about an assumed relationship existing between the variables involved. A brief treatment of the least squares method may be found on page 536 of Reference 15. In applying the method of least squares to find the relationship between observed variables one must first assume some form of the relationship. For example, if a large number of x, y points are observed, a second order polynomial may be the assumed relationship, i.e.

$$y = f(x) = a_0 + a_1 x + a_2 x^2 \tag{A-1}$$

or

$$f(x,y) = a_0 + a_1 x + a_2 x^2 - y = 0 \tag{A-2}$$

The problem is then to use a large number of data points to determine the best estimate of the coefficients a_0, a_1, a_2. This is accomplished in the following way. First, the partial derivative of f(x,y) is taken with respect to each coefficient and multiplied by the function f(x,y). Each result is then summed over the number of data points (x_i, y_i) and set equal to zero. i.e.

$$\sum_{i=1}^{n} f(x_i,y_i) \frac{\partial}{\partial a_0} [f(x_i,y_i)] = 0 \tag{A-3}$$

$$\sum_{i=1}^{n} f(x_i,y_i) \frac{\partial}{\partial a_1} [f(x_i,y_i)] = 0 \tag{A-4}$$

$$\sum_{i=1}^{n} f(x_i,y_i) \frac{\partial}{\partial a_2} [f(x_i,y_i)] = 0 \tag{A-5}$$

In the following example three linear equations with the three unknowns a_0, a_1 and a_2 result:

$$n a_0 + \sum_{i=1}^{n} x_i a_1 + \sum_{i=1}^{n} x_i^2 a_2 - \sum_{i=1}^{n} y_i = 0 \qquad \text{(A-6)}$$

$$\sum_{i=1}^{n} x_i a_0 + \sum_{i=1}^{n} x_i^2 a_1 + \sum_{i=1}^{n} x_i^3 a_2 - \sum_{i=1}^{n} x_i y_i = 0 \qquad \text{(A-7)}$$

$$\sum_{i=1}^{n} x_i^2 a_0 + \sum_{i=1}^{n} x_i^3 a_1 + \sum_{i=1}^{n} x_i^4 a_2 - \sum_{i=1}^{n} x_i^2 y_i = 0 \qquad \text{(A-8)}$$

The n data points are used to form the premultipliers and the equations are easily solved for the coefficients a_0, a_1, and a_2 by use of determinants. The resulting values establish the best estimate of a second order polynomial to fit the observed data.

The least squares method can be applied to the first stage moment data. The application becomes much more complex since many variables are involved. Control moments are a function of the Algol motor thrust, control deflection angle, altitude, dynamic pressure, Mach number and center of gravity location. Aerodynamic moments are higher order functions of dynamic pressure, Mach number, center of gravity, angles of attack and sideslip. In applying the least squares theory to a function of all these variables a system of nonlinear algebraic equations result which can not be solved as simply as the linear set given in the above example.

A detailed derivation of the application of least squares theory to the first stage moment problem is presented in Paragraph A.2. The solution of the resulting equations is beyond the scope of the current study, however, it is recommended that this approach be used at a later date.

The least squares approach was used in this study in analyzing one source of error at a time. Jet vane effectiveness as a function of time, aerodynamic center of pressure as a function of Mach number, and

pitching and yawing moment coefficient as a function of angles of attack and sideslip were analyzed separately by use of a standard least squares polynomial curve fitting computer routine (Recomp III program R3P-58).

A.2 Derivation of Least Squares Method of Estimating First Stage Parameters

The application of least squares theory to extracting stability derivatives in combination with control effectiveness and thrust misalignment for the first stage of the Scout vehicle is presented herein. The theory is based on a minimization of the deviations of a set of scattered data points from a selected functional relationship. The unknown constants in the describing functional relationship are to be determined. In the case of the first stage moments the equations of motion in pitch and yaw are the functions. The assumed form of the equation of motion is:

$$\Sigma M - I_{yy}\ddot{\theta} = 0 \qquad \text{(A-9)}$$

or

$$C_{m_0} qSd + C_{N_\alpha} qS(x_{cg} - x_{cp})\alpha + 2(L_\delta + C_{N_\delta} qS)(x_{cg} - x_\delta)\delta_p + C_{m_q} q\frac{Sd^2}{2V}\dot{\theta} + C_{L_\epsilon} qS(x_{cg} - x_{cp_{FIN}})\epsilon_{FIN} - T\epsilon_{r_p}(x_{cg} - x_r) - I_{yy}\ddot{\theta} = 0 \qquad \text{(A-10)}$$

The yawing equation of motion is:

$$\Sigma N - I_{zz}\ddot{\psi} = 0 \qquad \text{(A-11)}$$

$$C_{n_0} qSd + C_{y_\beta} qS(x_{cg} - x_{cp})\beta + 2(L_\delta + C_{N_\delta} qS)(x_{cg} - x_\delta)\delta_y + C_{n_r} q\frac{Sd^2}{2V}\dot{\psi} + C_{L_\epsilon} qS(x_{cg} - x_{cp_{FIN}})\epsilon_{FIN} - T\epsilon_{r_y}(x_{cg} - x_r) - I_{zz}\ddot{\psi} = 0 \qquad \text{(A-12)}$$

Equation (A-12) will not be developed in this treatment since it is similar to Equation (A-10).

The coefficients in Equation A-10 which will be treated as unknowns are C_{m_o} Sd, X_{cp}, L_δ, and ϵ_T. The fin misalignment, aerodynamic damping, fin tip effectiveness, normal force coefficient and inertia terms are assumed to be correct. The aerodynamic pitching moment at zero angle of attack will be assumed to be a function of Mach number only, i.e.

$$C_{m_o} Sd = a_1 + a_2 M + a_3 M^2 \tag{A-13}$$

The aerodynamic center of pressure is assumed to have the form,

$$X_{cp} = (a_4 + a_5 M + a_6 M^2)(a_7 + a_8 q) \tag{A-14}$$

Jet vane lift per degree deflection (L_δ) is assumed to be proportional to vacuum thrust and a second order function of altitude to account for exhaust pluming effects.

$$L_\delta = T_{VAC} (a_9 + a_{10} h + a_{11} h^2) \tag{A-15}$$

The thrust misalignment angle which should represent the mean value of all flights will be assumed to be constant with time, i.e.

$$\epsilon_T = a_{12} \tag{A-16}$$

Limiting of the above coefficients to low order functions is done to keep the calculation at a manageable level. Care must be exercised to limit the region of application to areas where the coefficients are not of higher order, (i.e., in the subsonic region only or the supersonic region only).

Equations (A-13) through (A-14) can be substituted into equation (A-10) to provide the relationship of the unknown coefficients to the known parameters.

$$\begin{aligned}&(a_1 + a_2 M + a_3 M^2) q + C_{N_\alpha} S \left[X_{CG} - (a_4 + a_5 M + a_6 M^2)(a_7 + a_8 q)\right] q\alpha \\ &+ C_{m_q} q \frac{Sd^2}{2V} \dot{\theta} + C_{L_\epsilon} q S (X_{CG} - X_{CP_{FIN}}) \epsilon_{FIN} + 2 (X_{CG} - X_\delta) \delta_p \left[C_{N_\delta} q S \right. \\ &\left. + T_{VAC} (a_9 + a_{10} h + a_{11} h^2)\right] - T (X_{CG} - X_T) a_{12} - I_{yy} \ddot{\theta} = 0\end{aligned} \tag{A-17}$$

For any given time point on a Scout flight all of the constants and variables other than the "a" coefficients of Equation (A-17) are known with a reasonable degree of accuracy. The task is then to use all of these data to find the best estimate of the coefficients a_1 through a_{12}. This is accomplished by application of the theory of least squares.

If we represent Equation A-17 as a function of the coefficients a_1 through a_{12}, i.e.

$$F_i(a_1, a_2, a_3, \cdots a_{12}) = 0 \tag{A-18}$$

where i denotes the value at one time point on one flight, then the best estimate of the coefficients "a" for "n" data points can be obtained by solution of the following 12 equations.

$$\begin{aligned}
&\sum_{i=1}^{n} F_i \frac{\partial F_i}{\partial a_1} = 0 \\
&\sum_{i=1}^{n} F_i \frac{\partial F_i}{\partial a_2} = 0 \\
&\vdots \\
&\sum_{i=1}^{n} F_i \frac{\partial F_i}{\partial a_{12}} = 0
\end{aligned} \tag{A-19}$$

The partial derivatives with respect to the coefficients become:

$$\begin{aligned}
\frac{\partial F_i}{\partial a_1} &= q_i \\
\frac{\partial F_i}{\partial a_2} &= M_i q_i \\
\frac{\partial F_i}{\partial a_3} &= M_i^2 q_i \\
\frac{\partial F_i}{\partial a_4} &= -(C_{N\alpha} S q \alpha)_i (a_7 + a_8 q_i) \\
\frac{\partial F_i}{\partial a_5} &= -(C_{N\alpha} S q \alpha)_i (a_7 + a_8 q_i) M_i \\
\frac{\partial F_i}{\partial a_6} &= -(C_{N\alpha} S q \alpha)_i (a_7 + a_8 q_i) M_i^2 \\
\frac{\partial F_i}{\partial a_7} &= -(C_{N\alpha} S q \alpha)_i (a_4 + a_5 M_i + a_6 M_i^2) \\
\frac{\partial F_i}{\partial a_8} &= -(C_{N\alpha} S q \alpha)_i (a_4 + a_5 M_i + a_6 M_i^2) q_i \\
\frac{\partial F_i}{\partial a_9} &= 2 (x_{cg_i} - x_\delta) \delta_i T_{VAC_i} \\
\frac{\partial F_i}{\partial a_{10}} &= 2 (x_{cg_i} - x_\delta) \delta_i T_{VAC_i} h_i \\
\frac{\partial F_i}{\partial a_{11}} &= 2 (x_{cg_i} - x_\delta) \delta_i T_{VAC_i} h_i^2 \\
\frac{\partial F_i}{\partial a_{12}} &= -T_i (x_{cg_i} - x_T)
\end{aligned} \tag{A-20}$$

Substituting Equations A-17 and A-20 into Equation A-19 yields a system of 12 nonlinear algebraic equations in the 12 unknown coefficients.

$$
\begin{aligned}
&\sum_{i=1}^{n} q_i F_i = 0 \; ; \quad \sum_{i=1}^{n} M_i q_i F_i = 0 \; ; \quad \sum_{i=1}^{n} M_i^2 q_i F_i = 0 \\
&\sum_{i=1}^{n} - (C_{N\alpha} S q \alpha)_i (a_7 + a_8 q_i) F_i = 0 \\
&\sum_{i=1}^{n} - (C_{N\alpha} S q \alpha)_i (a_7 + a_8 q_i) F_i M_i = 0 \\
&\sum_{i=1}^{n} - (C_{N\alpha} S q \alpha)_i (a_7 + a_8 q_i) F_i M_i^2 = 0 \\
&\sum_{i=1}^{n} - (C_{N\alpha} S q \alpha)_i (a_4 + a_5 M_i + a_6 M_i^2) F_i = 0 \\
&\sum_{i=1}^{n} - (C_{N\alpha} S q \alpha)_i (a_4 + a_5 M_i + a_6 M_i^2) F_i q_i = 0 \\
&\sum_{i=1}^{n} 2 (x_{CG_i} - x_\delta) \delta_i T_{VAC_i} F_i = 0 \\
&\sum_{i=1}^{n} 2 (x_{CG_i} - x_\delta) \delta_i T_{VAC_i} F_i h_i = 0 \\
&\sum_{i=1}^{n} 2 (x_{CG_i} - x_\delta) \delta_i T_{VAC_i} F_i h_i^2 = 0 \\
&\sum_{i=1}^{n} - T_i (x_{CG_i} - x_T) F_i = 0
\end{aligned}
\tag{A-21}
$$

The nonlinear terms in the system of equations (A-21) become apparent when the expression of F_i is included. The first of these equations becomes:

$$\sum_{i=1}^{n} q_i F_i = 0$$

or

$$
\begin{aligned}
&\sum_{i=1}^{n} q_i^2 a_1 + \sum_{i=1}^{n} q_i^2 M_i a_2 + \sum_{i=1}^{n} M_i^2 q_i^2 a_3 + \sum_{i=1}^{n} (C_{N\alpha} S q^2 \alpha x_{CG})_i \\
&- \sum_{i=1}^{n} (C_{N\alpha} S q^2 \alpha)_i a_4 a_7 - \sum_{i=1}^{n} (C_{N\alpha} S q^2 \alpha)_i a_4 a_8 - \sum_{i=1}^{n} (C_{N\alpha} S q^2 \alpha M)_i a_5 a_7 \\
&- \sum_{i=1}^{n} (C_{N\alpha} S q^2 \alpha M)_i a_5 a_8 - \sum_{i=1}^{n} (C_{N\alpha} S q^2 \alpha M^2)_i a_6 a_7 \\
&- \sum_{i=1}^{n} (C_{N\alpha} S q^2 \alpha M^2)_i a_6 a_8 + \sum_{i=1}^{n} (C_{mq} q^2 \frac{S d^2}{2V} \dot{\theta})_i + \sum_{i=1}^{n} \left[C_{L_\epsilon} q^2 S (x_{CG} - x_{CM}) \epsilon_{CM} \right]_i \\
&+ \sum_{i=1}^{n} 2 \left[(x_{CG} - x_\delta) \delta C_{N_\delta} q^2 S \right]_i + \sum_{i=1}^{n} 2 \left[(x_{CG} - x_\delta) \delta q T_{VAC} \right]_i a_9 \\
&+ \sum_{i=1}^{n} 2 \left[(x_{CG} - x_\delta) \delta q T_{VAC} h \right]_i a_{10} + \sum_{i=1}^{n} 2 \left[(x_{CG} - x_\delta) \delta q T_{VAC} h^2 \right]_i a_{11} \\
&- \sum_{i=1}^{n} \left[T (x_{CG} - x_T) q \right]_i a_{12} - \sum_{i=1}^{n} (I_{yy} \ddot{\theta} q)_i = 0
\end{aligned}
\tag{A-22}
$$

The remaining 11 equations will not be expanded here. The resulting non-linear equations may be solved by an iterative procedure using a high speed digital computer. Obviously the calculation of the coefficients (i.e., the summed quantities) of the unknown "a"s would also be accomplished by a digital computer. Both the pitch and yaw equations would require solution and the variables common to both pitch and yaw including jet vane effectiveness and center of pressure should be compared.

The resulting data would require verification. This would be accomplished by use of the data in a series of post flight trajectory calculations. The revised data would also be used in an attempt to null the residual moments which were calculated for several post flight analyses.

The application of the least squares method of extracting basic information from flight data is not only feasible but desirable. The major tasks involved in the application are (1) formulating and programming of the method of solution of the system of non-linear algebraic equations, (2) preparation of the input parameters, and (3) verification of the results.

APPENDIX B

SCOUT FIRST STAGE PARAMETER TIME HISTORIES

The time histories of the flight parameters for a number of Scout vehicles are presented herein. The Mach number, dynamic pressure, altitude, vacuum thrust, center of gravity location, angles of attack and sideslip, pitch and yaw control surface deflections and the pitch and yaw residual moment time histories are presented for the more recent Scout flights. These data, shown in figures B-1 through B-13b, were accumulated as part of the Scout post flight analysis and have been presented in the final flight reports.

K&E 10 X 10 TO THE CENTIMETER 47 1513
25 X 25 CM MADE IN U.S.A.
KEUFFEL & ESSER CO.

K&E 10 X 10 TO THE CENTIMETER 47 1513
KEUFFEL & ESSER CO

K&E 10 X 10 TO THE CENTIMETER 47 1513
KEUFFEL & ESSER CO.

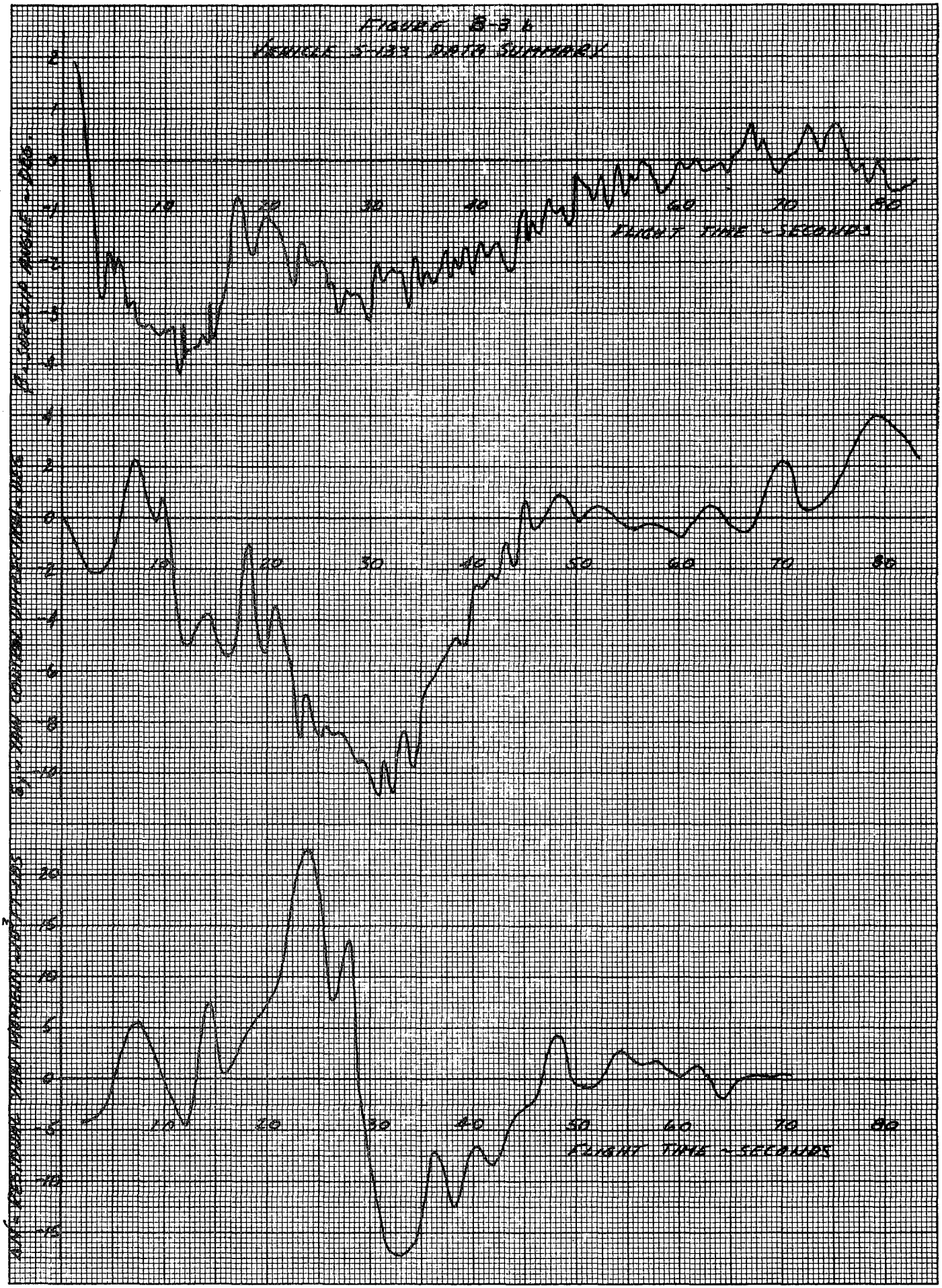
Figure B-3 k
Vessel S-123 Data Summary
FLIGHT TIME - SECONDS
FLIGHT TIME - SECONDS

K&E 10 X 10 TO THE CENTIMETER 47 1513
KEUFFEL & ESSER CO.

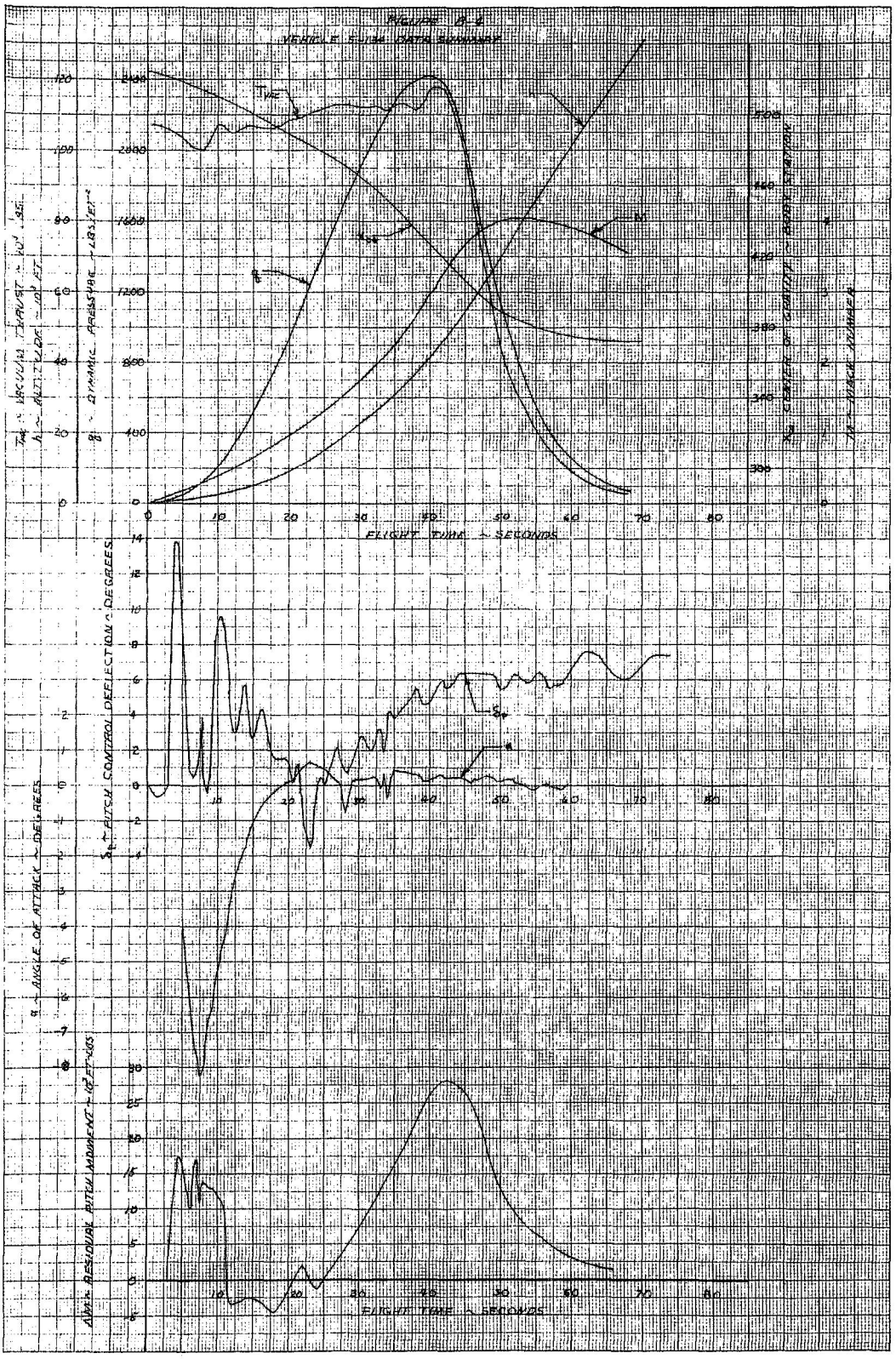

K&E 10 X 10 TO THE CENTIMETER 47 1513
KEUFFEL & ESSER CO.

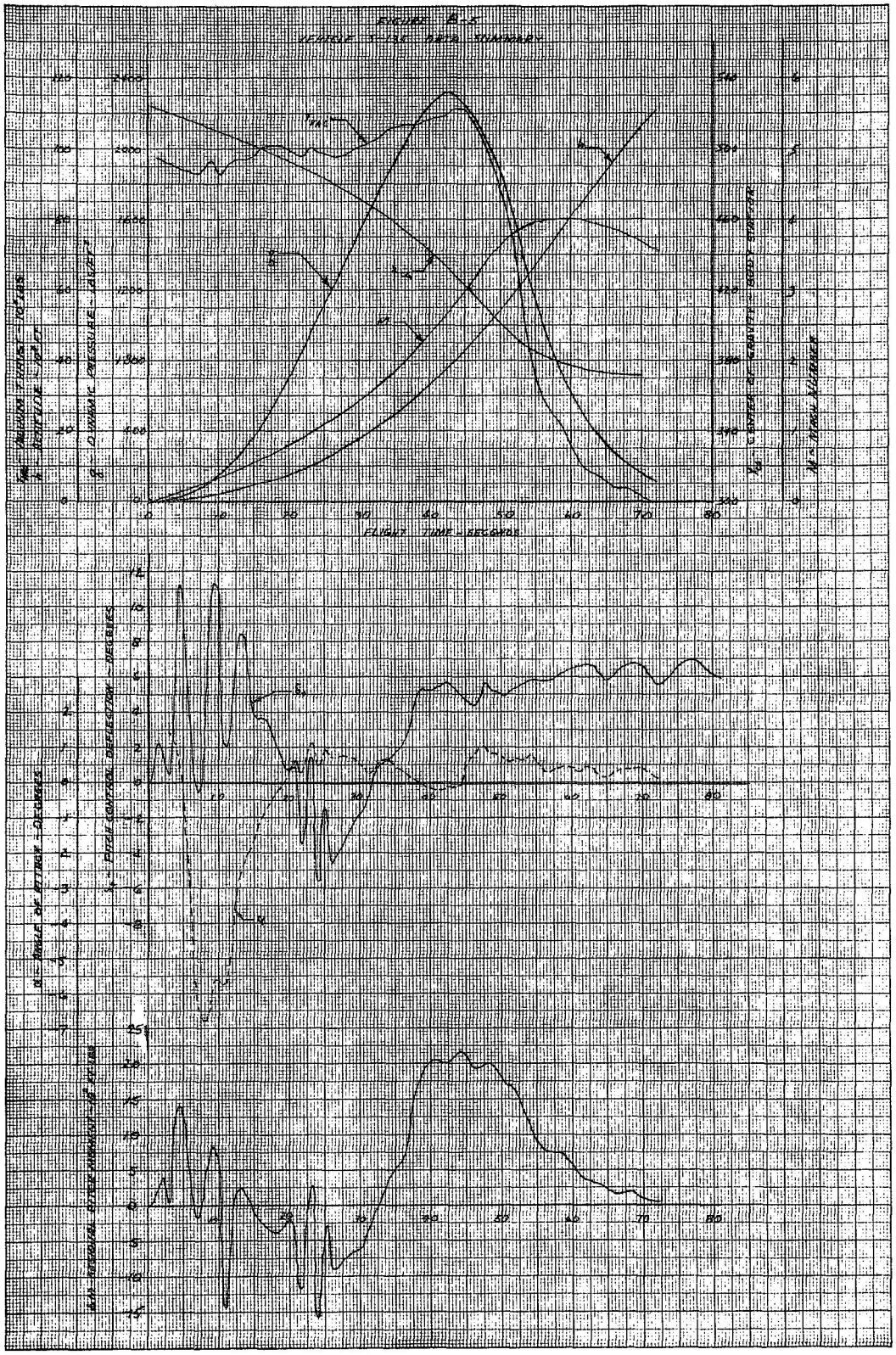

K&E 10 X 10 TO THE CENTIMETER 47 1513
KEUFFEL & ESSER CO.

FIGURE B-6.6
VEHICLE S-136 DATA SUMMARY

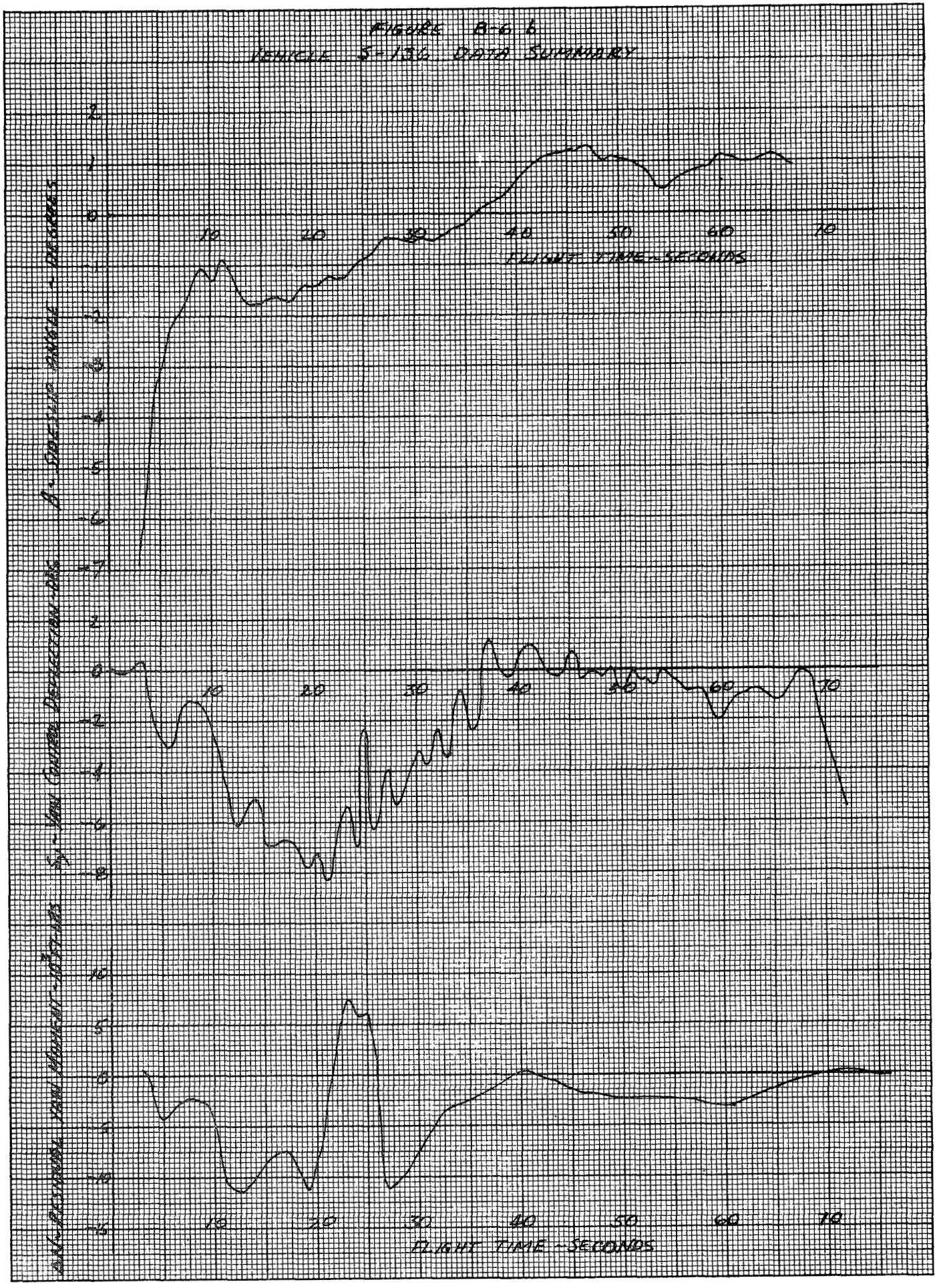

K&E 10 X 10 TO THE CENTIMETER 47 1513
KEUFFEL & ESSER CO

K•E 10 X 10 TO THE CENTIMETER 47 1513
25 X 25 CM MADE IN U.S.A.
KEUFFEL & ESSER CO.

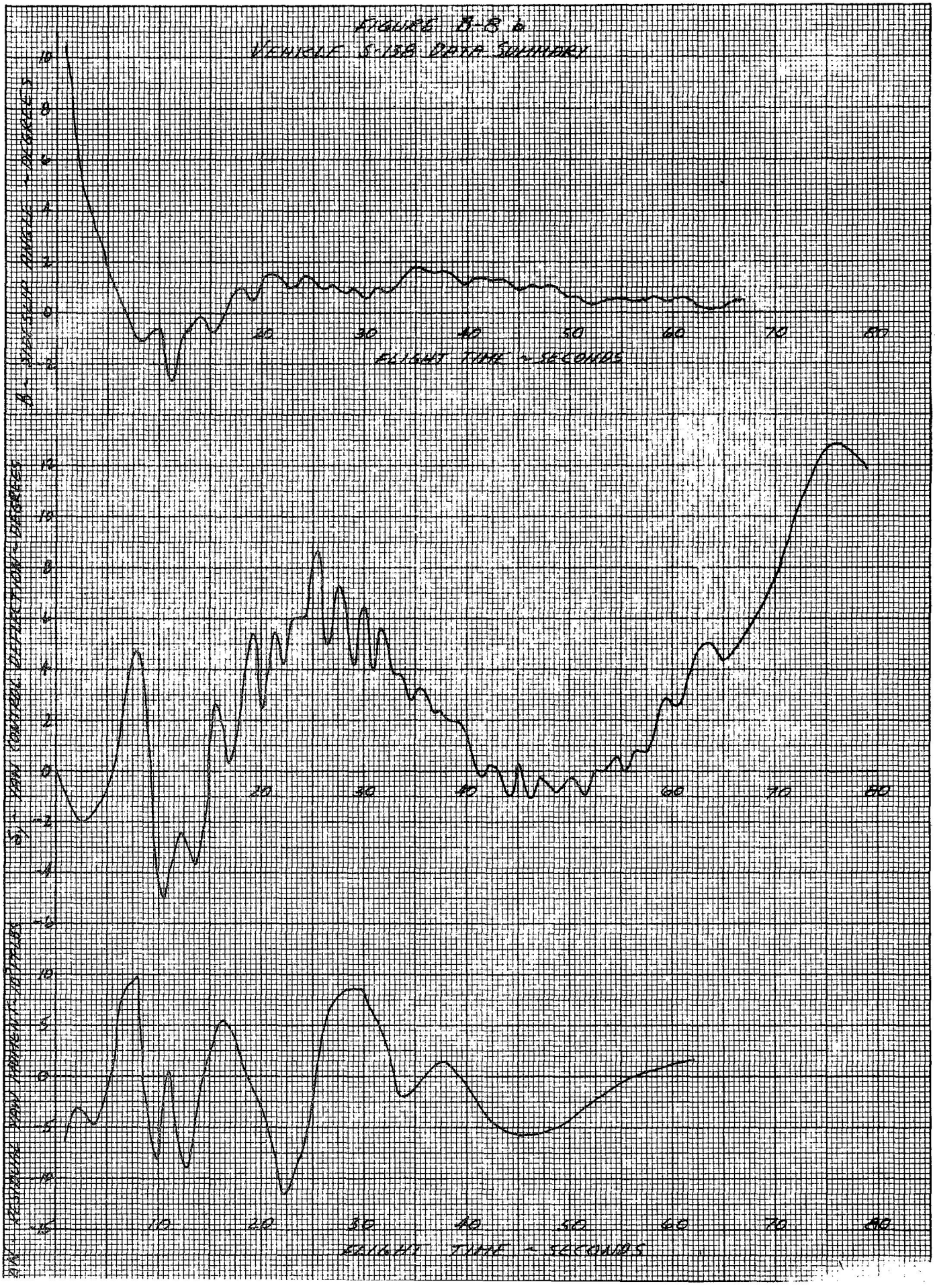
FIGURE B-8.b
VEHICLE S-158 PLANE SUMMARY
ELEVON DEFLECTION - DEGREES
ELEVATOR DEFLECTION - DEGREES
RUDDER DEFLECTION - DEGREES
FLIGHT TIME - SECONDS
FLIGHT TIME - SECONDS
FLIGHT TIME - SECONDS

K•E 10 X 10 TO THE CENTIMETER 47 1513
KEUFFEL & ESSER CO.

Figure B-9 b

Vehicle 5-139 Data Summary

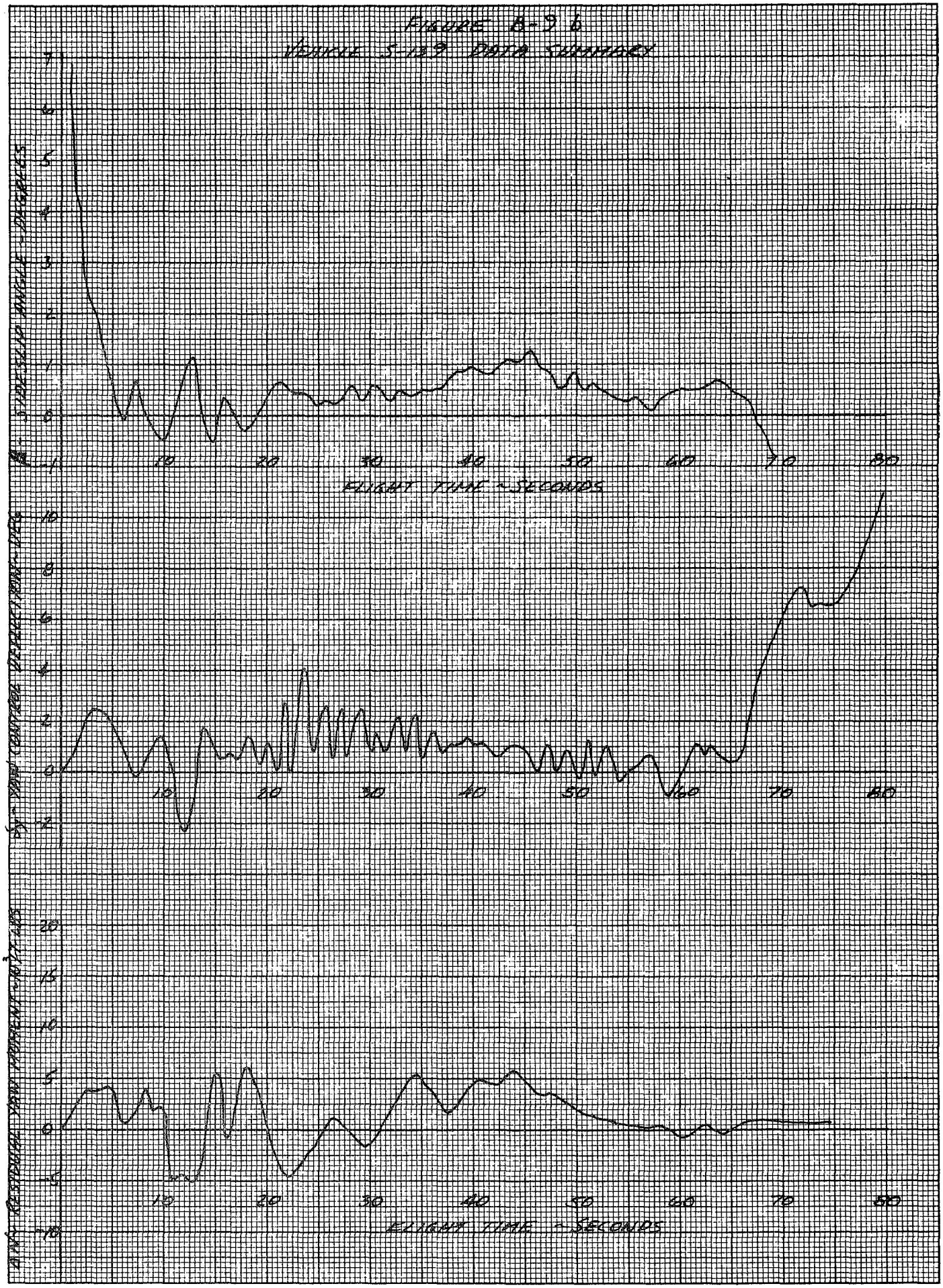

FLIGHT TIME - SECONDS
FLIGHT TIME - SECONDS
FLIGHT TIME - SECONDS

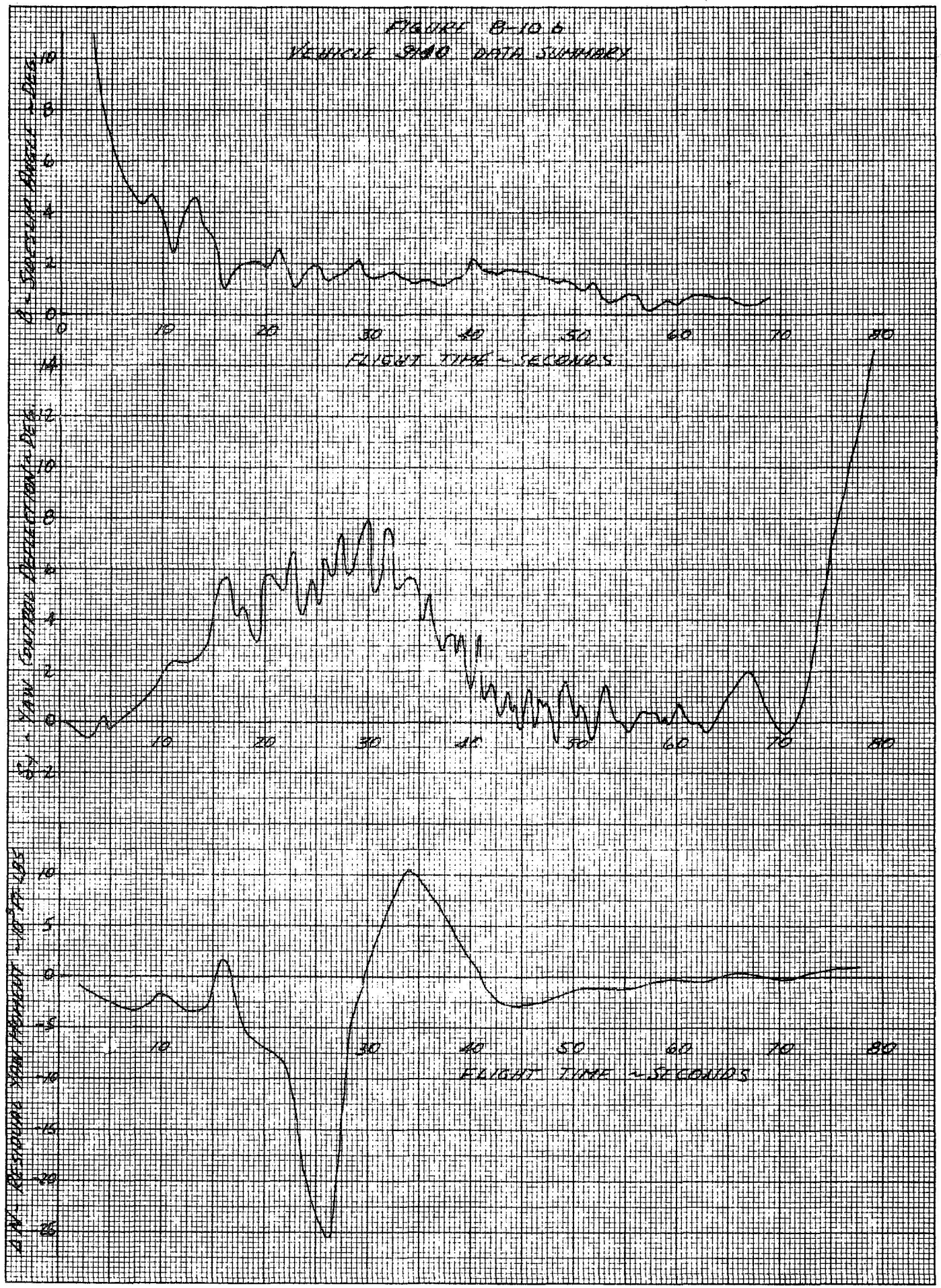
FIGURE B-10 b
VEHICLE 9&10 DATA SUMMARY
a - Spacecraft Angle of Attack - Degs
FLIGHT TIME - SECONDS
β - Spacecraft Angle of Sideslip - Degs
FLIGHT TIME - SECONDS
a_N - Spacecraft Normal Acceleration - Gs
FLIGHT TIME - SECONDS

K&E 10 X 10 TO THE CENTIMETER 47 1513
KEUFFEL & ESSER CO

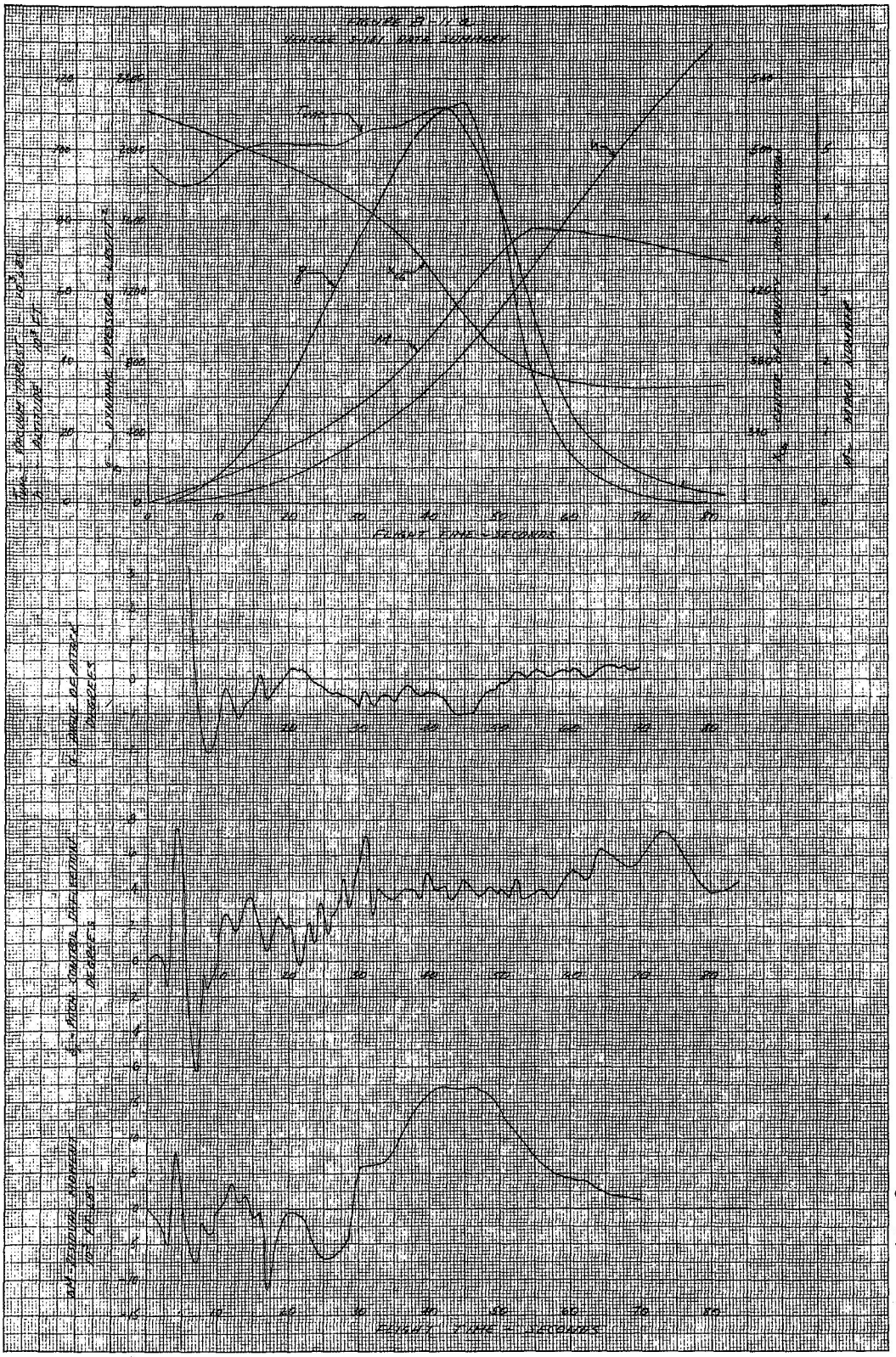

FIGURE B-11 b

VEHICLE S-IVB DATA SUMMARY

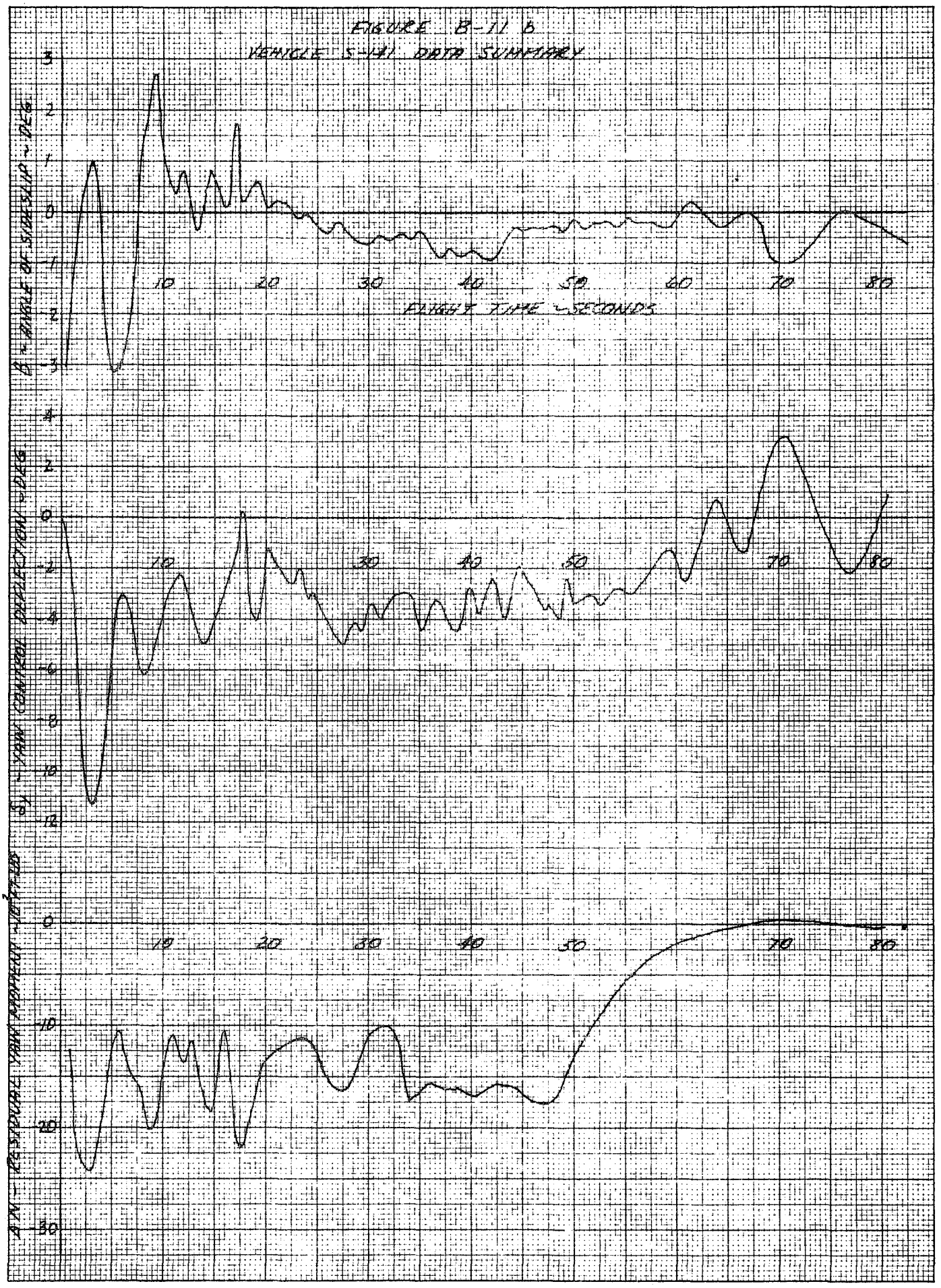

K-Σ 10 X 10 TO THE CENTIMETER 47 1513
25 X 38 CM. MADE IN U.S.A.
KEUFFEL & ESSER CO.

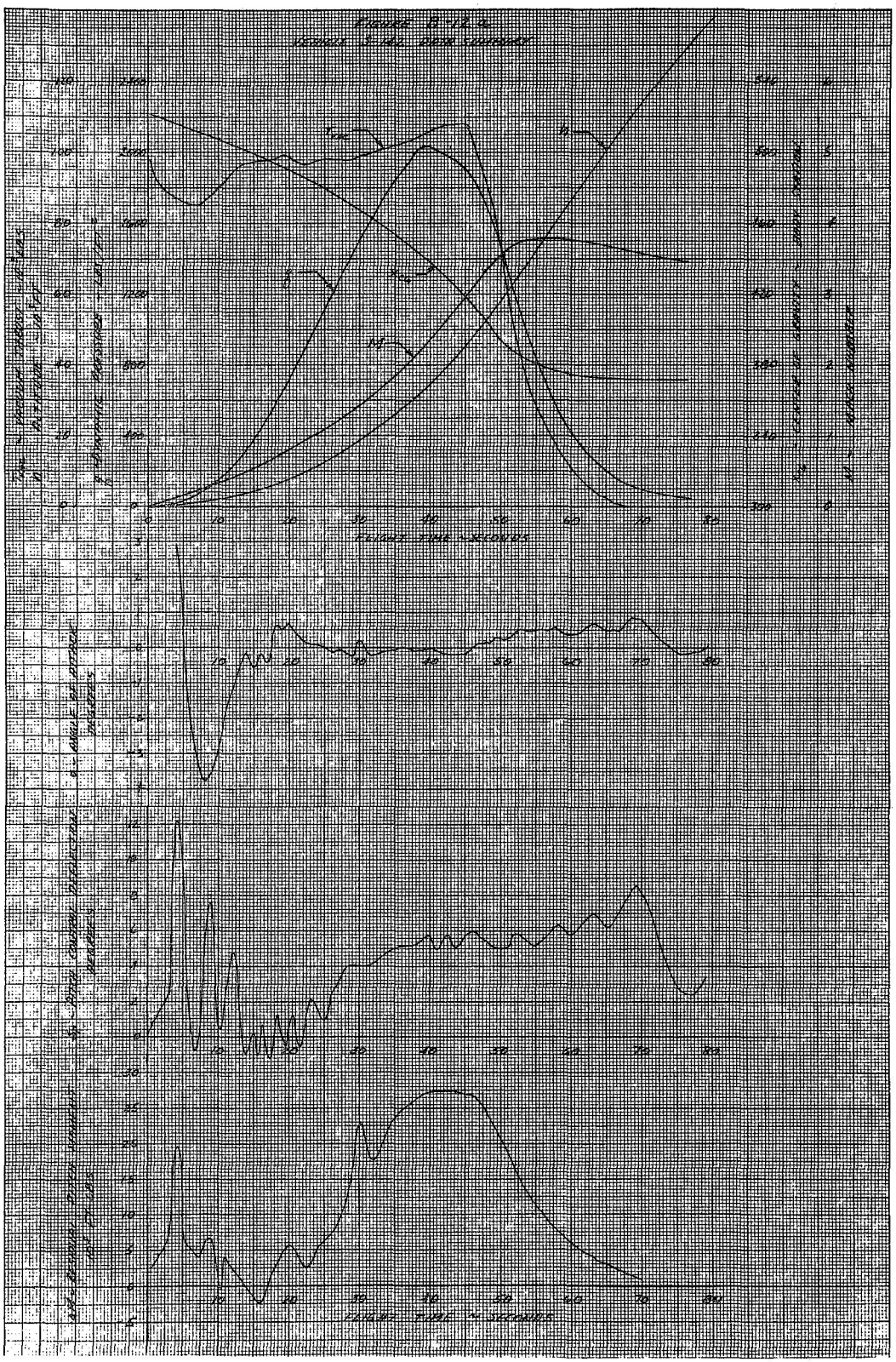

FIGURE B-12 6
VEHICLE 5-MR2 DATA SUMMARY

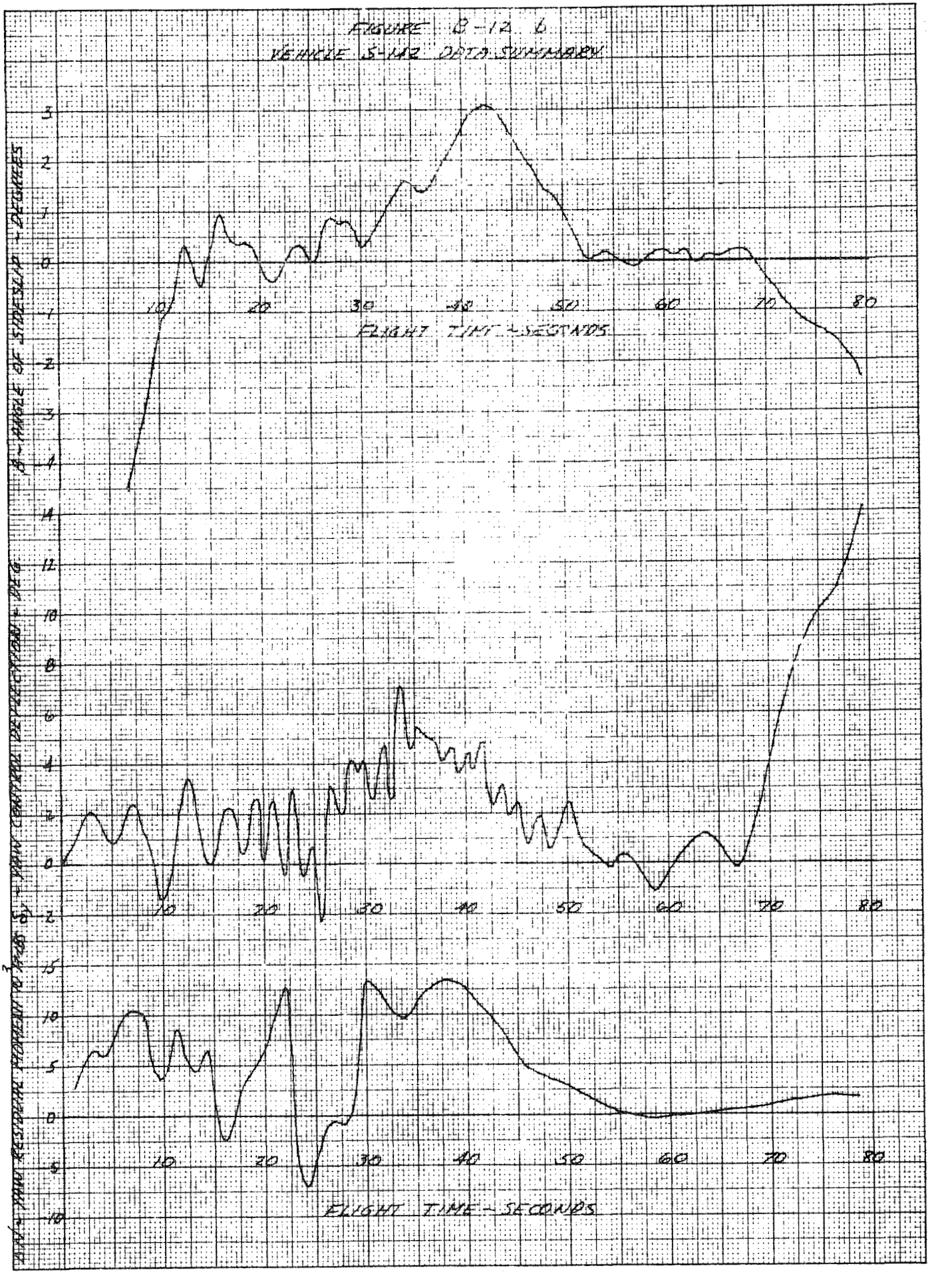

FIGURE 23-13 a
VEHICLE SHELL LOADS SUMMARY
FLIGHT TIME - SECONDS
FLIGHT TIME - SECONDS

FIGURE B-13.6

VEHICLE S-13 DATA SUMMARY

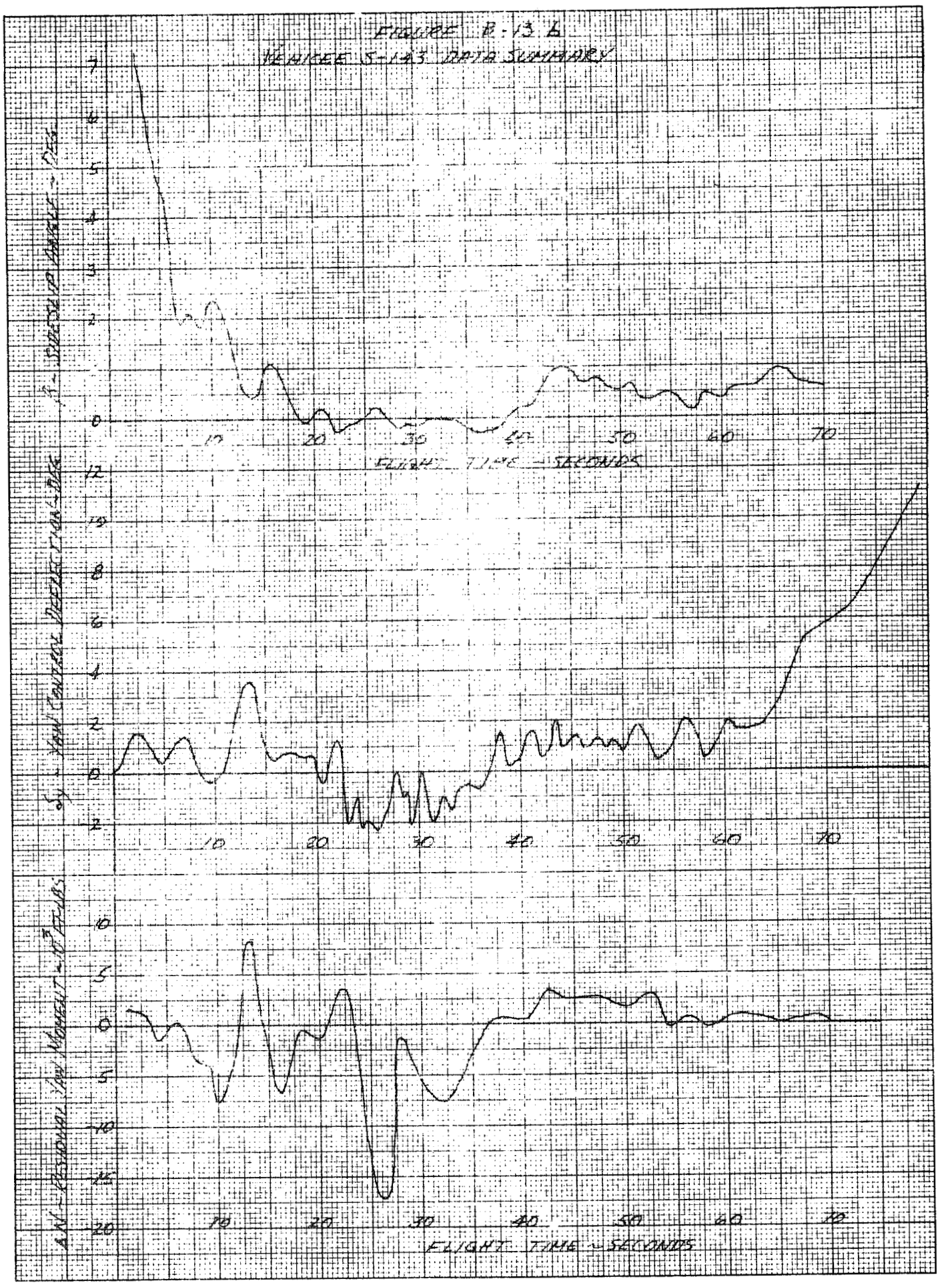

APPENDIX C

EFFECTS OF REDUCED JET VANE EFFECTIVENESS - SUPPLEMENTARY DATA

This appendix presents the effect of reduced jet vane effectiveness for vehicles S-133, S-137 and S-142. A comparison of the residual moments, effective aerodynamic center of pressure, and effective thrust misalignment is made for jet vane effectiveness values (L_{δ}/T_{vac}) of 0.00024 per degree and the predicted 0.00051 per degree. (Exception: reduced jet vane effectiveness used for S-133 evaluation is 0.000255 per degree) The results for vehicle S-133 are shown in figures C-1 through C-3; for S-137 in figures C-4 through C-6; and for vehicle S-142 in figures C-7 through C-11. The very erratic effective center of pressure shifts result directly from the near zero angle of attack used in the calculations . Angles of attack and sideslip as well as other pertinent flight parameters for these vehicles are presented in Appendix B.

FIGURE C-1

EFFECT OF REDUCED JET VANE EFFECTIVENESS ON RESIDUAL MOMENT

VEHICLE S-133

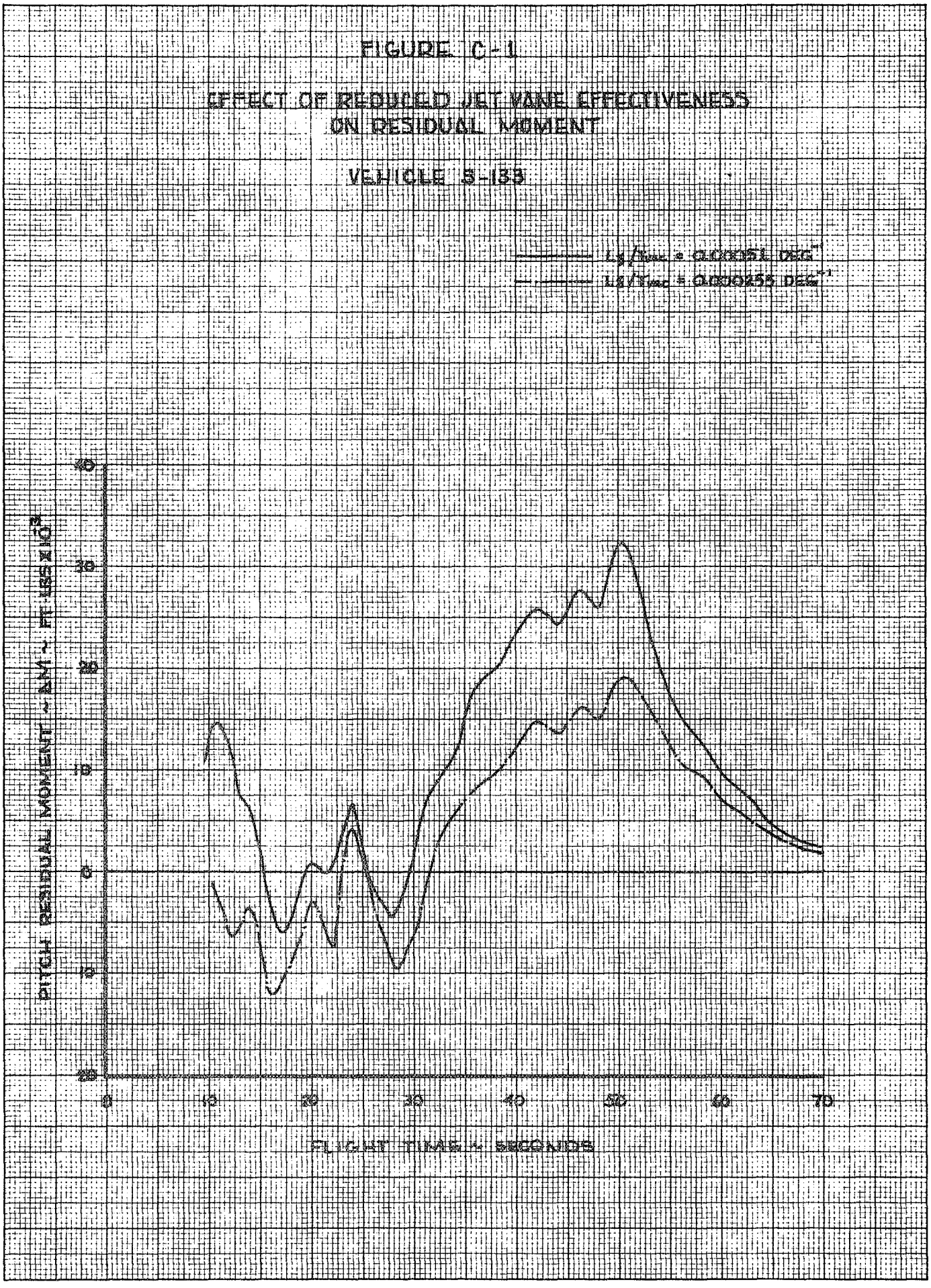

FIGURE C-2

PITCH CENTER OF PRESSURE HISTORY
AS A FUNCTION OF CONTROL EFFECTIVENESS

VEHICLE S-IB5

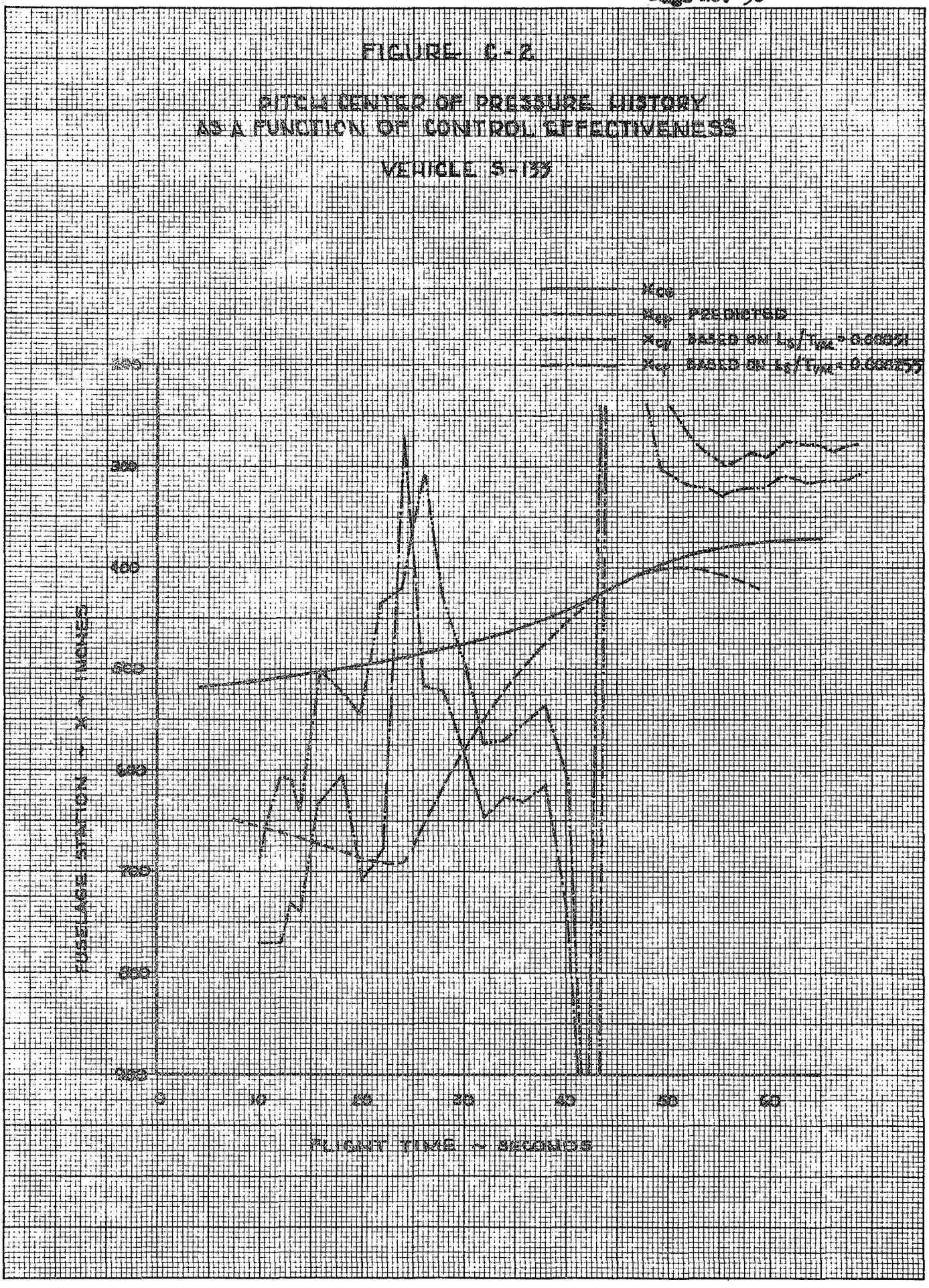

FIGURE C-3

PITCH THRUST MISALIGNMENT HISTORY
AS A FUNCTION OF CONTROL EFFECTIVENESS

VEHICLE S-133

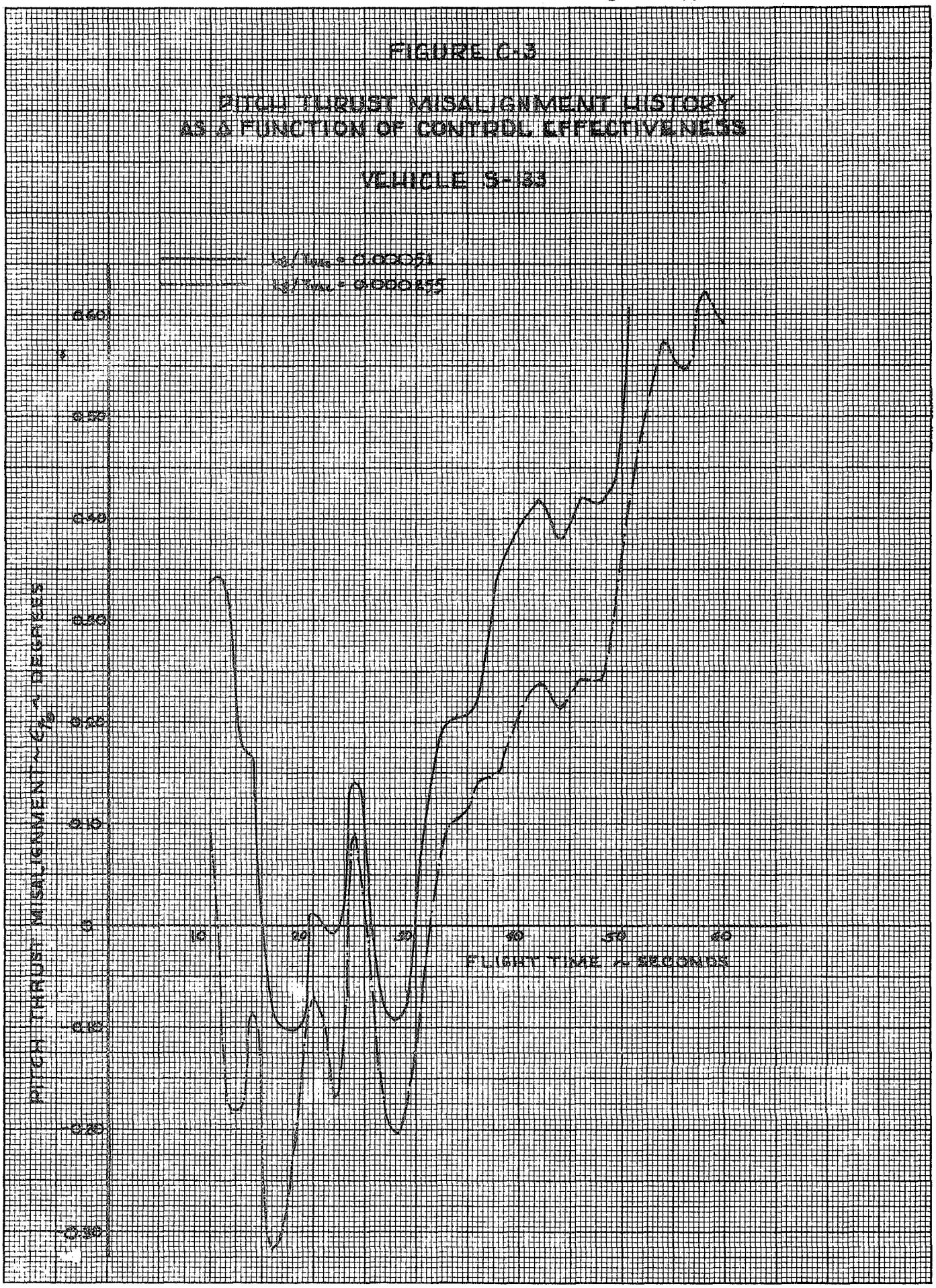

FIGURE C-4

EFFECT OF REDUCED JET VANE EFFECTIVENESS ON RESIDUAL MOMENT

VEHICLE 3-157

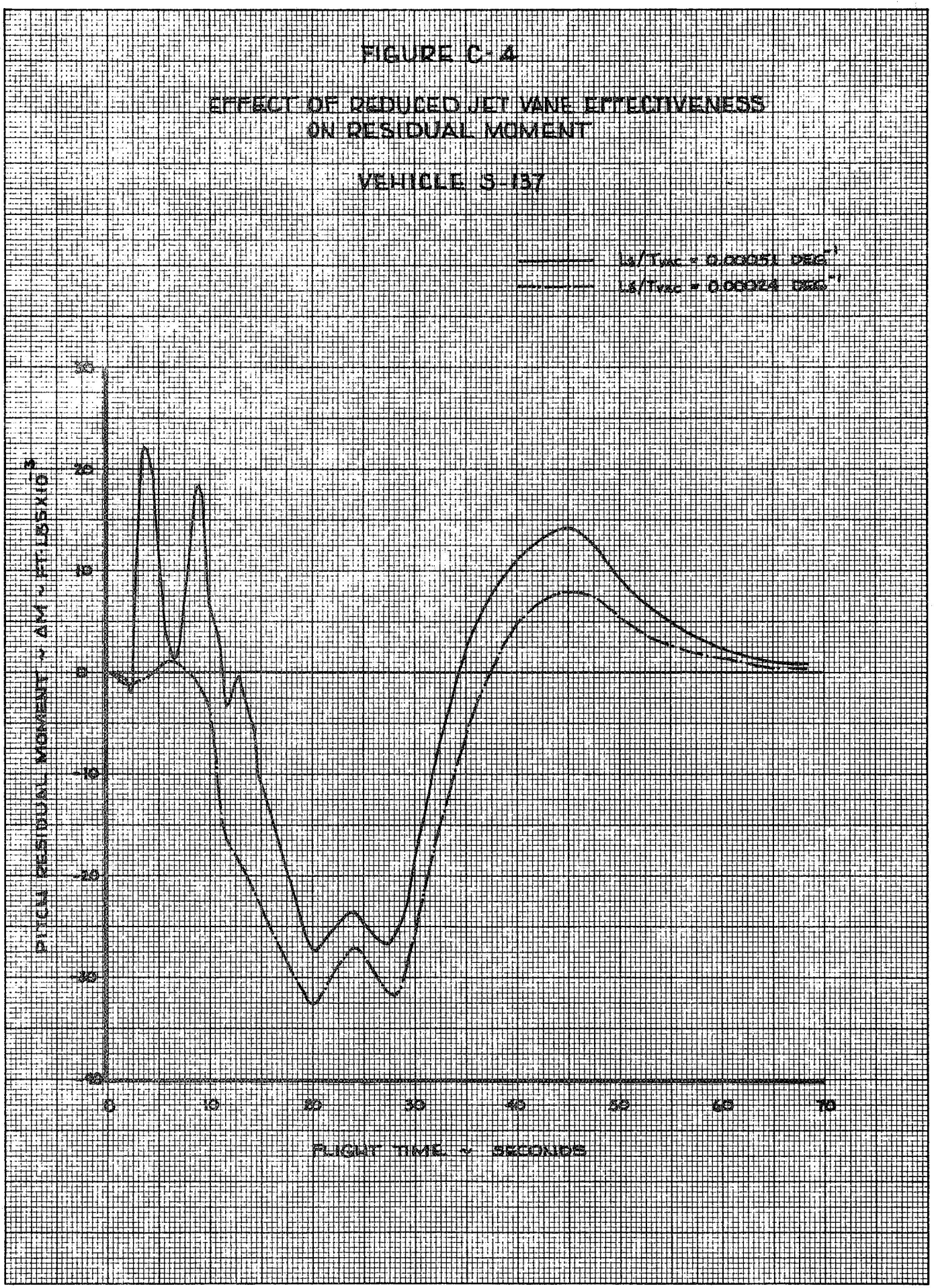

FIGURE C-5

PITCH CENTER OF PRESSURE HISTORY
AS A FUNCTION OF CONTROL EFFECTIVENESS
VEHICLE S-1B7

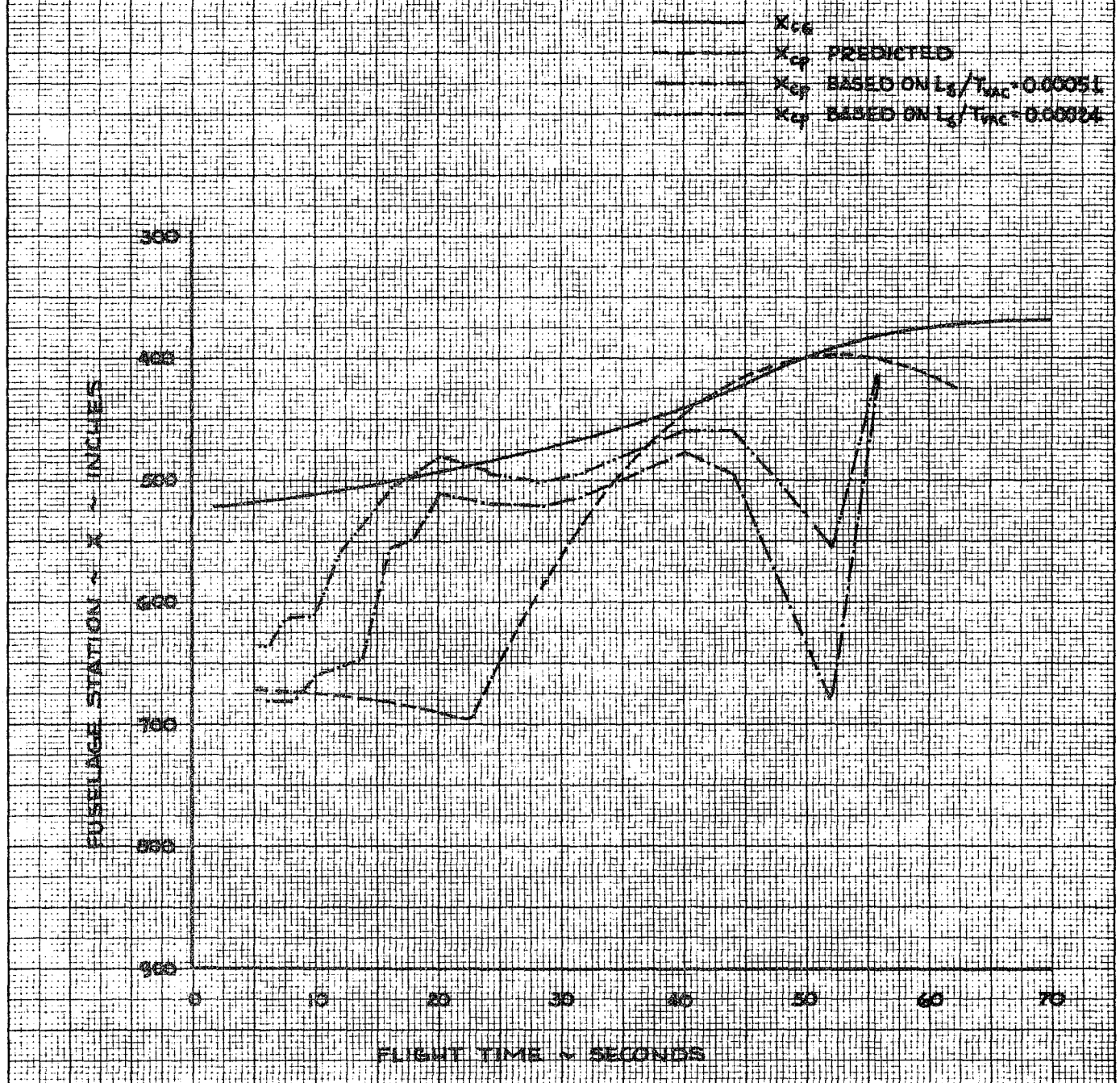

FIGURE C-6

PITCH THRUST MISALIGNMENT HISTORY
AS A FUNCTION OF CONTROL EFFECTIVENESS

VEHICLE S-137

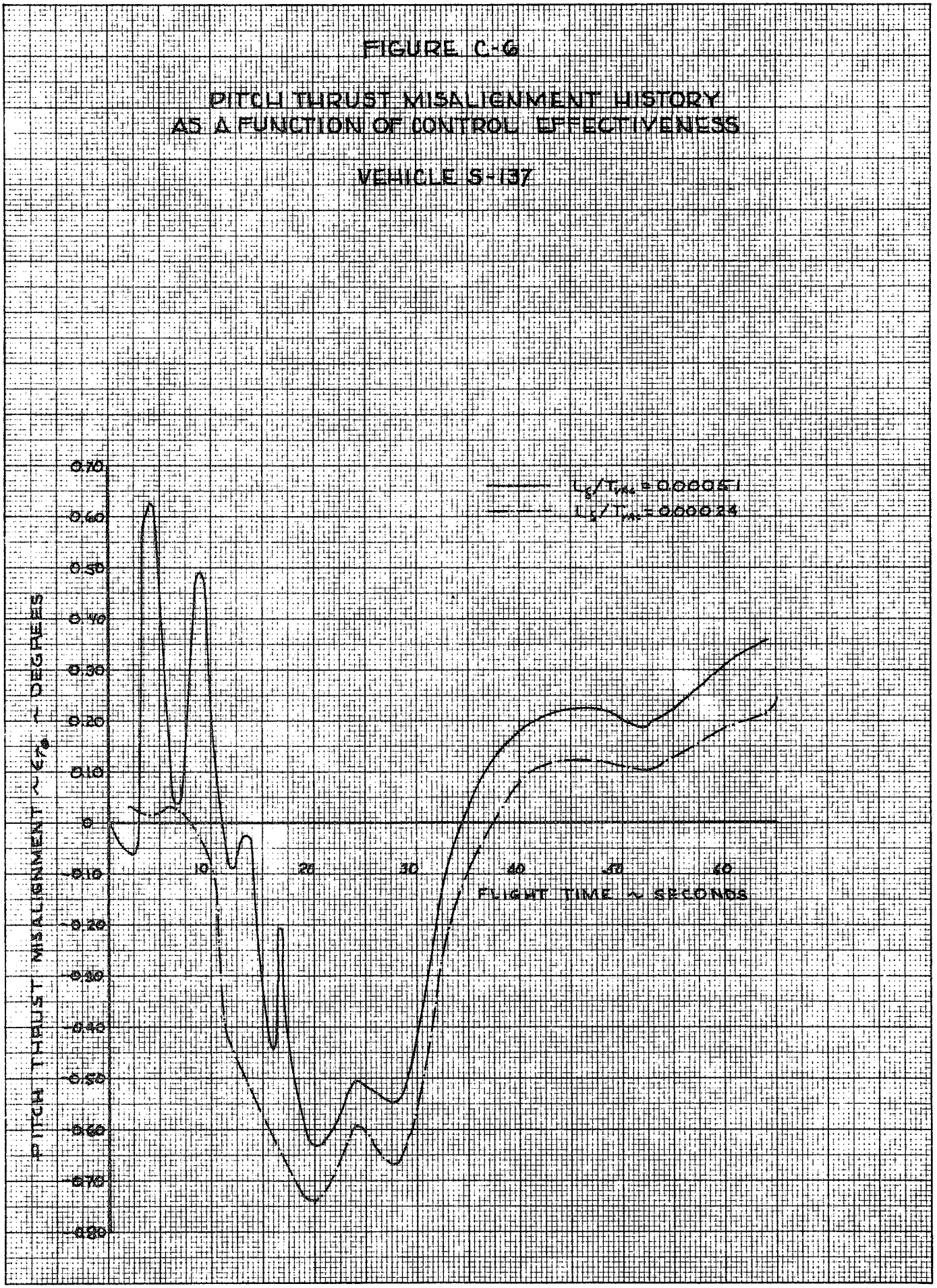

FIGURE C-7

EFFECT OF REDUCED JET VANE EFFECTIVENESS ON RESIDUAL MOMENT

VEHICLE S-142

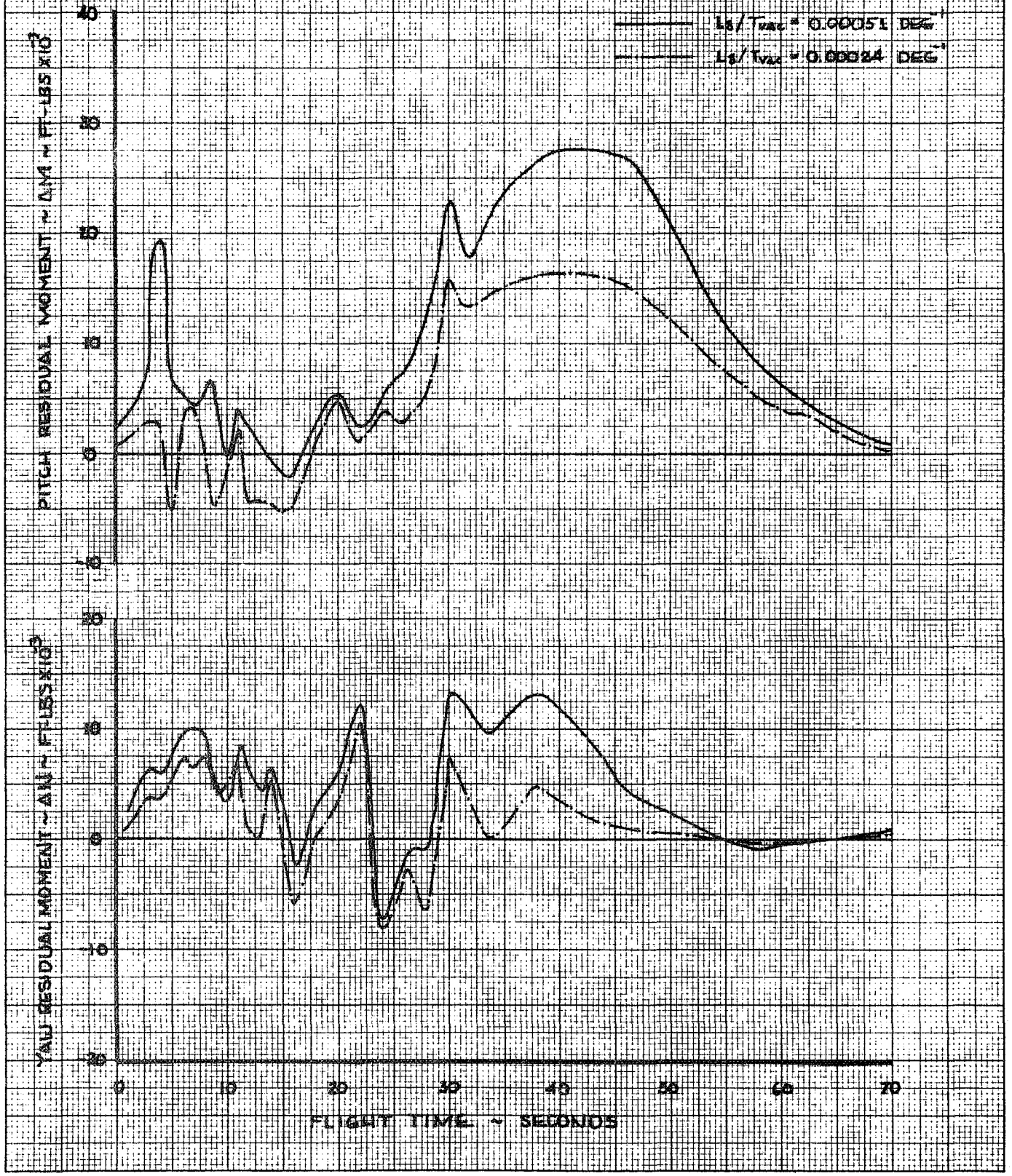

FIGURE C-8

PITCH CENTER OF PRESSURE HISTORY
AS A FUNCTION OF CONTROL EFFECTIVENESS

VEHICLE S-I42

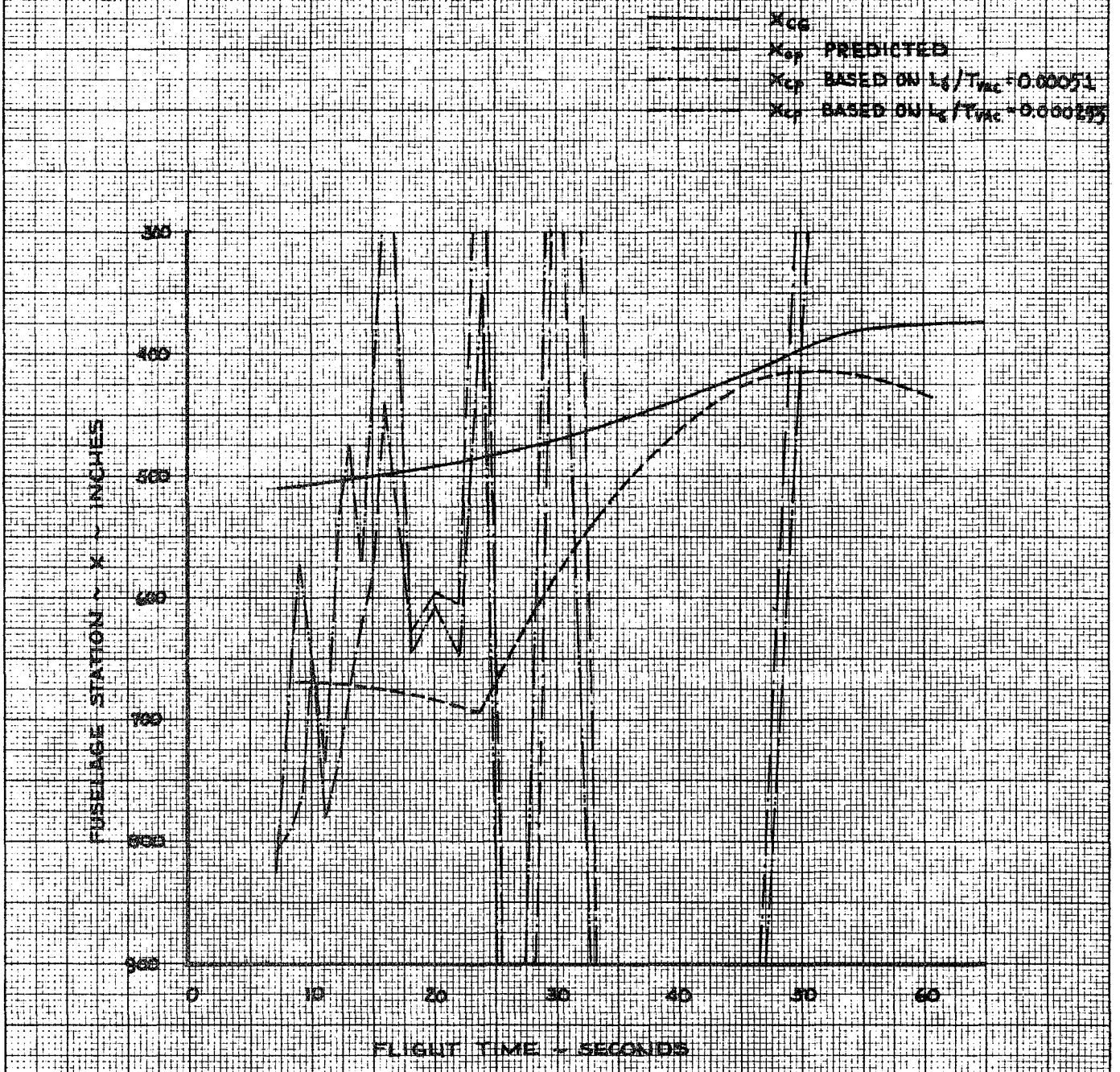

FIGURE C-9

YAW CENTER OF PRESSURE HISTORY
AS A FUNCTION OF CONTROL EFFECTIVENESS

VEHICLE S-42

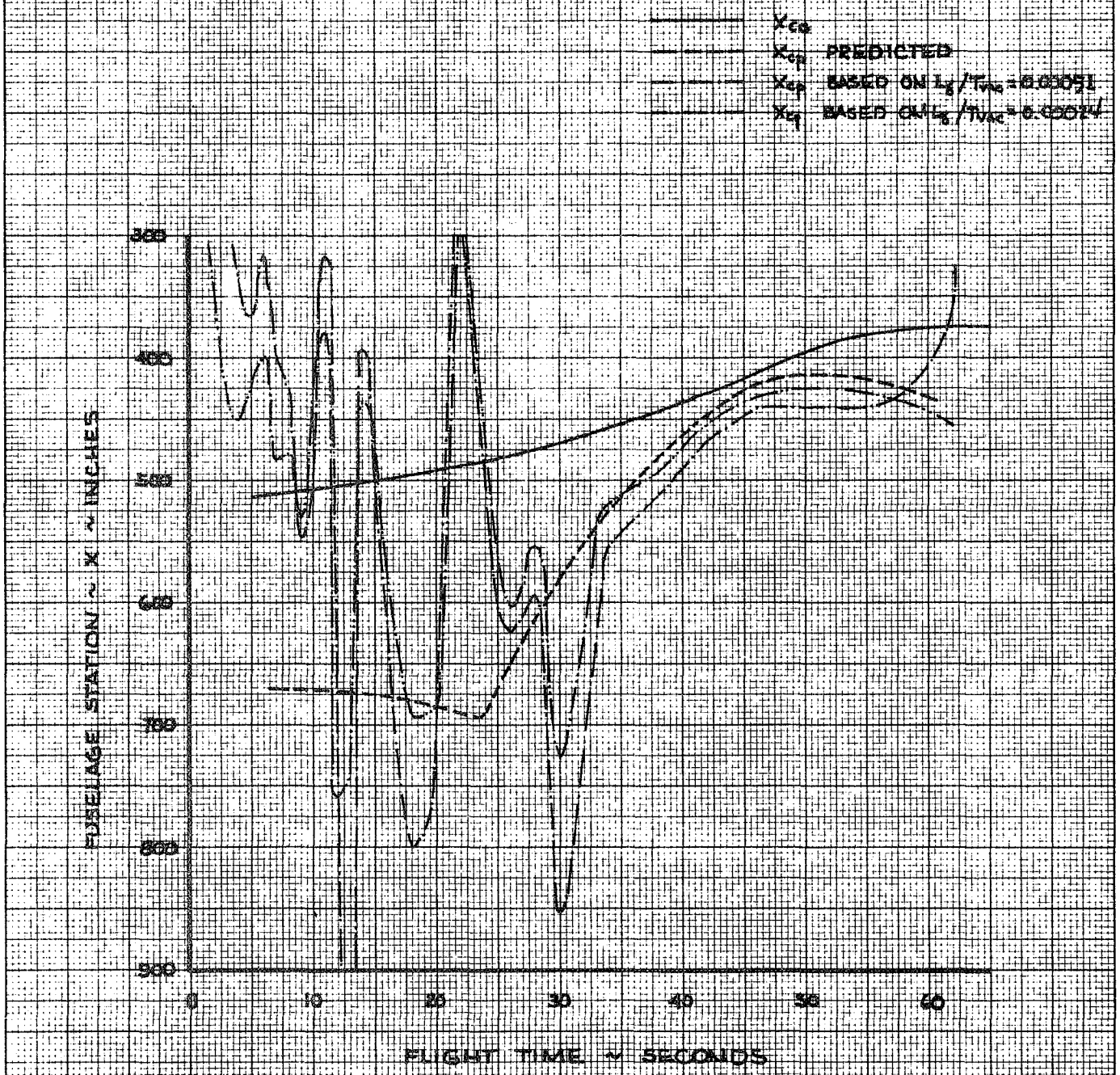

FIGURE C-10

PITCH THRUST MISALIGNMENT HISTORY
AS A FUNCTION OF CONTROL EFFECTIVENESS

VEHICLE S-142

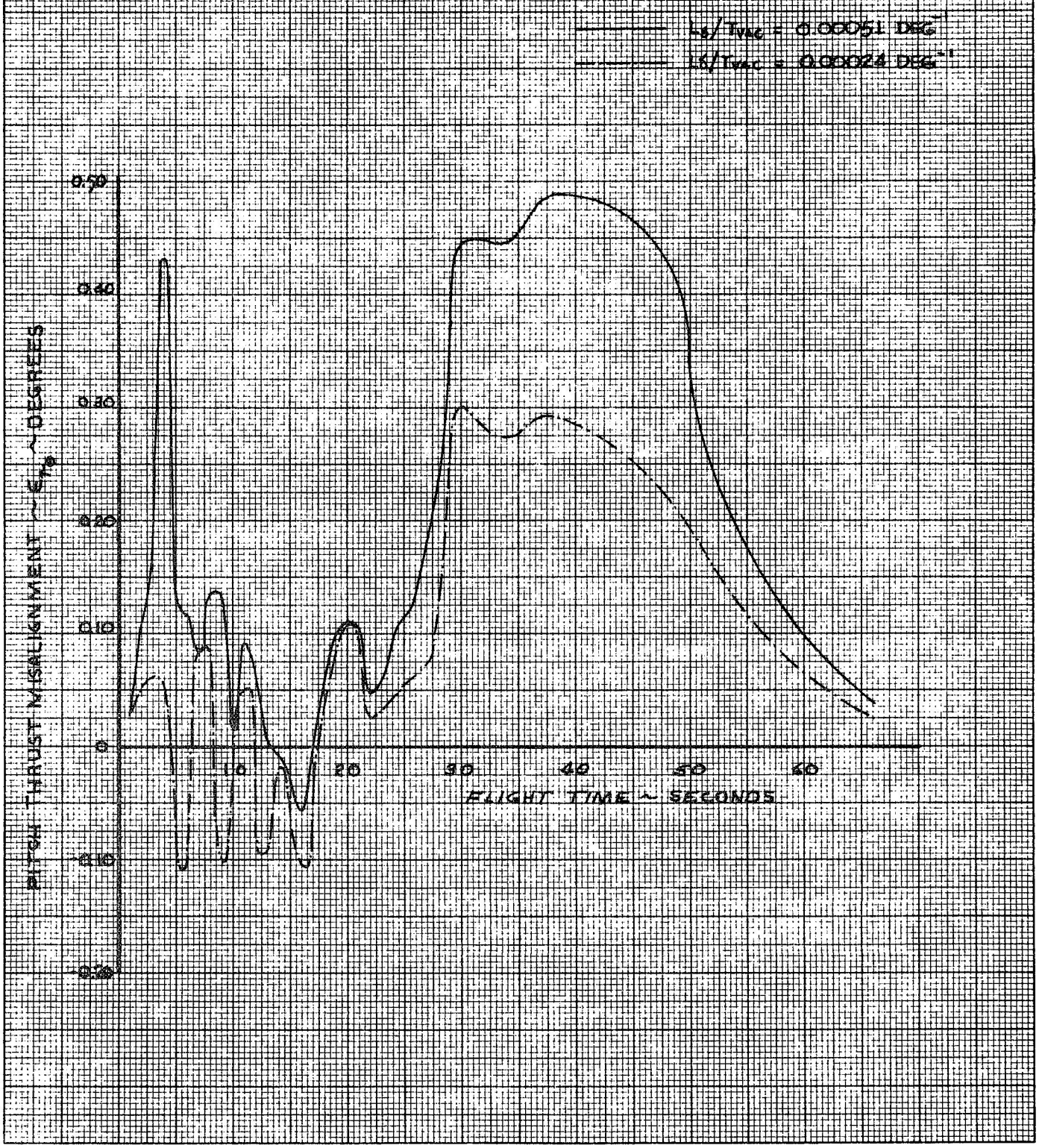

FIGURE C-11

YAW THRUST MISALIGNMENT HISTORY
AS A FUNCTION OF CONTROL EFFECTIVENESS
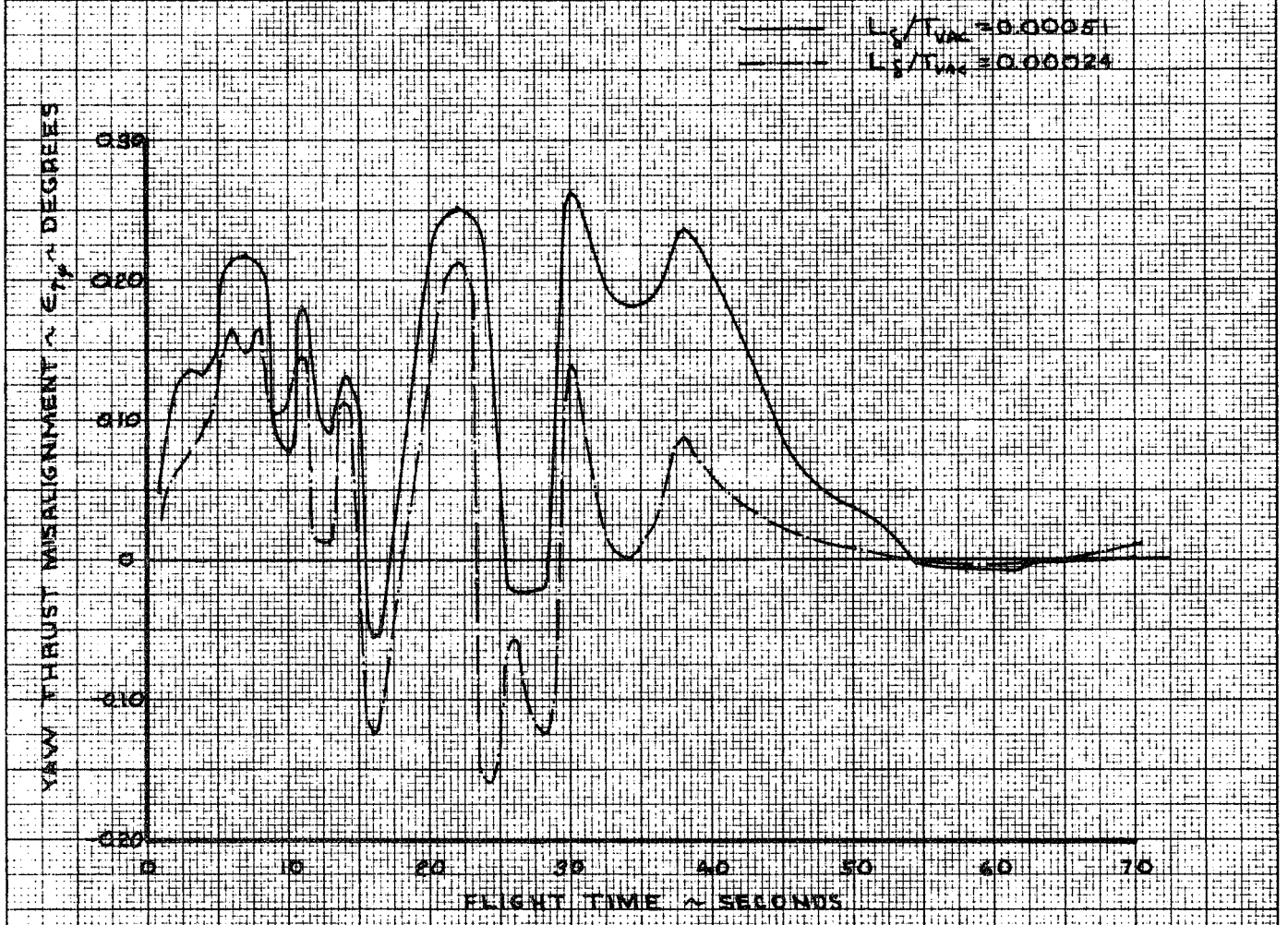
VEHICLE S-IVZ